

**Republic of Iraq
Ministry of Higher Education
and Scientific Research
University of Kerbala
College of Science**



**Determination of Natural Radioactivity for
Gamma and Alpha Emitters from Soil of
Kerbala University**

A Thesis

Submitted to the Council of College of Science, University of
Kerbala, in Partial Fulfillment of the Requirements for the
Degree of Master of Science in Physics

By

Abrrar Abbas Ibrahim

B. Sc., university of Babylon (2017)

Supervisor by

Prof. Dr. Abdalsattar Kareem Hashim

Prof. Dr. Ali Abid Abojassim

2021 A.D

1442A. H

Supervisor Certification

I certify that the preparation of this thesis, entitled “**Determination of natural radioactivity for Gamma and Alpha emitters from Soil of Kerbala University**” was made under my supervision by (**Abrrar Abbas Ibrahim**) at the College of science University of Kerbala in partial fulfilment of the requirements for the degree of (Master)of Science in Physics.

Signature:

Name: Dr. Abdalsattar Kareem Hashim

Title: Professor

Date: / / 2021

Signature:

Name: Dr. Ali Abid Abojassim

Title: Professor

Date: / / 2021

Head of the Department Certificate

In view of the available recommendations, I forward this thesis for debate by the examining committee.

Signature:

Name: Dr. Rajaa A. Madlool

Title: Professor

Head of Physics Department, College of Science

Date: / / 2021

ACKNOWLEDGMENTS

Praise to **Allah**, And the Prophet **Muhammad** and his Household and companions and peace. First of all, thanks go for the Almighty **Allah**. The Most Gracious and the most Merciful, for the capability granted to me to complete this research. I would like to express my heartfelt gratitude my deep appreciation to my Supervisors **Prof. Dr. Abdalsattar Kareem Hashim** and **Prof. Dr. Ali Abid Abojassim** for their suggestion for this project, and to provide assistance, guidance and my advice throughout the work and for many helpful discussions and suggestions. I would like to express my sincere thanks to head of the Department, **Prof. Dr. Raja Abdul Amir**, the Dean of the College, and **Assist. Dr. Nibras Mossa** for their support in carrying out this work. **Also**, I would like to thank to the head of Education for Pure Sciences Department (physics Department) **prof. Dr. Ali H.A. Jalaukhan**. I would also like to thank my dear friends who had the great role in completing this work (**Worood, Sara**).

Many thanks to all my colleagues and all members of the nuclear group for their support.

(My thanks and appreciation to my generous family for their moral support to help me in this research)

Abrrar



To

The land of peace, the good and tender land of Hussein (holy Karbala).

To

My family and all those who pray for my success, specially my father and my mother, those who are my story of existence of the secret of my success.

Dedicate to you my humble work

Abrrar

Abstract

The main source of radioactivity and nuclear radiation is called radionuclides, which represent a daily part of our lives. Alpha particles, and gamma rays represent the most important types of ionizing radiation. The soil is the important source of natural radioactive as terrestrial radiation that may be effect on human health.

The 100 samples were collected at different sites of the University of Kerbala that consist of many collages distributed in three sites such as Freiha site, the Al-Husseineya site (Agricultural college), and the Al-Mothafeen site. Gamma-ray emitters (^{238}U , ^{232}Th , and ^{40}K) and alpha emitters (^{222}Rn , ^{226}Ra , and ^{238}U) were measured by NaI(Tl) and CN-85 detectors, respectively. As well as, radiological hazard index due to gamma and alpha emitters of samples were determined. Then, the Geographic Information System (GIS) technique was used for the mapping of the most main results.

The results show that the average values of the specific activity for ^{238}U , ^{232}Th , and ^{40}K in Freiha site, were 17.02 ± 7.70 Bq/kg, 8.22 ± 2.9 Bq/kg, and 301.02 ± 77.5 Bq/kg respectively, while Al-Husseineya site were 21.75 ± 7.2 Bq/kg, 9.43 ± 3.2 Bq/kg, and 335.88 ± 82.2 Bq/kg respectively, however Al-Mothafeen site were 22.4 ± 8.8 Bq/kg, 11.19 ± 3.3 Bq/kg, and 333.11 ± 70.7 Bq/kg respectively. While, the results of the average values of radon concentrations, the specific activity Radium Content, and the specific activity uranium concentrations in Freiha site were 3769.71 ± 6.67 Bq/m³, 0.093 ± 0.03 Bq/kg, and 2.75 ± 0.18 Bq/kg

respectively, while Al-Husseineya site were $4308.25 \pm 7.17 \text{ Bq/m}^3$, $0.106 \pm 0.03 \text{ Bq/kg}$, and $3.15 \pm 0.18 \text{ Bq/kg}$, however Al-Mothafeen site were $5090.54 \pm 155.31 \text{ Bq/m}^3$, $0.125 \pm 0.03 \text{ Bq/kg}$, and $3.72 \pm 0.12 \text{ Bq/kg}$ respectively. Also, it is found a good correlation for the specific activity between ^{238}U and ^{222}Rn (0.88). Accordingly, the average value of gamma and alpha emitters, as well as radiological hazard index from Soil of Kerbala University, were within the global limitations of the organization UNSCEAR, OECD and ICRP recommended. At last, one may conclude that there is no danger from radiological hazard due to gamma and alpha emitter in soil samples of the present study on human health.

THE CONTEENTS

Section		Page
Abstract		I
List of Contents		III
List of Figure		VI
List of Tables		IX
List of Symbols		XI
Chapter One : General Introduction		1-18
1.1	Introduction	1
1.2	Radiation Sources	2
1.2.1	Natural Radiation	3
1.2.1.a	Cosmic Radiation	3
1.2.1.b	Terrestrial Radiation	4
1.2.1.c	Internal Radiation	6
1.2.2	Man-made (artificial) Source	6
1.3	Radon -222, Radium-226, Uranium-238	6
1.4	Natural Radionuclides in soil	8
1.5	Literature Survey	9
1.5.1	Using NaI(Tl) Technique	9
1.5.2	Using SSNTD Technique	13
1.5.3	Using others the Detector	16
1.6	Justification of This Study	17
1.7	The Aim of Study	18

Chapter Two: Theoretical Part		19-36
2.1	Introduction	19
2.2	Interactions of Gamma-ray with Matter	19
2.2.1	Photoelectric Effect	19
2.2.2	Compton Effect	20
2.2.3	Pair Production	21
2.3	Interactions of Alpha with Matter	22
2.4	Radioactive Equilibrium	23
2.4.1	Secular Equilibrium	24
2.4.2	Transient Equilibrium	24
2.4.3	Non Equilibrium	25
2.5	Health Risk of Gamma-Ray and Alpha-particle	26
2.6	Gamma-Ray Spectroscopy	27
2.7	Solid State Nuclear Track	28
2.7.1	Properties of SSNTDs	29
2.7.2	CN-85 Track Detector	30
2.8	Models of Track Formation	31
2.8.1	Thermal Spike Model	31
2.8.2	Ion-Explosion Spike Model	32
2.9	Chemical Etching	34
2.10	Track Formation Mechanism	35
Chapter Three: Materials and Methods		37-70
3.1	Introduction	37

3.2	Geological of Karbala Governorate	38
3.3	Area of Study	38
3.4	Sample Collection and Preparation	41
3.5	Systems of Measurement Used in This Study	52
3.5.1	NaI(Tl) System Spectroscopy	52
3.5.2	Preparation of the NaI(Tl) detector	54
3.5.2.a	Energy Calibration	54
3.5.2.b	Energy Resolution	55
3.5.2.c	Detector Efficiency	56
3.5.2.d	Gamma Radiation Measurement	58
3.6	Experimental Part of CN-85 Detector	61
3.6.1	Preparation of Samples and Detectors	61
3.6.2	Process of Chemical Etching	62
3.6.3	Calculation alpha particles track on the surface of detectors	62
3.7	Calculations	63
3.7.1	Calculations of Gamma-Ray emitters	63
3.7.1.1	Specific Activity (A)	63
3.7.1.2	Radium Equivalent Activity (Raeq)	64
3.7.1.3	Hazard Indices	64
3.7.1.3.1	External Hazard Index (Hex)	64
3.7.1.3.2	Internal Hazard Index (Hin)	64
3.7.1.3.3	Representative Level Index (I _γ)	65

3.7.1.3.4	Alpha Index (I_{α})	65
3.7.1.4	Exposure Rate (X')	65
3.7.1.5	Radiological doses	66
3.7.1.5.1	Absorbed Dose Rate in Air (D_r)	66
3.7.1.5.2	Annual Gonadal Equivalent Dose (AGED)	66
3.7.1.5.3	The Annual Effective Dose Equivalent (AEDE)	67
3.7.1.6	Excess life-time Cancer Risk (ELCR)	67
3.7.2.	Calculations of Alpha Emitters	67
3.7.2.1	Radon Concentration	68
3.7.2.2	Radium Concentration	69
3.7.2.3	Radon Exhalation Rates	69
3.7.2.4	Uranium Concentration	70
Chapter Four: Results and Discussions		71-147
4.1	Introduction	71
4.2	Gamma-Ray Emitters	71
4.2.1	Gamma Emitters in Freiha Site	71
4.2.1.1	Specific Activity	71
4.2.1.2	Radiological Effects	78
4.2.2	Gamma Emitters in Agricultural College	84
4.2.2.1	The specific Activity	84
4.2.2.2	Radiological Effects	90
4.2.3	Gamma Emitters in Al-Mothafeen Site	93
4.2.3.1	The specific Activity	93

4.2.3.3	Radiological Effects	99
4.2.4	Compare the results of gamma emitters between sites in present study	102
4.2.5	Compare the results of gamma emitters with other study	105
4.3	Alpha Particles Emitters	107
4.3.1	Alpha Emitters in Freiha Site	107
4.3.1.1	Radon Concentration and Annual effective dose	108
4.3.1.2	Radium Content and Radon Exhalation Rates	108
4.3.1.3	Uranium Concentration	109
4.3.2	Alpha Emitters in (Agricultural college)	119
4.3.2.1	Radon Concentration and Annual effective dose	119
4.3.2.2	Effective radium content and Radon exhalation rates	120
4.3.2.3	Uranium Concentration	120
4.3.3	Alpha Emitters in -Mothafeen Site	129
4.3.3.1	Radon Concentration and Annual effective dose	129
4.3.3.2	Effective radium content and Radon Exhalation Rates	130
4.3.3.3	Uranium Concentration	130
4.3.4	Compare the Results of Alpha Emitters Between Sites in present Study	138
4.3.5	Compare the results of Alpha emitters between sites in present study	140
4.5	Correlation Between Gamma and Alpha Emitters	142
4.6	Conclusions	146
4.7	Recommendations	147
Reference		148-160

LIST OF FIGURES

Chapter One : General Introduction		
(1-1)	Radiation back ground	3
(1-2)	shows the decay scheme of three nuclear chains	5
(1-3)	Potassium-40 decay scheme	5
(1-4)	Uranium-238 decay	7
Chapter Two : Theoretical Part		
(2-1)	Photoelectric effect	20
(2-2)	Compton scattering	21
(2-3)	Pair production	22
(2-4)	Secular equilibrium	24
(2-5)	Transitional balance	25
(2-6)	No Equilibrium	25
(2-7)	Schematic picture of NaI(Tl) detector	28
(2-8)	Chemical formula of CN-85 (C ₆ H ₈ O ₉ N ₂)	31
(2-9)	The ion explosion spike phase for inorganic solid track formation: The initial ionization produced by the passage of the charged particle (a) is unstable and throws in strong ions producing Vacancies and interstitials (b) The stressed area later relaxed elastically (c) Straining the matrix undamaged	33
Chapter Three: Materials and Methods		
(3-1)	A flow chart of the main parts of the current study	37
(3-2)	Iraq map with a selected window represents Karbala city	40
(3-3)	GPS device	41
(3-4)	Map of location sample for Freiha site	47
(3-5)	Map of location sample for Al-Husseineya site	48
(3-6)	Map of location sample for Al-Mothafeen site	49
(3-7)	Oven used in this study	50
(3-8)	Electric mill	50

(3-9)	Sieve used in this study	51
(3-10)	Balance used in this study	51
(3-11)	Sketch of the equipment set up of NaI(Tl) detector	53
(3-12)	Shielding, (a) :Schematic diagram of the shielding chamber and (b): Photograph of the shielding chamber with detector position	53
(3-13)	Energy Calibration Curve of NaI(Tl) "3×3"	55
(3-14)	Spectrum of ^{137}Cs using (Maestro-32)	56
(3-15)	The efficiency calibration curve of NaI(Tl) ("3×3")	57
(3-16)	Sample of soil in marinelli beaker	58
(3-17.a)	The spectrum of sample U2 (university of Kerbala Freiha site) in Maestro-32.	59
(3-17.b)	The spectrum of sample U65 (university of Kerbala agricultural college) in Maestro-32.	60
(3-17.c)	The spectrum of sample U85 (university of Kerbala Al-Mothafeen Site) in Maestro-32.	60
(3-18)	A test tube technique used in the study	61
(3-19)	Water Path	62
(3-20)	Optical microscope	63
Chapter Four: Results and Discussions		
(4-1)	Map of the values of specific activity of ^{238}U in Freiha site of Kerbala university	75
(4-2)	Map of the values of specific activity of ^{232}Th in Freiha site of Kerbala university	76
(4-3)	Map of the values of specific activity of ^{40}K Freiha site of Kerbala university	77

(4-4)	Map of the values of specific activity of ^{238}U in Agricultural College of Kerbala university	87
(4-5)	Map of the values of specific activity of ^{232}Th in Agricultural College of Kerbala university	88
(4-6)	Map of the values of specific activity of ^{40}K in Agricultural College of Kerbala university	89
(4-7)	Map of the values of specific activity of ^{238}U in Al-Mothafeen Site of Kerbala university	96
(4-8)	Map of the values of specific activity of ^{232}Th in Al-Mothafeen Site of Kerbala university	97
(4-9)	Map of the values of specific activity of ^{40}K in Al-Mothafeen Site of Kerbala university	98
(4-10)	Comparing of specific activity for ^{238}U in all locations under study.	103
(4-11)	Comparing of specific activity for ^{232}Th in all locations under study.	103
(4-12)	Comparing of specific activity for ^{40}K in all locations under study.	104
(4-13)	Comparing of Radiological hazard Due to Gamma Emitters in all locations under Study	104
(4-14)	Comparing of Radiological hazard Due to Gamma Emitters in all locations under Study	105
(4-15)	AED of radon for soil samples collected from Kerbala university of Freiha Site	114
(4-16)	Map of the values of C_{Rn} in Freiha site of Kerbala university	115
(4-17)	Map of the values of C_{Ra} in Freiha site of Kerbala university	116

(4-18)	Map of the values of C_U in Freiha site of Kerbala university	117
(4-19)	Map of the values of C_U in Freiha site of Kerbala university	118
(4-20)	AED of radon for soil samples collected from Kerbala university of (Agricultural college)	124
(4-21)	Map of the values of C_{Rn} in agricultural college of Kerbala university	125
(4-22)	Map of the values of C_{Ra} in agricultural college of Kerbala university	126
(4-23)	Map of the values of C_U in agricultural college of Kerbala university	127
(4-24)	Map of the values of C_U agricultural college of Kerbala university	128
(4-25)	AED of radon for soil samples collected from Kerbala university of Al-Mothafeen site	133
(4-26)	Map of the values of C_{Rn} in Al-Mothafeen Site of Kerbala university	134
(4-27)	Map of the values of C_{Ra} in Al-Mothafeen Site of Kerbala university	135
(4-28)	Map of the values of C_U Al-Mothafeen Site of Kerbala university	136
(4-29)	Map of the values of C_U in Al-Mothafeen Site of Kerbala university	137
(4-30)	Comparing of C_{Rn} , C_{Ra} and C_U in all locations under study.	138
(4-31)	Comparing of Radiological hazard due to Alpha Emitters in all locations under Study.	139

(4-32)	Correlation between ^{222}Rn for CN-85 and ^{238}U NaI(Tl) detectors for Freiha Site.	144
(4-33)	Correlation between ^{222}Rn for CN-85 and ^{238}U NaI(Tl) detectors for Al-Husseineya Site	144
(4-34)	Correlation between ^{222}Rn for CN-85 and ^{238}U NaI(Tl) detectors for Al-Mothafeen Site	145
(3-35)	Correlation between ^{222}Rn for CN-85 and ^{238}U NaI(Tl) detectors for all values of Kerbala University	145

LIST OF TABLES

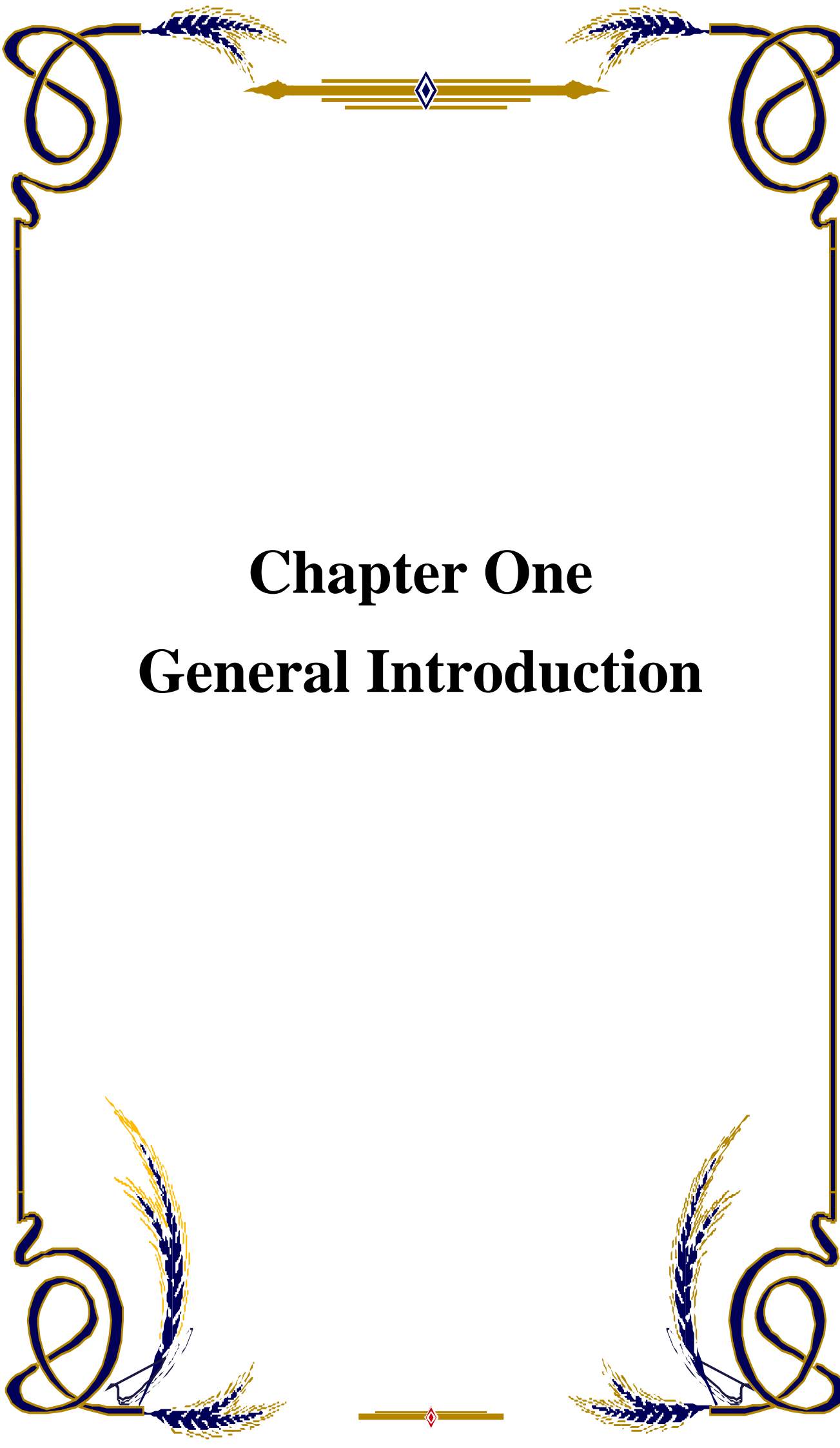
No	Table title	page
(3.1)	Location of Freiha site samples	42
(3.2)	Location of Agricultural college in Al-Husseineya site	45
(3.3)	Location in Al-Mothafeen Site samples	46
(3.4)	Properties of Radioactive Sources used in the Present Study with Compare Experimental (I_γ)	54
(4.1)	Results of specific activity in Kerbala university of Freiha site	72
(4.2)	Results of R_{aeq} , H_{ex} , H_{in} , $I_{\gamma\text{r}}$ and I_α in Kerbala university of Freiha site	78
(4.3)	Results of X , D_r , AGED, $\text{AEDE}_{\text{outdoor}}$, ELCR in Kerbala university of Freiha site	81
(4.4)	Results of specific activity in Kerbala university of agricultural college	85
(4.5)	Results of R_{aeq} , H_{ex} , H_{in} , $I_{\gamma\text{r}}$ and I_α in Kerbala university of Agricultural College	90
(4.6)	Results of X , D_r , AGED, $\text{AEDE}_{\text{outdoor}}$, ELCR in Agricultural college of Kerbala university	93
(4.7)	Results of specific activity in Al-Mothafeen Site of Kerbala university	94
(4.8)	Results of R_{aeq} , H_{ex} , H_{in} , $I_{\gamma\text{r}}$ and I_α in Al-Mothafeen Site of Kerbala university	99
(4.9)	Results of X , D_r , AGED, $\text{AEDE}_{\text{outdoor}}$, ELCR in Al-Mothafeen Site of Kerbala university	101

(4.10)	Comparison of the present study Results in Soil with Different Countries.	106
(4.11)	Comparison of the current Study Results in Soil with Different locations in Iraq.	107
(4.12)	Results of track density(ρ), radon concentration (C), concentration of radon in samples(C_{Rn}) , annual effective dose(AED) in Freiha Site of Kerbala university	110
(4.13)	Results of effective radium content (C_{Ra}), surface (E_s)and mass(E_M) exhalation rates. Uranium concentration(C_U) and uranium concentration in unit Bq/kg (C_U) in Freiha Site of Kerbala university	112
(4.14)	Results of track density(ρ), radon concentration (C), concentration of radon in samples(C_{Rn}), annual effective dose(AED) in Agricultural college of Kerbala university	121
(4.15)	Results of effective radium content (C_{Ra}), surface (E_s)and mass(E_M) exhalation rates. Uranium Concentration(C_U)and uranium Concentration in unit Bq/kg (C_U) in agricultural college of Kerbala university	122
(4.16)	Results of track density(ρ), radon concentration (C), concentration of radon in samples(C_{Rn}), annual effective dose (AED) in Al-Mothafeen Site of Kerbala university	131
(4.17)	Results of effective radium content (C_{Ra}), surface (E_s)and mass(E_M) exhalation rates. Uranium Concentration(C_U)and uranium Concentration in unit Bq/kg (C_U) in Al-Mothafeen Site of Kerbala university	132
(4.18)	Comparison of the present Study with others Studies of many Different Countries.	141
(4.19)	Correlation between Gamma and Alpha Emitters in all value of Kerbala university	142
(4.20)	Correlation between Gamma and Alpha Emitters in present study	142

LIST OF SYMBOLS & ABBREVIATIONS

Symbols	Description
α	Alpha particle
I_{α}	Alpha Index (I_{α})
AGED	Annual Gonadal Equivalent Dose
AEDE	Annual Effective Dose Equivalent
ADC	Analog to Digital Convertor
β	Beta particle
BDL	Below Detection Limit
C	Concentration of radon
K	Calibration Factor
H_{ext}	External Hazard Index
\dot{X}	Exposure Rate
ELCR	Excess Lifetime Cancer Risk
ε	Efficiency
FWHM	Full width at half maximum
γ	Gamma- Ray
D_{γ}	Gamma Dose Rate
$I_{\gamma r}$	Gamma Index Representative
GIS	Geographic Information System
Gy	Gray
HPGe	High Purity Germanium
IR	Infrared
ICRP	International Commission on Radiological Protection.
H_{int}	Internal Hazard Index
IR	Infrared
L	Liter
MeV	Million electron Volt.
MCA	Multichannel analyzer
E_M	Mass exhalation rate
mSv y^{-1}	Milli sieverts per year
NORM	Naturally Occurring Radioactive Material
OECD	Organization for Economic Co-operation and Development

H	Occupancy factor.
⁴⁰ K	Potassium-40
PMT	photo Multiplier Tube
²²² Rn	Radon-222
²²⁶ Ra	Radium -226
R _{aeq}	Radium Equivalent Activity
AD _r	Rate dose absorbed in soli
RF	Risk Factor
R _a	Radium content
Nal (TI)	Sodium Iodide Thallium Detector
SSNTDs	Solid State Nuclear Track Detectors
E _A	surface exhalation rate
ρ	Track density
²³² Th	Thorium-232
T	The number of hours per year.
²³⁸ U	Uranium-238
C _U	Uranium Concentration



Chapter One
General Introduction

Chapter One

General Introduction

1.1 Introduction

NORM is an abbreviation for the natural radioactive materials always present within the environment, natural sources of radiation are the most important contributors to exposure to the general public. There are two main categories of NORM supported their origins [1]. Terrestrial radionuclides consist of a natural chain such as ^{238}U and ^{232}Th and are non-sequenced like ^{40}K which are usually long-lived with a half-life over one hundred million years. The presence of (NORM) within the environment is understood to be liable for exposure to large radiation against humanity. Radionuclides may either emit from alpha or beta particle and that they are often transferred to the body by swallowing or inhalation. This will cause a rise in internal exposure, a number of these nuclear types are liable for gamma emission, which is that the main source of human exposure. This means that humans are vulnerable not only to natural sources but also to internal and external radiation, internal exposure is caused by the ingestion of radionuclides through inhalation or ingestion[2]. The dose of inhalation exposure is closely related to the presence of dust particles in the air which include radionuclides from the ^{238}U and ^{232}Th series in addition to ^{40}K . The largest contribution is in inhalation exposure comes from short-lived radon degradation products, radon is one of the noble gas chains in the periodic table. Radon has three natural isotopes which are: actinone (^{219}Rn), thoron (^{220}Rn), and radon (^{222}Rn) resulting from the radioactive decay of the actinium ^{235}U chain, thorium ^{232}Th , and uranium ^{238}U , respectively. ^{222}Rn consists of ^{226}Ra decay, the direct origin of the ^{238}U series, while his ^{220}Rn counterpart decays from ^{224}Ra , it is a part of the ^{232}Th series[3]. Actinon

series is usually neglected due to its low concentration in the air radon is released as a gaseous element in the natural radioactive chain in the atmosphere from the earth's crust. Radon gas emits rocks and soil and tends to focus indoors like underground mines or homes[4]. Radiation Protection Agency is one of the United Nations agencies concerned with Peaceful use of atomic energy and preventing radioactive pollution, in addition to protecting National Societies in all countries of the world its citizens, and numerous studies and research have emerged to estimate the level of radioactivity in the soil, Air, water, and plants and their effect on living organisms[5]. The soil is one of the most important contributors to the background, and it is very important to understand the radioactivity content of the soil. Therefore, a study evaluating the radioactive impact of radionuclides in soil samples collected from Kerbela University, to determine the effect of radiation from this soil on human health. The Environmental Radiological Guidance Programmer plays a vital role in ensuring the safety and security of society. This is why it is so important to know the amount of increase in radiation levels because of its effect on many aspects. Most of them are closely related to the genetic impact of the body, its health, and negativity[6].

1.2 Radiation Sources

The radiation in the physics view is an energy that takes the state of waves or moving sub-nuclear particles [7]. Radiation has two types which can be identified as ionizing or non-ionizing radiation depending on the impact on nuclear matter ionizing radiation that has adequate energy. To ionize atoms or molecules like (x-ray, γ - rays, α , and β) and non-ionizers for example(ultraviolet, microwave, IR, radio waves, and visible light) [8]. The radiation sources can be classified into (natural and man-made radiation). Figure (1-1) illustrates the average annual percentage of

radiation exposure which is contributed by every major source. These sources are known as low-level radiation everywhere "background". Nature participates about (85) percent. As for industrial, medical, and consumer sources, the participation reaches (15%) percent.

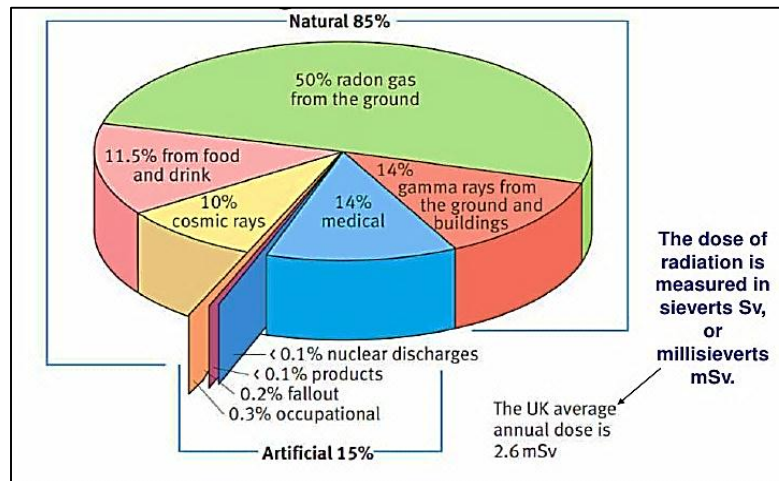


Figure (1-1) Radiation back ground [10].

1.2.1 Natural Radiation Source

1.2.1.a Cosmic Radiation

Cosmic ray's original in space and solar particles inside the earth's atmosphere and start a cascade of secondary interactions and decays, cosmic rays consist of high-energy molecules with an average energy of approximately [9]. (10^4 MeV) such as protons, high-energy electrons, alpha particles, and light atomic nuclei the cosmic rays contains (87%) protons and (11%) alpha particles and about (1%) nuclei of the number (Z) between (4 - 26) and about (1%) electrons of high kinetic energy[10].

1.2.1.b Terrestrial Radiation

Only nuclides with a half-life are comparable with the age of the earth or decay products whose concentrations are governed by their existence in terrestrial materials, in terms of dose, the primary radionuclides are ^{40}K , ^{232}Th , and ^{238}U whereas ^{86}Rb and ^{235}U are of secondary importance [10]. In disparity, two radionuclides of uranium and one of thorium decay to give rise to two families of radionuclides which decay in three distinct series. All three series contain alpha emitters. The first one begins with the decay of ^{238}U half-life (4.5×10^9 years) and, is called the uranium chain and starts with the second (^{232}Th) half-life (1.4×10^{10} years), which is called the thorium chain, and the third begins with ^{235}U half-life (7.1×10^8 years), which is called actinium series. All three decay through three complex series of stable isotopes of lead (^{206}Pb , ^{208}Pb , and ^{207}Pb) respectively [11]. There is a fourth series called Neptunium series ^{237}Np , this series was reformed after ^{241}Pu was made in nuclear reactors. This series does not take place in a natural method since the (half-life) of the longest-lived. Member of the chains (^{237}Np) is only (2.14×10^6 y), shorter than the earth's lifetime finally, it is important to know that not all radionuclides in the chains emit distinct gamma rays, only those radionuclides under lined shown in Figure (1-2) can be measured with a gamma-ray spectrophotometer [12].

Natural potassium contains 0.012% ^{40}K and has a half-life of (1.28×10^9 y) and has 31.4 Bq/g a specific activity for normal potassium, ^{40}K is degraded through beta decay to ^{40}Ca 89.28% of the time. The remaining 10.72% of the ^{40}K undergoes decay by electron capture to the stable ^{40}Ar and the decay branch also emits the characteristic gamma rays at 1.461 MeV. This line is very useful in determining and measuring ^{40}K by gamma spectrometry [13]. ^{40}K decay scheme can be shown in Figure (1-3)

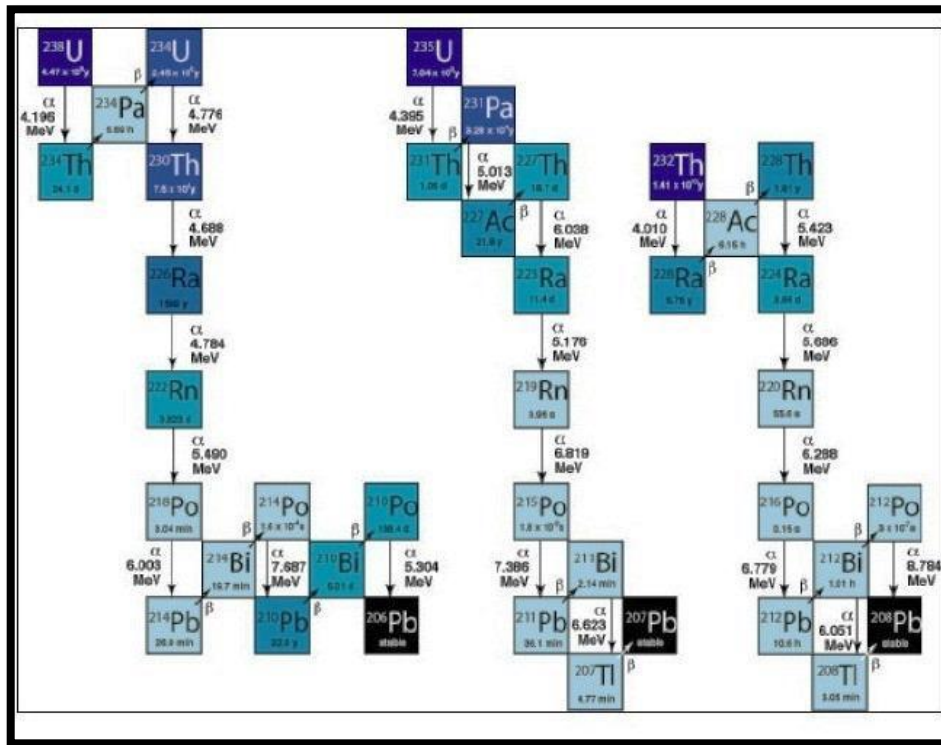


Figure (1-2): Shows the decay scheme of three nuclear chains[12].

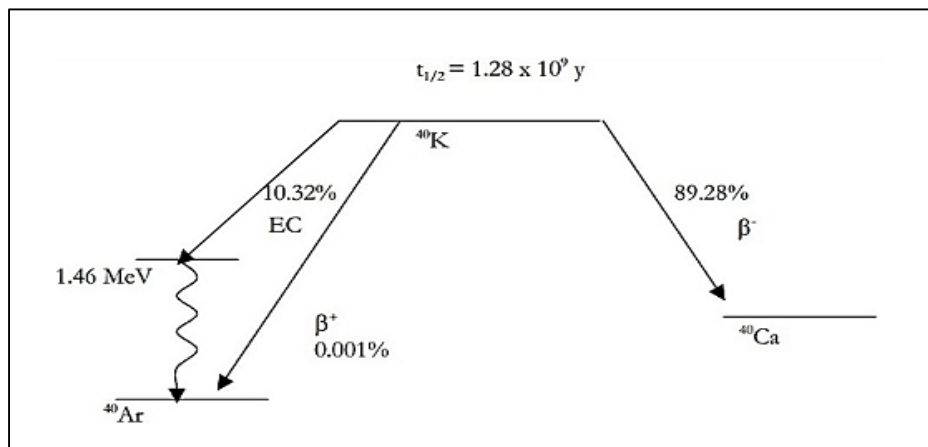


Figure (1-3): Potassium-40 decay scheme [13].

1.2.1.c Internal Radiation

A significant contribution to radioactivity in the human body originates from the gassy decay products of the thorium radioactive series, namely (radon and thoron) and uranium. The rocks and soil diffuse these kinds of gases and they also exist in readily commensurable concentrations in the atmosphere. After spreading over in the air they are inhaled by mankind during the process of decay products. Similarly, when plants and animals take up the above-mentioned gassy decay products, such products [14]. It will eventually be transferred to most foodstuffs leading to measurable amounts of natural radioactivity. Ordinary cereals and foods contain high radioactivity, but the situation seems quite different regarding milk products, fruit, and vegetables; they contain a low content of radioactivity [15].

1.2.2 Man-made (artificial) Source

Another source of radioactivity is man-made radionuclides emitted to the atmosphere. As a result of nuclear weapons tests, or nuclear power plant accidents [16]. Many artificial radionuclides (^{134}Cs , ^{137}Cs , ^{131}I , ^{90}Sr , etc.) were released as a result of these events [17].

1.3 Radon -222, Radium-226, Uranium-238

Radon, radium, and uranium are in the same group because they are radionuclides. They are major unstable components that are highly involved in the release of ionizing radiation. These three elements uranium, radon, and radium occur naturally in the environment. Radon (^{222}Rn) was born as a result of spontaneous decomposition automatic degradation element radium ^{226}Ra present in the earth's crust (10-11%), the presence of radium in the natural region depends on the presence of uranium, which is

estimates the presence of geologists in the earth's crust at 3 parts per million, because, radium is the main source of radon[18]. (^{238}U) is decomposed by 16 radioactive atoms until lead and the non-radioactive element ^{206}Pb are reached. When radioactive materials are released, these substances fall into two main states, first, they either change to different isotopes, or to a completely different element. The decay of radioactivity is usually defined as the process that emits radioactivity, and transforms one element into another substance, uranium and radium are found in various types of rock as solids, Radon can be present in dissolved in water or in the air, but it is not commonly existed in food. Radon cannot be found at any considerable concentration in surface water. The background level of radon in air is 0.4 pixels /liter. Radon is the most dangerous (^{222}Rn) which is inhibited to form very small solid radioactive particles, including (^{218}Po) and (^{214}Po) that become bound to air and natural dust particles. When inhaled, it contributes to lung cancer, exposure to high radon concentrations. For a longer period of time increases the risk of lung cancer[19]. Since radionuclides are usually associated with rocks, wells of rocky water may have higher levels of radionuclides than shallow or drilled wells. Radionuclides are described as undetectable to determine if they are present in water. An analytical test must be performed. Uranium is a very important element because it supplies us with nuclear fuel used to generate electricity in nuclear power plants. It is also the main material through which uranium is manufactured[20]. The uranium fuel used in the nuclear reactors is enriched with uranium-235. The military also uses uranium to power nuclear submarines and nuclear weapons. Radium is used to produce radioactive radon gas that is used to treat some types of cancer. Radium is a million times more effective tha

1.4 Natural Radionuclides in Soil

Soil consists of mineral and organic matter, water, and air arranged in a complicated physiochemical system that provides the mechanical foothold for plants in addition to supplying their nutritive requirements[7]. The inorganic part of the surface soils may fall into several textural classes, depending on the concentration of silt, sand, and clay. Sand consists largely of primary minerals such as quartz and has a particle size ranging from (60 μ m) to about (2 mm). The silt consists of particles in the range of (2 to 60 μ m), while the clay particles are smaller than (2 μ m), In diameter [21]. Substantial amounts of radionuclides are found in the earth's crust. Natural radioactivity is largely responsible for the fact that the interior of the earth is hot and molten. The term radiometric fingerprinting describes the identification of mineral species based on the difference in radionuclide concentrations[21]. In soil measurements, a correlation between activity concentrations and grain size has been determined in previous studies. While ^{40}K activity concentration varies slightly with grain size, ^{238}U and ^{232}Th concentrations increased with an increase in grain size [22]. The extent of radioactivity in the soil changes widely and is the (Source of people's) continued, exposure to ground activity depending on the type of soil. Some of the ingredients are macronutrients (Mg, S, Ca, K, N, and P), micronutrients (B, Co, Cl, Fe, Cu, Mn, Ni, Mo, Se, Zn, and Si). Fluorine and dangerous ingredients (Pb, Hg, As, Al, Cd) such as the normal radionuclides of U, thorium, radium (Ra), and potassium (K). Ingredients may spread in soil and" water. iron, aluminum, and phosphate" reduce the diversity of uranium in nature. The spatial difference in soil permeability, the concentration of carbon dioxide, and soil porosity. Atmospheric pressure, gas, and moisture affect soil emission of carbon dioxide. It works

as a radon carrier in the soil, which enhances its concentration in the soil atmosphere[21].

1.5 Literature Survey

Literature survey is classified in three types according to the techniques that used to measure natural radioactivity as follows:

1.5.1 Using NaI(Tl) Technique

Author, Year and Reference	Country	Results
Al-Hamarneh and et al (2009) [23]	Jordan	The results show that the average values of specific activity in (^{238}U , ^{232}Th and ^{40}K) 49, 70, 291 Bq.kg ⁻¹ respectively.
Mandić and et al (2010) [24]	Serbia	The results show that of concentration the average, value of in (^{238}U , ^{232}Th , and ^{40}K) were (2.52 ± 0.73 , 9.40 ± 2.86 and $1.60 \pm 0.40\%$) mg kg ⁻¹ , respectively.
Al-Leswas (2010)[25]	Thailand	The results show that the average values of specific activity in ^{238}U , ^{232}Th and ^{40}K (64.48,67.04, 447.7 Bq/kg) respectively.
Al-Sulaiti et al (2010) [26]	Qatar	The results show that The average values of specific activity in ^{238}U , ^{232}Th , and ^{40}K (25.5, 7.7, 165.8 Bq/kg) respectively.

Rasheed and et al (2013)[27]	Iraq (Kurdistan)	The results show that, the average values of specific activity in ^{238}U , ^{232}Th and ^{40}K were (83.337, 19.147 and 284.86Bq/kg) respectively.
Hatif and et al(2015)[28]	Babylon	The results show that, the average values of specific activity ^{238}U , ^{232}Th and ^{40}K (14.07,12.32,416.65 Bq/kg).
Abojassim (2016)[29]	Iraq (Babylon)	The results show that, the average values of specific activity ^{238}U , ^{232}Th and ^{40}K (16.07±2.89,9.60±0.954and271.42±11.60) Bq/kg respectively.
Jassim and et al (2016)[30]	Missan	The results show that, the average values of concentrations in ^{238}U , ^{232}Th and ^{40}K (21.19,9.72,453.91)Bq/kg respectively.
Arnedo and et al . (2016)[31]	Spain	The results show that, the average values of specific activity in ^{226}Ra ^{232}Th and ^{40}K were 25.2 ,28.9 and 384.4 Bq/kg respectively. Also use a commercial global positioning system GPS.
Kadhim and at al(2016) [32]	Karbala	The results show that, the average values of concentration in ^{238}U , ^{232}Th and ^{40}K (19.45, 24.47 ,245.1) Bq kg . respectively.

Abojassim (2017)[33]	Al-Najaf	The results show that, the average values of concentration ^{238}U , ^{232}Th and ^{40}K (17.48,8.59,298.31) Bq/kg ,respectively.
Shayeb and et al(2016)[34]	Saudi (Arabia)	The result show that concentration ^{226}Ra , ^{232}Th , ^{40}K in building materials it differs from 12.6 to 121.4, 13.6to 142, and 69.5 to 620.6Bq/kg respectively.
Yildirim (2017) [35]	Turkey	The results show that, the average values of ^{238}U (7.4-79.8) , ^{232}Th (9.5-170.8) ,and ^{40}K (35.79-13.8) Bq/kg ,respectively.
Saleh Kotahi (2017)[36]	Iran	The results show that the average values of specific activity in ^{238}U , ^{232}Th and ^{40}K (23,31,453)Bq/kg ,respectively.
El-Taher and et al (2018)[37]	Saudi Arabia	The results show that the average values of specific activity in ^{238}U , ^{232}Th , and ^{40}K (14.22,14,968.19) Bq/kg respectively.
Gbadamosi and et al 2018[38]	Nigeria	The results show that, the average values of ^{238}U , ^{232}Th , and ^{40}K from Below Detection Limit 76.00 ± 12.00 , -204.48 ± 13.02 and 755.6 ± 40.15 Bq/kg respectively.

Akbar Abbasi et al (2020)[39]	Cyprus	The results show that, the average values of ^{238}U , ^{232}Th , and ^{40}K from (49.7 ± 3, 18.1 ± 1.5, 103.5 ± 27) Bq/kg respectively.
Ibrahim and et al 2020 [40]	Kerbala	The results show that, the values of specific activity of ^{238}U , ^{232}Th and ^{40}K in Bq/kg were ranged from (10 to 23, from 2 to 12 and from 100 to 500) respectively
Ibrahim and et al 2021 [41]	Kerbala	The results showed that the mean value of specific activity with a standard error of ^{238}U , ^{232}Th , and ^{40}K in Al- Hussania site was (21.7±7.2, 9.43±3.2 and 335.8±82.2) Bq/kg respectively, while in Al-Mothafeen site were (22.4±8.8, 11.2±3.3 and 333.1±70.7) Bq/kg respectively

1.5.2 Using solid state nuclear Track detectors technique.

Author, Year and Reference	Country	Results
Mujahid and et al(2010)[42]	Punjab (Pakistan)	The result show that , measured radon concentration found in the ranges of 34 ± 7 to 260 ± 42 Bq m ⁻³ and Radon Exhalation Rate found in the ranges of 38 ± 8 to 288 ± 46 mBq m ⁻² h ⁻¹ respectively.
Rafique and et al(2011) [43]	Pakistan	The result show that, were found the mean of radon concentrations in kitchen (84Bq/m ³)and in drawing room (85 Bq/m ³) and bed room (93Bq/m ³) respectively.
Iqbal and et al.(2011)[44]	Pakistan	The result show that, the radon concentrations in sample were (50 ± 11.6 and 167.1 ± 21.4 Bq·m ⁻³ with an overall average of (95.1 ± 15.8 Bq·m ⁻³) respectively.
Drweesh and et al(2012)[45]	Iraq(Baghda)	The result show that the concentrations of uranium in soils samples (3.67 and 3.99 ppm)with average of 3.82 ppm.
Tabar and et al (2013)[46]	Turkey	The result show that, the ²²² Rn radon concentrations of sample Soil in the study area varied from (0.098-8.594

		kBq/m ³) with an average values of (1.920kBq/m ³) respectively.
Alsaadi and et al(2013)[47]	Iraq (Karbala)	This results have shown that the radon gas concentration altogether dates and their seeds samples is below the permissible limit from International Commission of Radiation Protection (ICRP).
Kunovska and et al(2013)[48]	Bulgaria	The result show that, the radon concentration in soil samples was found to be (log-normal) distributed within a varied of (3–97) kBq.m ⁻³ With the arithmetic mean of (26) kBq.m ⁻³ . respectively.
Kakati and et al(2013)[49]	(India)	The result show that uranium concentration found in the ranges of (1.47) ppm to (10.6) ppm. While radium concentrations vary from 10.54 Bq/kg to 49.67Bq/kg respectively.
Hashim and et al (2015)[50]	Iraq(Kerbala)	The result show that, the values of radium concentration in all the soil samples were less than there commended by organization for Economic Cooperation and Development (OECD) 1979. Also the radium concentration and radon

		exhalation rate in these samples has been found to be well below of 40 Bq/kg and 57.6 Bq.m ⁻² .s, respectively.
Battawy and et al(2016)[51]	Iraq(Tikrit)	The results show that , the very best concentrations of radon was (45.97kBq/m ³)found in Jihann tea ,while rock bottom value is recorded in Mahmoud tea which was about(25.44 kBq/m ³).
Mittal and et al (2016)[52]	India	The results show that radon concentrations in soil samples differed from (941 to 10,050 Bq m ⁻³),with the mean value of 4561Bqm ⁻³ respectively.
Abojassim (2018)[53]	Iraq(Al-Najaf)	The result show that the values of radon concentrations were range between from 506.84 Bq/m ³ to 1194.69 Bq/m ³ with an average of 894.21±77.80 Bq/m ³ respectively.
Nayif and et.al (2019)[54]	Iraq(karbala)	The results showed that of radon concentration in buildings was (36.972±11.33) Bq/m ³ and36.481±9.66 Bq/m ³ .
Jaber and et al 2020 [55]	Kerbala	The results with the global calculated results, the radiation levels of the studied models were found to be within permissible limits.

IBRAHIM and et al 2021 [56]	Kerbala	The results showed that radon concentrations with an average of $4308.25 \pm 7.17 \text{ Bq} \cdot \text{m}^{-3}$. AED with an average of $3.48 \pm 0.203 \text{ mSv/y}$. Radium content in Bq/kg varied from with an average of 0.1064 ± 0.035 ., respectively.
-----------------------------	---------	--

1.5.3 Using others the detector

Author , Year and Reference	Country	Results
Hashim and et al (2016)[57]	Lebanon	The result show that concentrations uranium concentration varies from (0.131)ppm to (6.77) ppm with average values of (1.467) ppm.
Hashim and et al (2017)[58]	Freiha(Iraq)	The results show that the ^{222}Rn varied between (17.969 Bq/m^3) to (88.975 Bq/m^3) with an mean value ($51.554 \pm 28.284 \text{ Bq/m}^3$) respectively.
Abojassim and et al (2017)[59]	Iraq(KufA)	The results showed that radon concentrations were generally low which are ranging from 38.4 to 77.2 Bq/m^3 , with a mean value of 50 Bq/m^3 the average equilibrium radon concentration and annual effective dose were evaluated to be 19.9 Bq/m^3 and 1.2 mS/y respectively.

Bajwal and (2017) [60]	India	The results show that the ranged concentration from a specific activity ^{40}K , ^{238}U , ^{232}Th from 260.1 ± 17.3 to 728.2 ± 27.7 . Below Detection Limit to 41.9 ± 10.3 and 29.5 ± 7.1 to 88.1 ± 6.2) Bq/kg respectively.
Pourimani and et al (2018)[61]	East of Shazand	The result show that the Radon concentration the Specific activities of (^{226}Ra , ^{232}Th , ^{40}K) and ^{137}Cs in the soil samples differed from 18.92 to 43.11, 25.31 to 54.27, 230.17 to 728.25 and from <1.49 to 9.52 Bq/kg, respectively.
Günay and et al (2019)[62]	Izmir(Turkey)	The result show that the Radon concentration in the soil samples ranged from No Below Detection Limit ^{226}Ra 24.1 Bq.kg, ^{232}Th 40.2 Bq.kg, and ^{40}K 315.9Bq.kg
Henryk Bem and et al (2020)[63]	Central Poland	The overall results of this radiometric survey from concentration were generally low, and lying within the range of the normal background levels.

1.6 Justification of This Study

1. The University of Kerbala is very Many students and professors.
2. The soil is one of the most natural sources of ionizing radiation radioactivity nuclides like ^{238}U series nuclides and ^{232}Th , and ^{40}K . In

addition to ^{222}Rn which exists a lot in the soil which in one way or another affects human health

3. The absence of previous studies covering the University of Kerbala, as well as no study covering the risk factors to this extent in previous studies.

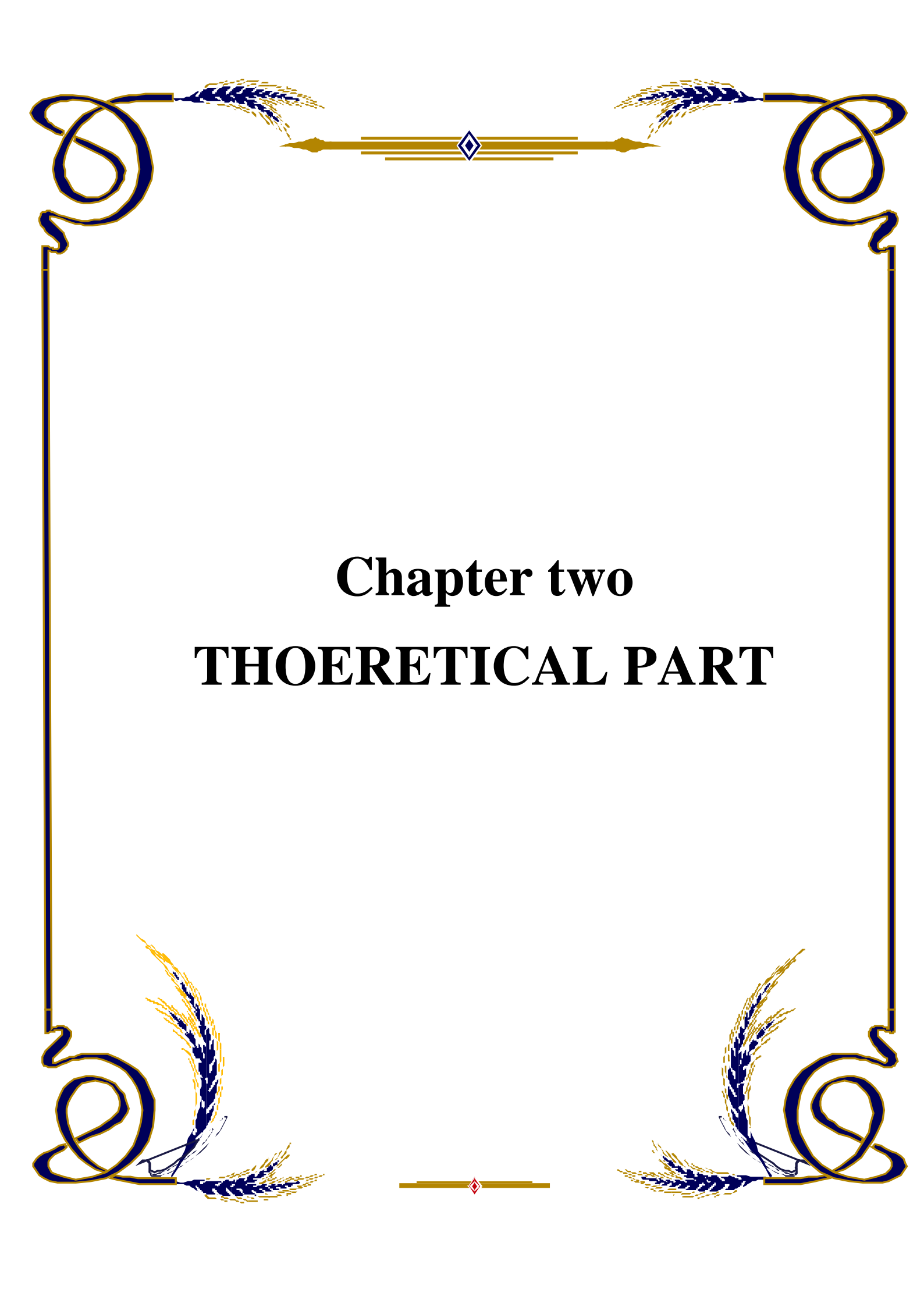
4. It was subjected to military bombardments as well as too many blasts. Also, agricultural area containing chemical fertilizer

5. The absence of a radiation map for the Karbala Governorate and there's no national number of allowed levels for Iraq, just like the remainder of the Arab world and therefore the world.

1.7 Aim of the Study

The overall aim of this present study is to measure gamma and alpha emitters levels in selected samples of the soil at the University of Kerbela in Karbala governorate in Iraq. Objects can be explored in the study as follows:

1. Determine the specific activity and the radiological due to gamma emitters (^{214}Bi (^{238}U), ^{208}Tl (^{232}Th), and ^{40}K).
2. Determine the concentration of alpha emitters (^{222}Rn , ^{226}Ra , and ^{238}U) and radiological parameters in the same samples of soil.
3. Compare the results with the recommended international values for safety standards.
4. Finally, it is drawn to establish natural radioactivity and radiological map to be a reference to the next studies using GIS technology.



Chapter two
THOERETICAL PART

CHAPTER TWO

THEORETICAL PART

2.1 Introduction

This chapter is to provide an overview of the gamma-ray and alpha particles considering four axes as how interactions with matter, radioactive equilibrium, the health risk of them, and techniques that used for measurement

2.2 Interactions of Gamma-ray with Matter

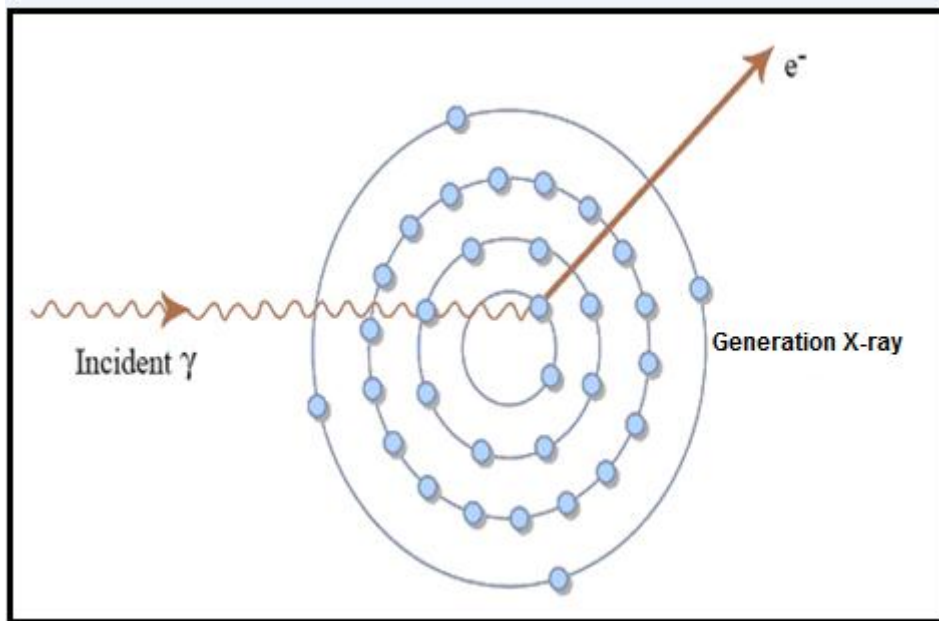
Understanding the γ -ray interactions with a detector is an important issue in order to know how γ -ray's photons are detected and attenuated. From, the number of possible interactions processes for γ -ray in the matter, three mechanisms play the most significant roles in interactions with γ -ray detectors to transfer their energy partially or completely to the detection medium. The interaction probability in one of these processes depending on the energy of the gamma-ray and the atomic number of the material there are three processing of interaction gamma with the matter, as following[64].

2.2.1 Photoelectric Effect

In general, in this process, the incident photon interacts with matter (the detector atoms) as result, the photon, completely vanished and the electron is released by the atom. This electron is called the photoelectron. If the energy of the incident photon larger than the electron binding energy in atom(work function of the matter), the photoelectron will be emitted from the more tightly bound (K) shell with kinetic energy, is given as [64].

$$E_{e^-} = h\nu - E_b \dots\dots\dots (2.1)$$

Where E_b represents the binding energy of the photoelectron original's shell[65]. This effect (photoelectric) is the common mode of interaction of gamma -rays of relatively low energy, (<0.5) MeV, with the matter as shown in Figure (2-1)



Figure(2-1):The photoelectric Effect[65].

2.2.2 Compton Effect

This phenomenon is a reaction collision between incident γ -ray's photons and an electron in the absorber. The gamma photons are deflected through an angle θ for its original direction. The recoil electron gains a portion of the photon energy. Depending on the dispersion angle, this energy can range from zero to a considerably large fraction of the initial gamma-ray energy. As seen in Fig. (2-2) [66]. It is also the prevailing interaction mechanism for γ -ray energies of (0.5-5) MeV radioisotope sources. The incoming γ -ray is scattered over an angle for to its original path. A part of the photon energy is transferred to the compton electron.

The cross-section for compton scattering (σ) per unit mass can be expressed as follows[66]:

$$\sigma = \text{Constant} / E\gamma \quad \dots\dots (2.2)$$

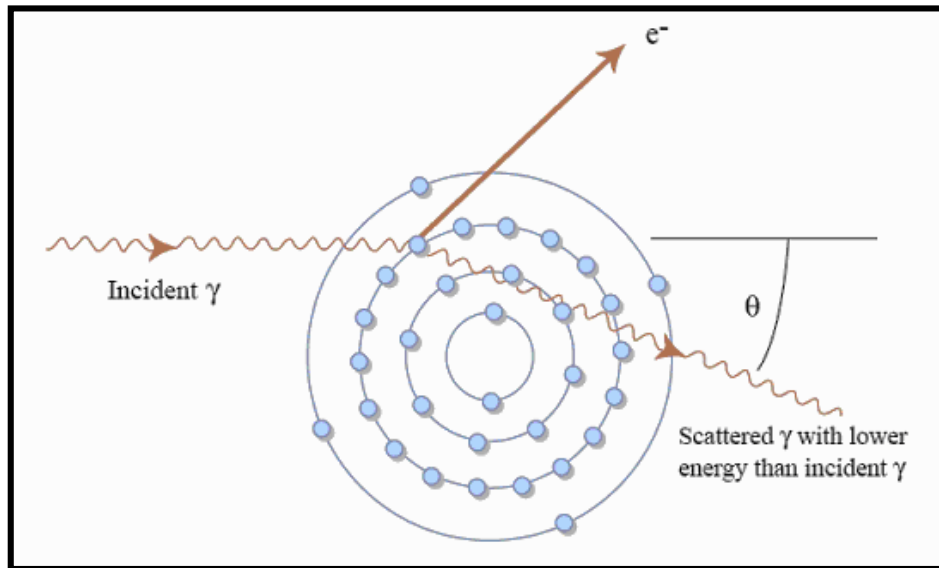


Figure (2-2): Compton Scattering[66].

2.2.3 Pair Production

The third significant photon interaction process in the matter is pair production. Because of the strong electric field at this stage[67]. This process happens close to the nuclei of the absorbing material. As shown in Figure (2-3), the incident γ -ray photon disappears and an electron-positron pair formed in its place in this process requires the energy of $(2m \cdot c^2)$ to create an electron-positron pair and therefore minimum γ -ray energy of (1.022 MeV) is required for any incident photon to undergo this process. Any excess energy above this value is transferred into kinetic energy which is shared by the electron-positron pair. The total kinetic energy of the electron-positron pair will then be[67]:

$$E_{e^-} + E_{e^+} = h\nu - 2m \cdot c^2 \dots\dots (2.3)$$

Usually, the electron and positron move a few millimeters in the substance until they lose their energy in the medium of the absorption. A positron can be combine of with another electron from the absorption medium when the positron is slowed down due to collisions, and this leads to the annihilation of both particles that are replaced by two photons, each of energy $m_e c^2$ (i.e.,0.511MeV) which are emitted back-to-back to achieve law of conserve linear momentum[67]:

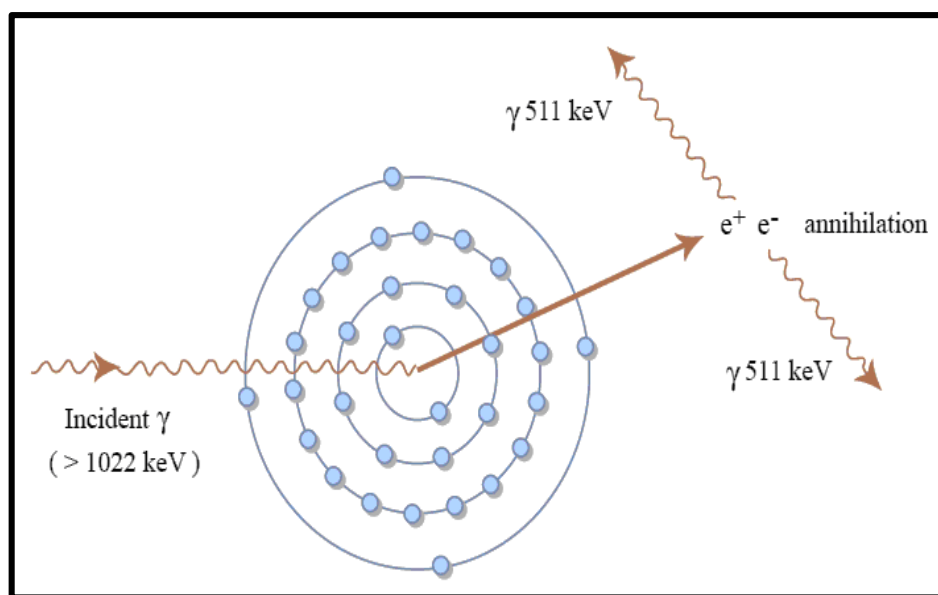
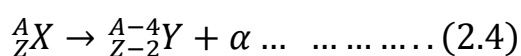


Figure (2-3): Pair Production [67].

2.3 Interactions of Alpha with Matter

The nuclides with atomic numbers greater than (82) have an unstable structure of protons and neutrons, therefore an alpha decay process occurs in these nuclides. An alpha particle consisting of (2) protons and (2) neutrons. The general atomic equation for alpha decay is[18]:



Alpha particles have a double positive charge due to the protons present. This allows ionization within a specific substance (solid, liquid, or gaseous) by forming an ion pair. Due to Columbus's attraction between a traversing the alpha particle and atomic electrons, they give it additional mass, making it easier to ionize. Electrostatic attraction between positive and negative positive and negative particles with orbital electrons leads to ionization and excitation events. When a positively charged alpha particle moves through the material, it attracts many orbital electrons that leave the heel of ionic pairs. Ion pairs are produced by this process until their kinetic energy is completely dissipated within the materials that pass through them. When the speed slows down enough, the alpha particle picks up electrons to produce helium atom. The ionizing effect of the alpha particle is very high and that because of its strong positive charge and mass and relatively low speed so it interacts with a large number of medium atoms. That is, they create multiple pairs of ions in a very short path. The alpha particles lose all of its energy in very short distance. The range in the air is only several centimeters. Since the range of alpha particles in matter is finite, it does not pose any danger to the external radiation of humans. Many alpha particles cannot penetrate the protective layer of the skin. However, alpha emitters pose an internal danger[18].

2.4 Radioactive Equilibrium

Decay series occur when all radionuclides decompose, at an equivalent rate in equilibrium. There are three differing types of balance: secular equilibrium, transient equilibrium, and no equilibrium depending on the relationship between the decomposition constant of the mother and daughter nucleus [68]:

2.4.1 Secular Equilibrium

A (secular equilibrium) usually occurs when the radionuclide has a much "longer" half-life than any other radionuclide in the series ($A_P = A_D$) daughter activity is equal to parent activity shown in Figure(2-4) [69].

$$\lambda_D \gg \lambda_P \quad \text{or} \quad (t_{D\ 1/2} \ll t_{P\ 1/2}) \quad \dots \dots (2.5)$$

$$\frac{A_D}{A_P} = 1 \quad \dots \dots (2.6)$$

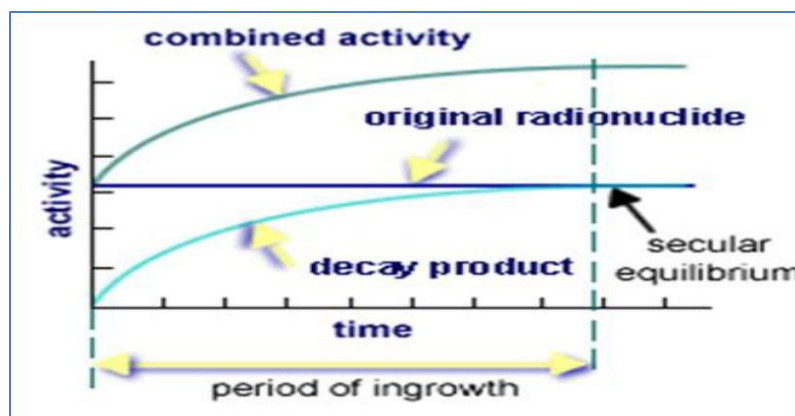


Figure (2-4): Secular Equilibrium[69].

2.4.2: Transient Equilibrium

When (half-life) of the parent the radionuclides is longer than the daughter's half-life, Transient Equilibrium occurs[70]. Shown in Figure (2-5). The daughter's activity will increase until the activity of the parents exceeds, then the daughter will dissolve in the half-life if the parents has the same half-life. The daughter's activity is ($A_2 = \lambda_2 N_2$) and accumulates steadily[71]. Over time, ($e^{-\lambda_2 t}$) became negligible with respect to ($e^{-\lambda_1 t}$) then we will get

$$A_2 = \frac{\lambda_1 \lambda_2 N_1 e^{(-\lambda_1 t)}}{\lambda_2 - \lambda_1} \quad \dots \dots (2.7)$$

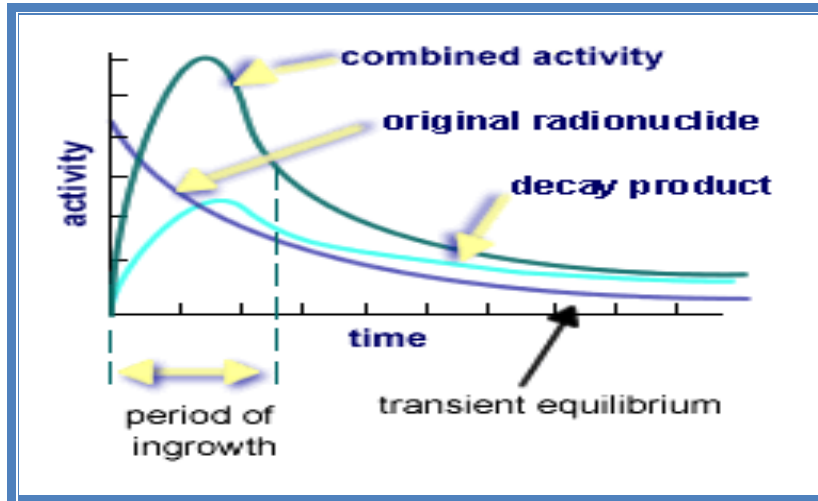


Figure (2-5): Transitional Equilibrium[71].

2.4.3 No Equilibrium

If the half-life of the parent is less than the half-life of the daughter. No equilibrium occurs [70, 72]. The daughter's activity will increase and decrease, Parent activity decreases shown in Figure (2-6)

$$(t_{1/2})^1 < (t_{1/2})^2 \quad \dots \quad (2.8)$$

$$\text{or } \lambda^1 > \lambda^2$$

$$\lambda_P > \lambda_D \quad \dots \dots \dots (2.9)$$

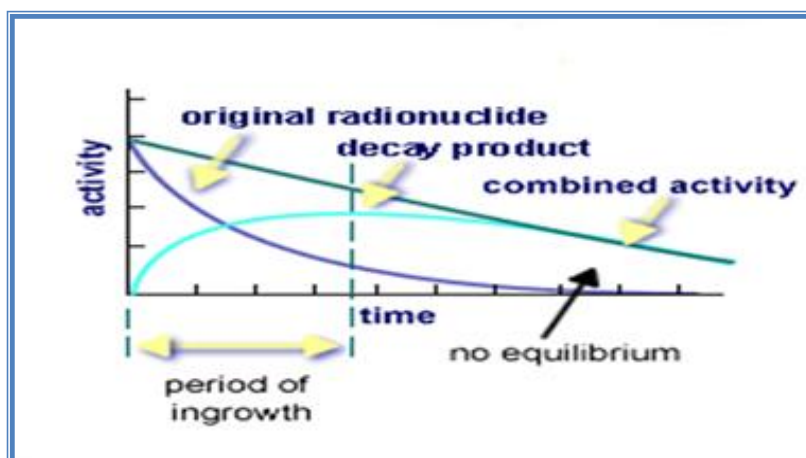


Figure (2-6) : No Equilibrium[72].

2.5 Health Risk of Gamma-Ray and Alpha-particle

Radon is more likely to develop cancer of the lung in people who have smoked in the past than non-smokers throughout their lives. However, it is the leading cause of lung cancer among people who have never smoked. The Environmental Protection Agency calculates that radon is mainly responsible for the death of a person (1,000) with lung cancer annually. In the risk analysis study, 413 women and 235 were evaluated. A man with lung cancer, as long exposure to radon increases the risk of infection [73]. When molecules in a living cell interact with radiant energy through precipitation or exposure, the biological effects of ionizing radiation begin. When ionizing radiation causes excitation, in the same molecule, the direct effect occurs, as it is deposited and absorbed directly affects the (DNA) molecules by primary radiation, direct ionization in the target tissues of atoms in the (DNA) molecules by Compton reactions and the photoelectric effect is the result of energy absorption. this energy is sufficient to expel electrons from the molecule, bonds that can break one or both of the (DNA) strands will be broken[73]. When the ionizing radiation is absorbed into the water molecule in the human body, indirect effects occur and produce short-lived chemical reaction products that interact with other molecules at other locations in the body[74, 75]. Radiation is harmful to organic matter and one must take into account the ingredients of lunch. In the human body, up to 61% is composed of water. The components of the metabolism They are proteins, fats, nucleic acids, and enzymes. Regarding the internal arrangement of the body, (Human body) contains weight is about 10% H and 18% C, 3% N, 65 % O, 1.5% Ca and 1% P, and other components that contribute less than (1%)[73].

2.6 Gamma Spectroscopy

The gamma-ray detection method is based on the interaction of gamma-ray photons with the detector. Each (major) type of gamma-ray interaction can occur within the volume of the detector, but the most common types that take an important role in photon detection are the photoelectric effect and Compton dispersion. For these reactions, the primary and/or secondary gamma ray photons are dispersed. For these interactions, the main gamma-ray photons and/or the secondary scattered photon interfere with the detector atoms and produce fast electrons within the detector volume that are energy-proportional to the primary photon [76]. These fast electrons will then produce secondary electrons as they pass through the volume of the detector. These secondary electrons can be collected as generators. These secondary electrons can be collected to generate electrical pulses. The charges can be converted via a preamplifier to a voltage, the size of which is proportional to the original gamma -ray energy deposited in the detector.

Scintillation devices consist of a crystal and a photomultiplier tube(PMT) which converts light into an electrical signal. The scintillation counter can be divided in to two stages;

(1) Absorption of radiation energy caused by the scintillation then the assembly of photons within the visible part of the electromagnetic spectrum.

(2) The photomultiplier tube amplifies the electrons and produces the output pulse. The most commonly used spectral gamma-ray detector is NaI(Tl), because it is cheap and readily available. It can be larger than room temperature and does not require any cooling system to work[77]. A change of the radiant energy in the electric pulse is the principle of

operation for NaI(Tl) detectors. It consists of two parts, a photomultiplier tube (PMT) and a scintillation crystal. The structure of the NaI(Tl) detector is shown in the Figure (2-7) [78].

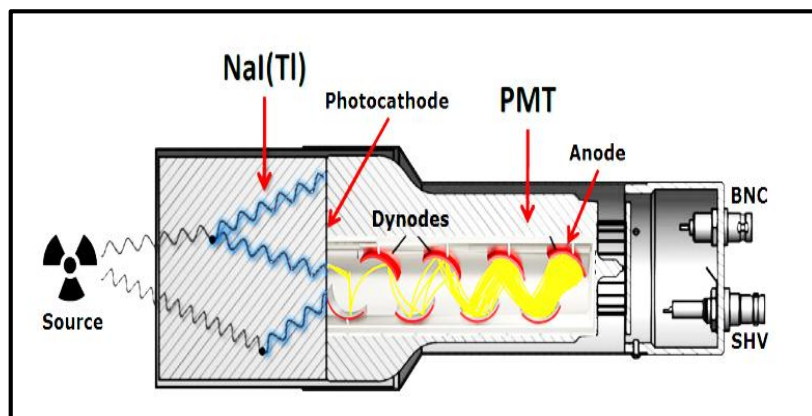


Figure (2-7): Schematic picture of NaI(Tl) detector[77].

2.7 Solid state Nuclear Track

Solid-state nuclear track as well is known as drilled path detectors, it is mostly used for long radon monitoring periods, SSNTD is a small piece of plastic or film inside a container the principle of these detectors is their ability to detect and record charged particles. Heavy charged particles will cause a wide range of ionizing materials when they pass through an intermediate. The passage of heavy ionizing nuclear particles through most of the solid materials creates a barrier of narrow paths (damaged tracks) these "pathways" are often detected at the top of the measurement period, the detectors are placed during a caustic solution that accentuates the damaged paths in order that they will be counted using an automatic counting system. The number of paths per unit area associated with the radon concentration within the air. There are many types of these reagents, while inorganic reagents such as mica and glass. The other (organic) plastic detectors include (CR-39, CN-85, LR-115, Lexan, Makrofol), the solid-state nuclear track contains (SSNTD) is sensitive to alpha the particles are

in the energy range of the emitted particles from radon cross-sensitivity of the thoron can be avoided with diffusion, a room with significant spread resistance to the gas entering the room, and are largely insensitive to gamma and beta rays [79].

2.7.1 Properties of SSNTDS

There are several advantages of SSNTDS which are described below:

1. They are powerful and easy to use, so they can be used at the highest level, cosmic ray spectroscopy
2. They have the best charging and energy decisions
3. Sources that give very high efficiency and sensitivity. Reagents can be placed in direct connection with the fission part
4. They are passive detectors, unlike devices, and do not require power supplies while using
5. SSNTD has different sensitivities, sensitive to alpha particles in the particle energy rang radon emits
6. These detectors have geometrical the flexibility that makes it suitable for angular measurements.
7. Heavy charged particle (such as fission fragments) can be distinguished from lighter charged particles e.g. alpha particles[79].
8. Detailed information is available for these reagents such as size and shapes these tracks the mass and the charge, the motion direction of the projected particle
9. SSNTDs are visually transparent, homogeneous and corrosive

2.7.2 CN-85 Track Detector

The CN-85 consists of a plate with a thickness of (12 μ m) of cellulose nitrate capable of recording the paths of the ionized particles. These films are covered with lithium borate scattered in a water-soluble coating and widely used to obtain the neutron radiation images by the interaction of neutron and alpha particles. It is a French company (Kodak-Path producing various types of cellulose nitrate films for use as track detectors, the CN-85 solid polymer nuclear detector "SSNTDs" the chemical formula for CN-85 is (C₆H₈O₉N₂) as shown in Figure (2-8). It is very sensitive to the active alpha particles because it causes great damage to damage as it passes. It is widely used to detect alpha particles that range from (0.5-8) MeV to detect and measure radon levels from the soil and uranium (CN-85) films are made to convert each pathway by the ionizing particle to hole in sensitive cellulose nitrate layer. Scanning pathways under a microscope is facilitated by large nodes between perforation and background. The best case for (CN-85) is drilling in sodium hydroxide concentrations of (2.5N), for (90) minutes at a temperature of (60° C). Possibly scanning for detection using an optical microscope or spark counter, (CN-85) is the most efficient detector. This behavior is related to the different detection properties of the tested detector[80].

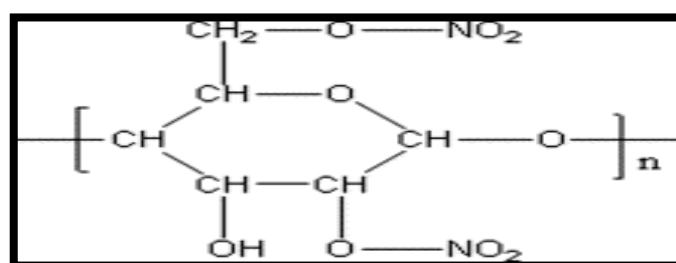


Figure (2-8) Chemical formula of CN-85 (C₆H₈O₉N₂)[80].

2.8 Models of Track Formation

2.8.1 Thermal Spike Model

The energy loss mechanism of the (projectile-ion) leads to electronic and atomic collision cascades the atomic collision-cascade deposits its energy in the close vicinity of the ion trajectory while the electronic (collision-cascade) has a long-range so its thermal effects may be neglected. The thermal spike version simplifies the complicated outcomes of the atomic collision collection through supposing a simple thermal distribution. In step with the thermal spike model the stored power corresponds to an abrupt temperature upward thrust, in a small cylindrical extent around the ion trajectory on the time of passage $t=zero$ after the passage of the ion i.e. for ($t > zero$); the thermal strength diffuses far away from the ion trajectory, the thermal spike produces defect by thermal activation which are remaining as frozen defects along the ion trajectory due to rapid quenching of the temperature. If α - particle deposits energy(Q) per unit (length) at the time ($t =zero$); then the temperature (T) as a function of (t) and of radial distance (r) from the axis of the ion course is given by[81]:

$$T(r, t) = \frac{Q}{4c\rho\pi Dt} \exp\left(-\frac{r^2}{4Dt}\right) + T_0 \quad \dots\dots\dots (2.10)$$

Where (T_0) is the initial temperature of the lattice, (c) is the capacity of the medium, (ρ) is its density, and (D) is the thermal diffusivity. If it's far assumed that a high temperature is maintained (many thousands of degrees Kelvin) for a short time via an incident fission fragment; processes which include (melting and recrystallization) could occur and as a consequence point defects (e.g., vacancies and interstitials) would be quite possibly. For all this to manifest; conductivity within the fabric need to be low [82]. This

explains the incapacity of metals to provide tracks as the thermal spike turns into large and diffuses in the steel lattice, where in as in insulators, a narrow, extreme spike is produced. this leads to enough localized radiation harm able to generating an etch capable track[83].

2.8.2 Ion-Explosion Spike Model

The mechanism for the latent track, track formation based on the ion explosion spike model is depicted shown in Figure (2-9) suggest by Fleischer et al., 1975[84]. According to this model, the high concentration of ions positive along its path is resulted from a charged particle passing through an insulator and its interaction to coulomb potential. That time of recombination is long relative to the time of vibration. Positive ions will repel each other, ions pushing interstitial ions and leaving behind a vacancy-rich cylindrical center. This is a cylinder with a radius of 2-4 nm and a few (mm) long shaped, which can be seen under a microscope transmission electron [85, 86]. If it is enlarged chemically then the tracks etched can be seen under an optical microscope. According to this model, requirements for track formation are that:

- (a) the electrostatic stress (i.e. the coulomb repulsive forces within the ionized region), should be greater than the mechanical strength, or lattice-bonding forces; which implies that materials of low mechanical strength or low dielectric constant are more likely to store etchable tracks.
- (b) The maximum permissible density of free electrons must be low. This condition restricts track formation to good insulators and excludes metals.
- (c) At present, this model is the most commonly known in the field of tracks; however, it is very likely that any combination of the models might

provide a more detailed image of the actual process by which solids shape nuclear tracks. In materials with high holes' mobility, tracks will not be formed; the explanation is that the core atoms will be neutralized by a fast external diffusion of holes; this in turn will prevent track formation. So semiconductors like (silicon and germanium) with high overall mobility; do not record tracks[87].

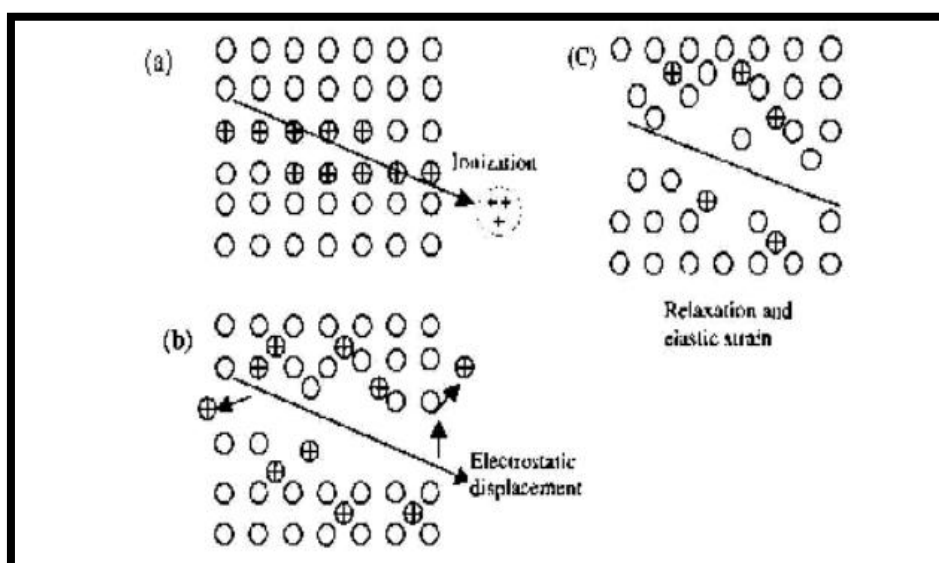


Figure (2-9): The ion explosion spike phase for inorganic solid track formation: The initial ionization produced by the passage of the charged particle (a) is unstable and throws in strong ions producing Vacancies and interstitials (b) The stressed area later relaxed elastically (c) Straining the matrix undamaged [87].

2.9 Chemical Etching

Ionizing particles that pass through polymeric path reagents (passive paths) which are pathways of radioactive damage the best way to monitor pathways is by drilling an (SSNTD), substance with a chemical solution. Which preferably attacks damaged materials and increases the size of the original pathway to the size that can be seen in optical microscopy[88]. Chemical drilling of plastic reagents is usually performed in a thermally controlled bath (maintained constant $\sim \sim 0.1^\circ\text{C}$). For plastic the most widely used block is the aqueous solution of (NaOH). At concentrations (2.5N) and at temperature usually used ($70 \pm 0.1^\circ\text{C}$). Usually a large glass is placed in the etching solution inside the temperature controlled bathroom. In a suspension with a cap covering the highest of the beaker to scale back evaporation and therefore the resulting increase within the solute concentration of the answer..... Etc. (NaOH) solution was used with normal position (2.5) of the etching process, the normal value is calculated using the following formula [89]:

$$W = W_{\text{eq}} \times N \times V \quad \dots\dots\dots (2.11)$$

W: is the weight of (NaOH)

W_{eq} : is the equivalent weight of (NaOH)

N, is the normality = 2.5N

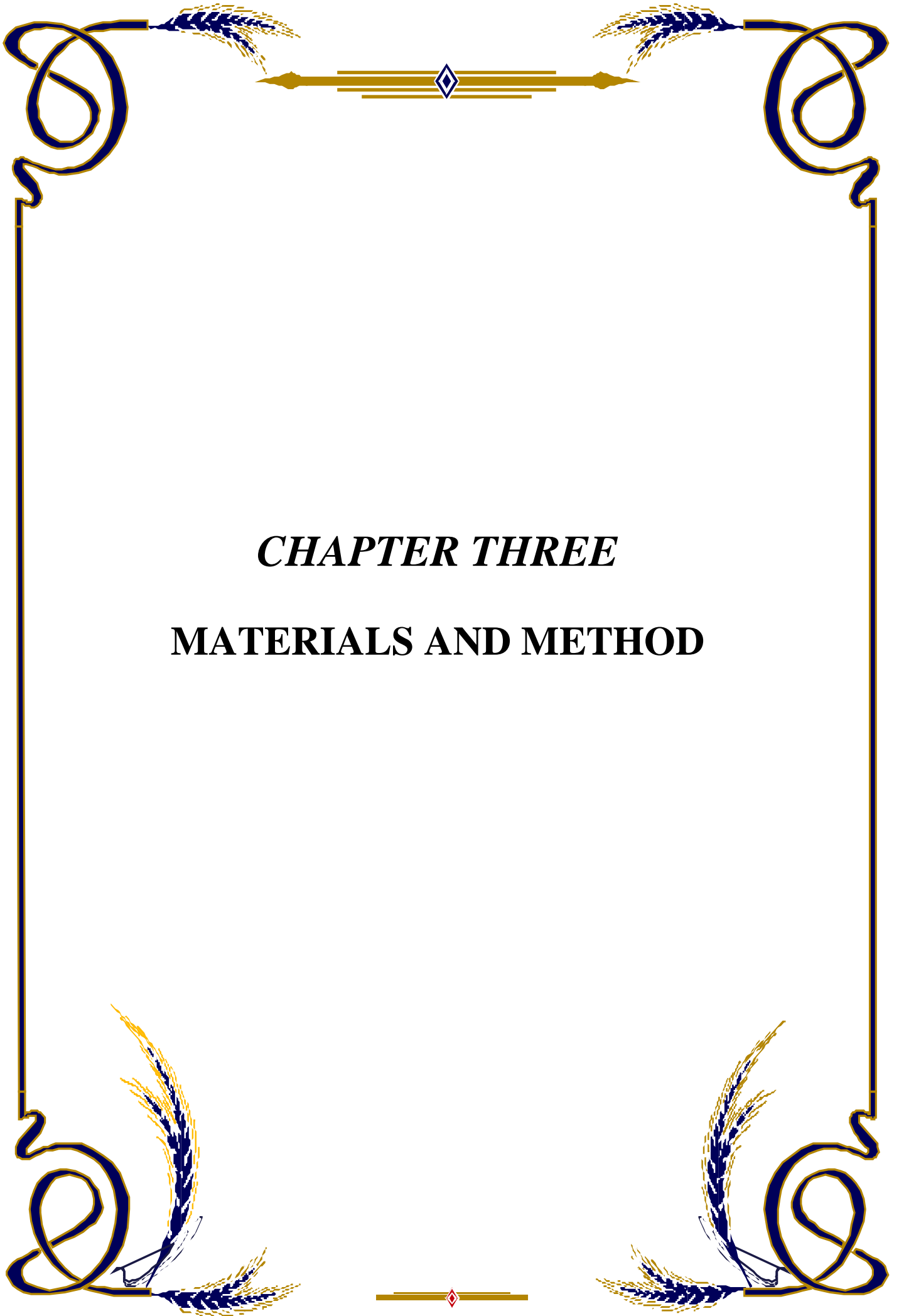
V, is the volume of distilled water.

In the current study and based on the equation, (2.11) has been the use of (15gm) from (NaOH) and (150) ml of distilled water for the purpose, of chemical etching.

2.10 Track Formation Mechanism

When a strongly charged nuclear particle passes through an insulating solid. It transfers a part or group of its energy to the electrons of the medium in a linear fashion energy loss rate (dE / dx), which is a function of particle properties such as (mass, the charge, energy), and reagents used. Causes physical, chemical, and other properties the solid matter along and around the path of the particle change and the path is narrow serious damage is created. This radiative damage may consist of broken links displacement atoms, electronic and ionic defects, voids, defects, etc. This narrow path is known as the "latent path." When the energy loss is greater than the critical value (dE / dx) m Joule per meter, it is called (Threshold Recording), without which paths do not consist of solids and are specific to the reagent used. Then the primary path is formed. The typical diameter is about (1 nm to 10 nm)[86]. Depending on their size, latent paths can only be visualized under very extreme magnification through electron microscopes or other similar tools the etching process is formed to enlarge tracks up to a diameter of few (μm) with the assistance of a focused hot chemical occasion like alkaline materials (such as NaOH or KOH) or acid (for example, HF or HNO₃) [90]. Depending on nature (SSNTD) is used. Based on experimental tests conducted. It has been accessed there are two separate track forming mechanisms, one for inorganic and solid materials glasses and other materials for organic solids or polymers. The first is about measuring effects of electronic radiation on the rates of chemical dissolution of solid and other solids measurement of the radial distribution of biodegradable damage in solids. For inorganic solids and glasses, according to the proposed model, the positively charged particles are multiplied outside the orbital electrons of the atom near its path, thus producing a cylindrical region filled with positive ions. These positive ions

are present when they expel each other, thus disturbing, distorting the natural network in a crystalline solid and producing a more or less cylindrical region[91].



CHAPTER THREE
MATERIALS AND METHOD

CHAPTER THREE

MATERIALS AND METHOD

3.1 Introduction

This part of the project includes important steps (materials and methods), which have been followed to analyze the soil samples of the university of Kerbela, area of study and collection samples, preparation of the samples, systems of measurement NaI(Tl) and CN-85 detector of which are used in this study (as shown in Figure 3-1), and also a theoretical consideration (theoretical equations).

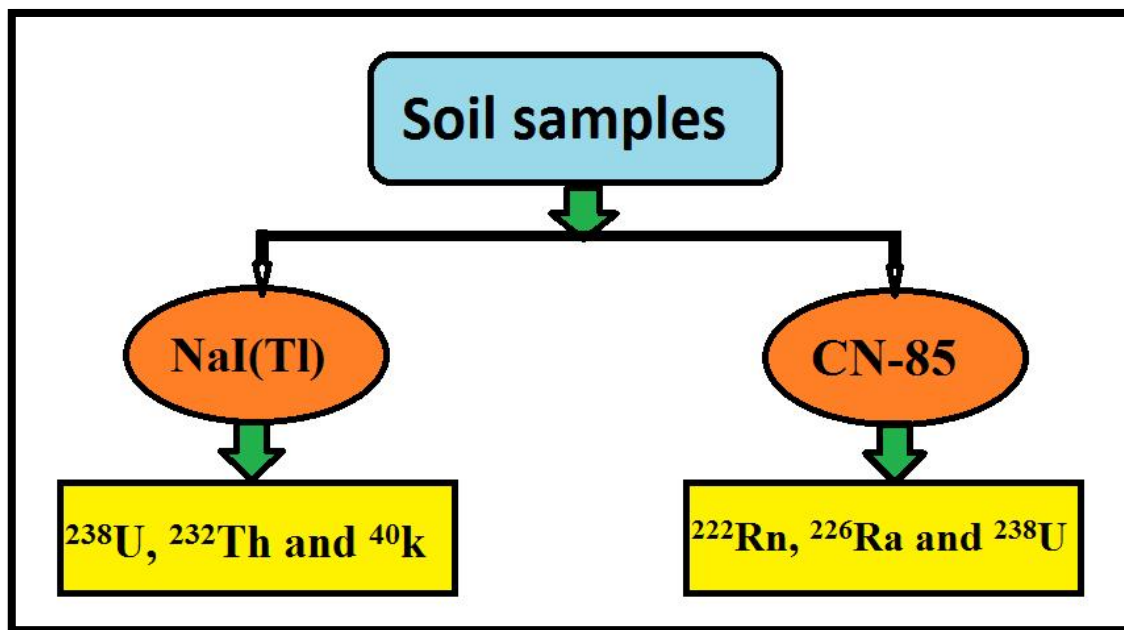


Figure (3-1): A schematic Diagram of the main parts of the Current Study.

3.2 Geological of Karbala Governorate

Karbala Governorate is one among the foremost important Iraq middle cities from its religious point of view. It covers a neighborhood of 5034 km² and features a population that exceeds a million capita [92]. The governorate of Karbala is one of Iraq's smallest governorates and is located in the southwest of the country. Irrigated farmland extends along the euphrates river in the east of Karbala, while the desert plains cover the most western parts of the governorate. A saline lake located to the west of the governorate's capital called Razazah. The aligned governorates to Karbala city are Anbar from the northwest, Najaf from south and Babil from east. It is located between latitude 32N, to latitude 33N, and longitude 43E, to longitude 44E, [93]. The Karbala city contains three provinces which are the center of Karbala, Hindiyah, and Ean-tamer.

3.3 Area of Study

The university of Kerbala was established in the city of Karbala by decision of the Ministry of Higher Education and scientific research No. 15 of 2002. Since then, the university has expanded to become one of the top universities, not only within the country but also in the region. The University of Kerbala is one of the leading institutions in its higher education and knowledge because of its innovative way of academic administration, human resources development, and capacity to excel in research and education on various levels of science, art, humanities, medicine and social sciences. Kerbala university offers an excellent education to Iraqi and foreign students. There are 16 colleges in the university which are the faculty of medicine. College of dentistry, college

of engineering, college of applied medical Sciences, college of Education, faculty of management and economics, faculty of law, college of science, college of agriculture, college of Islamic sciences, college of religious tourism, faculty of human education, college of education for Pure Science, and faculty of nursing. The university of Kerbala is consists of many collages that distribution in three regions such as the Freiha site, Al-Husseineya site, and Al-Mothafeen site.

Firstly, Freiha site is located in a very popular city, Kerbala, which is bounded by $32^{\circ}36'33''$ N north latitudes and $44^{\circ}0'11''$ E east longitude. There are nine colleges law, sciences, Islamic sciences, management, economics, engineering, tourism, education and human sciences, and pure education. The Gypsum soil; It is considered a strong and cohesive soil in the dry state as a result of the presence of gypsum material between its granules, but when the water runs through it or saturated it with rain water will occur sudden collapses as a result of washing gypsum from the soil leaving voids in it for this must be studied the properties of this soil under conditions as close as possible to reality and find a modern way of improving. Secondly, the agriculture colleges in Al-Husseineya site located between $32^{\circ}40'.37''$ N north latitudes and $44^{\circ}09'.98''$ E east longitude. It has consisted of two colleges, agriculture and animal production. The soil was of silt type which was characterized by high fertility rate, in addition to its lightweight and ability to maintain moisture, ease to compact, and washed by rainwater. Adding organic matter to it helped inholding soil formation and structure together and transforming these into more stable ones. Thirdly Al-Mothafeen site is located between $32^{\circ}36'.36''$ N north latitudes and $44^{\circ}00'.1''$ E east longitude. It has consisted

of six colleges, nursing, pharmacy, Dentistry, applied medical sciences, and Medicine, Sports Sciences, physical education. The soil was of Sandy type it contains small particles of rocks and minerals, in this study, the natural radioactivity (^{238}U , ^{232}Th , and ^{40}K) and (^{222}Rn , ^{226}Ra , and ^{238}U) were measured in soil samples that were distributed across residency quarters that are belonging to each of university of Kerbala Figure (3-2) displays the location of Karbala represented by the red area of the Iraq map and a magnified window represents the study area.

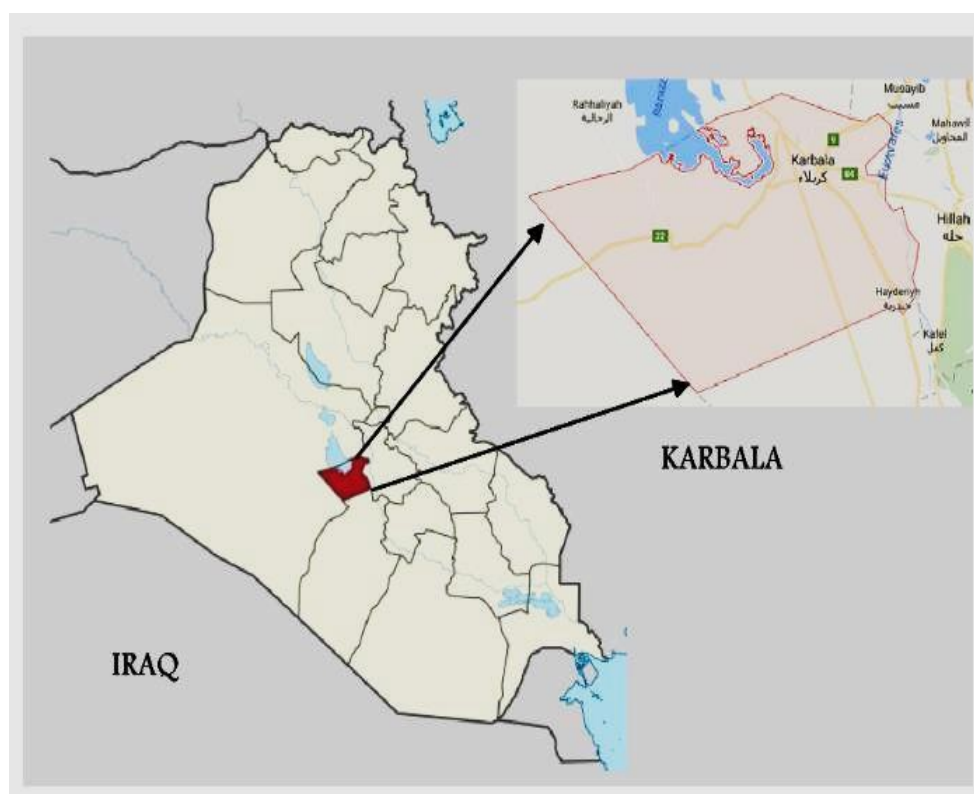


Figure (3-2):A selected window map of Iraq represents Karbala city[93].

3.4 Sample Collection and Preparation

The 100 soil sample from residential (60 in Freiha site, 20 in Al-Husseineya site for agricultural college, and 20 in Al-Mothafeen site) were collected from various sites of the university of Kerbala, Karbala governorate during October and November 2019 at a depth of (10) cm from the soil surface. The samples were located using the Global Positioning System (GPS) shown in Figure (3-3). Tables (3-1), (3-2) and (3-3) show name, code, coordinate for samples of soil in Freiha site, Al-Husseineya site, and Al-Mothafeen site respectively, while Figures (3-4), (3-5) and (3-6) show maps of the area of study that maps using geographic information system (GIS) technical.



Figure (3-3): GPS device

Table (3.1): Location of Freiha site samples

No.	Location name	Sample code	Coordinates	
1	In front of the internal department for female students	U 1	3235'36.17"N	4405'22.17"E
2	Behind the student's internal departments	U 2	3235'33.49"N	4405'25.62"E
3	Near the female student's internal departments	U 3	3235'37.29"N	4405'24.34"E
4	In front of the College of Science	U 4	3235'45.09"N	4405'21.24"E
5	To the right of the college of science	U 5	3235'43.31"N	4405'25.99"E
6	Left of the college of sciences	U 6	3235'52.62"N	4405'27.19"E
7	From behind the college of science	U 7	3235'47.31"N	4405'28.27"E
8	Near the deanship of the college of engineering	U 8	3235'53.78"N	4405'24.07"E
9	In front of the college of engineering deanship	U 9	3235'52.1"N	4405'25.97"E
10	Near the College of pure education	U 10	3235'50.29"N	4405'29.89"E
11	Right the College of pure education	U 11	3235'49.59"N	4405'17.87"E
12	In front of the College of pure education	U 12	3235'53.05"N	4405'18.59"E
13	Near of the College of human education	U 13	32035'51.75"N	4404'21.60"E
14	Behind f the College of human education	U 14	3235'44.50"N	4405'21.60"E
15	In front the College of human education	U 15	3235'53.58"N	4405'22.69"E
16	In front of the central club	U 16	3235'54.58"N	4405'29.74"E
17	Behind the central club	U 17	3235'55.16"N	4405'29.87"E
18	In Front Of The College of engineering	U 18	3235'56.31"N	4405'34.12"E
19	Behind Of The College of engineering	U 19	3235'58.35"N	4405'30.68"E

20	Beside the College of biomedical engineering	U 20	3235'55.98"N	4405'35.27"E
21	In front of the College of biomedical engineering	U 21	3235'56.51"N	4405'35.52"E
22	Near of the College of biomedical engineering	U 22	3235'51.48"N	4405'35.49"E
23	Behind the college of engineering, life medicine	U 23	3235'54.72"N	4405'35.26"E
24	In front of the electrical station	U 24	3235'52.62"N	440545.72"E
25	Right of the power station	U 25	3235'52.95"N	4405'46.62"E
26	Behind the power station	U 26	3235'52.94"N	4405'48.73"E
27	The side of the electrical station	U 27	3235'53.51"N	4405'47.75"E
28	In front of the presidency	U 28	3236'01.38"N	4405'14.61"E
29	Side of the presidency	U 29	3236'01.88"N	4405'16.63"E
30	Behind the presidency	U 30	3236'04.44"N	4405'17.87"E
31	In front of the college of Islamic sciences	U 31	3236'01.74"N	4405'21.72"E
32	Behind of the college of Islamic sciences	U 32	3236'01.92"N	4405'20.14"E
33	Near the College of Islamic Sciences	U 33	3236'03.53"N	4405'20.14"E
34	In front of the college tourism of sciences	U 34	3236'05.83"N	4405'21.82"E
35	Near of the college tourist of sciences	U 35	3236'05.15"N	4405'21.87"E
36	Behind of the college tourist of sciences	U 36	3236'05.22"N	4405'40.18"E
37	In front of the central library	U 37	3236'10.57"N	4405'29.67"E
38	Left of the central library	U 38	3236'13.73"N	4405'27.97"E
39	Behind the central library	U 39	3236'14.64"N	4405'29.43"E
40	Right the central library	U 40	3236'78.87"N	4405'30.14"E

41	Near the College of veterinary medicine	U 41	3236'14.2"N	4405'30.31"E
42	In front of the College of veterinary medicine	U 42	3236'13.0"N	4405'30.51"E
43	Beside the College of veterinary medicine	U 43	3236'12.73"N	4451'34.43"E
44	Behind the College of veterinary medicine	U 44	3236'13.67"N	4405'34.68"E
45	Right of the of university gate	U 45	3236'15.43"N	4405'33.97"E
46	Near of the of university gate	U 46	3236'15.31"N	4405'30.91"E
47	In front of the of university gate	U 47	3236'11.12"N	4405'24.81"E
48	Left of the of the of university gate	U 48	3236'16.45"N	4405'20.61"E
49	In front of the internal departments for students	U 49	3236'08.65"N	4405'14.14"E
50	Behind of the internal sections	U 50	3236'08.51"N	4405'12.72"E
51	right of the internal sections	U 51	3236'14.16"N	4405'11.78"E
52	Left of the internal sections	U 52	3236'07.85"N	4405'12.29"E
53	Near of the College of Administration and Economics	U 53	3236'14.16"N	4405'11.78"E
54	Left of the College of Administration and Economics	U 54	3236'07.85"N	4405'17.17"E
55	Central of the College of Administration and Economics	U 55	3236'07.47"N	4405'19.28"E
56	Right of the College of Administration and Economics	U 56	3236'15.99"N	4405'27.05"E
57	Side of the college of law	U 57	3236'07.83"N	4405'24.49"E
58	Behind of the college of law	U 58	3236'07.37"N	4405'26.44"E
59	Before of the college of law	U 59	3236'04.66"N	4405'24.06"E
60	Right of the college of law	U 60	3236'03.49"N	4405'27.54"E

Table (3.2): Location sample for Agricultural College.

No.	Location name	Sample code	Coordinates	
61	In Front of plant protection department	U 61	324033.37"N	4409'51.95"E
62	Near of plant protection department	U 62	3240'32°.83"N	4409'59.03"E
63	Behind of plant protection department	U 63	3240'38.18"N	4409'52.8"E
64	Behind the College of garden engineering and horticulture	U 64	3240'33.79"N	4409'53.6"E
65	In front of the College of horticulture engineering	U 65	3240'33.23"N	4409'52.57"E
66	Near of the College of horticulture engineering	U 66	3240'34.31"N	4409'52.66"E
67	Side of the College of horticulture engineering	U 67	3240'32.49"N	4409'52.26"E
68	Central College	U 68	3240'30.58"N	4409'52.25"E
69	In front of the field crops section	U 69	3240'30.52"N	4409'51.57"E
70	Besides of the field crops	U 70	3240'32.36"N	4409'49.83"E
71	Behind of the field crops	U 71	3240'29.29"N	4409'49.92"E
72	Beside the College of animal Production	U 72	3240'29.72"N	4409'51.38"E
73	In front of the College of animal production	U 73	3240'24.65"N	4409'51.93"E
74	Behind of the College of animal production	U 74	3240'28.95"N	4409'51.45"E
75	Left of the College of animal production	U 75	3240'29.75"N	4409'52.66"E
76	Amid a field of agricultural crops	U 76	3240'30.43"N	4409'54.55"E
77	In front of the faculty of agriculture gate	U 77	3240'31.06"N	44o9'53.31"E
78	Left of the faculty of agriculture gate	U 78	3240'32.33"N	4409'50.91"E
79	Right of the faculty of agriculture gate	U 79	3240'32.92"N	4409'49.6 "E
80	Near of the faculty of agriculture gate	U 80	3240'31.7"N	4409'50.98"E

Table (3.3): Location in Al-Mothafeen Site samples

No.	Location name	Sample code	Coordinates	
81	In front of the faculty of physical education	U 81	3236'31.36"N	4400'05.58"E
82	Near the faculty of physical education	U 82	3236'32.95"N	4400'06.04"E
83	In front of the Deanship of the college of pharmacy	U 83	3236'33.25"N	4400'07.16"E
84	In front of the college of pharmacy	U 84	3236'33.85"N	4400'15.42"E
85	Near the college of engineering	U 85	3236'31.16N	4400'03.9"E
86	In front of the college of engineering	U 86	3236'29.25"N	4400'04.75"E
87	Deanship of the college of engineering	U 87	3236'29.94"N	4400'04.7"E
88	Behind of the college of engineering	U 88	3236'27.51"N	4400'30.57"E
89	In front of the faculty of applied sciences	U 89	3236'33.65"N	4400'08.93"E
90	Behind the faculty of applied sciences	U 90	3236'35.63"N	4400'09.28"E
91	Near the faculty of applied sciences	U 91	3236'35.63"N	4400'09.28"E
92	Near the college of Nursing	U 92	3236'33.43"N	4400'12.83"E
93	In front of the college of Dentistry	U 93	3236'33.43"N	4400'11.94"E
94	Behind of the college of Dentistry	U 94	3236'32.69"N	4400'10.35"E
95	Near of the college of Dentistry	U 95	3236'37.23"N	4400'10.3"E
96	In front of the faculty of medicine	U 96	3236'35.2"N	4400'15.33"E
97	Near of the faculty of medicine	U 97	3236'35.07"N	4400'14.87"E
98	Behind of the faculty of medicine	U 98	3236'36.83"N	44 00'13.39"E
90	Near of the faculty of medicine gate	U 99	3236'34.68"N	4400'15.17"E
100	In front of the faculty of medicine gate	U 100	3236'33.67"N	4400'15.1"E

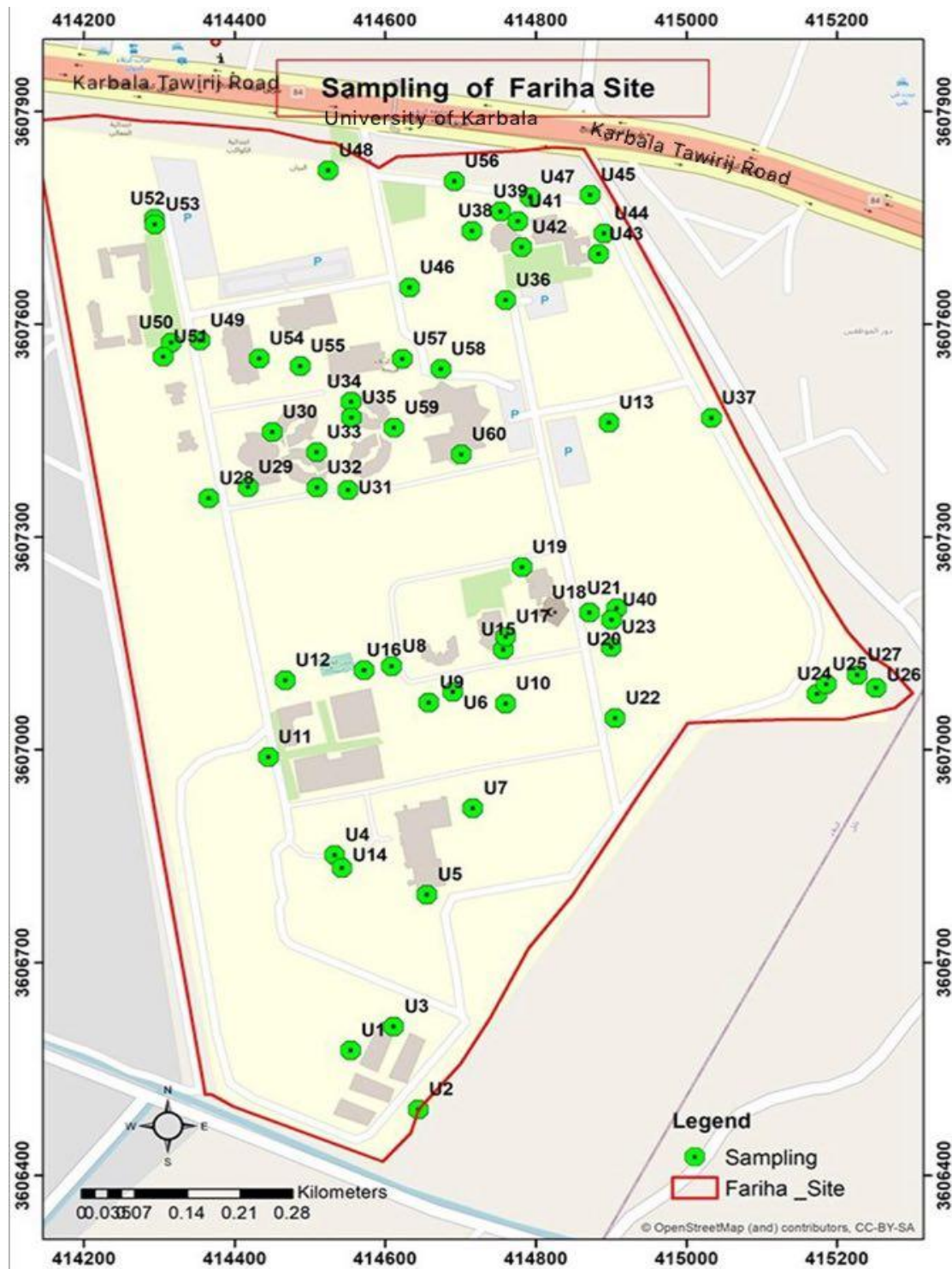


Figure (3-4): Map of location sample for Fariha site

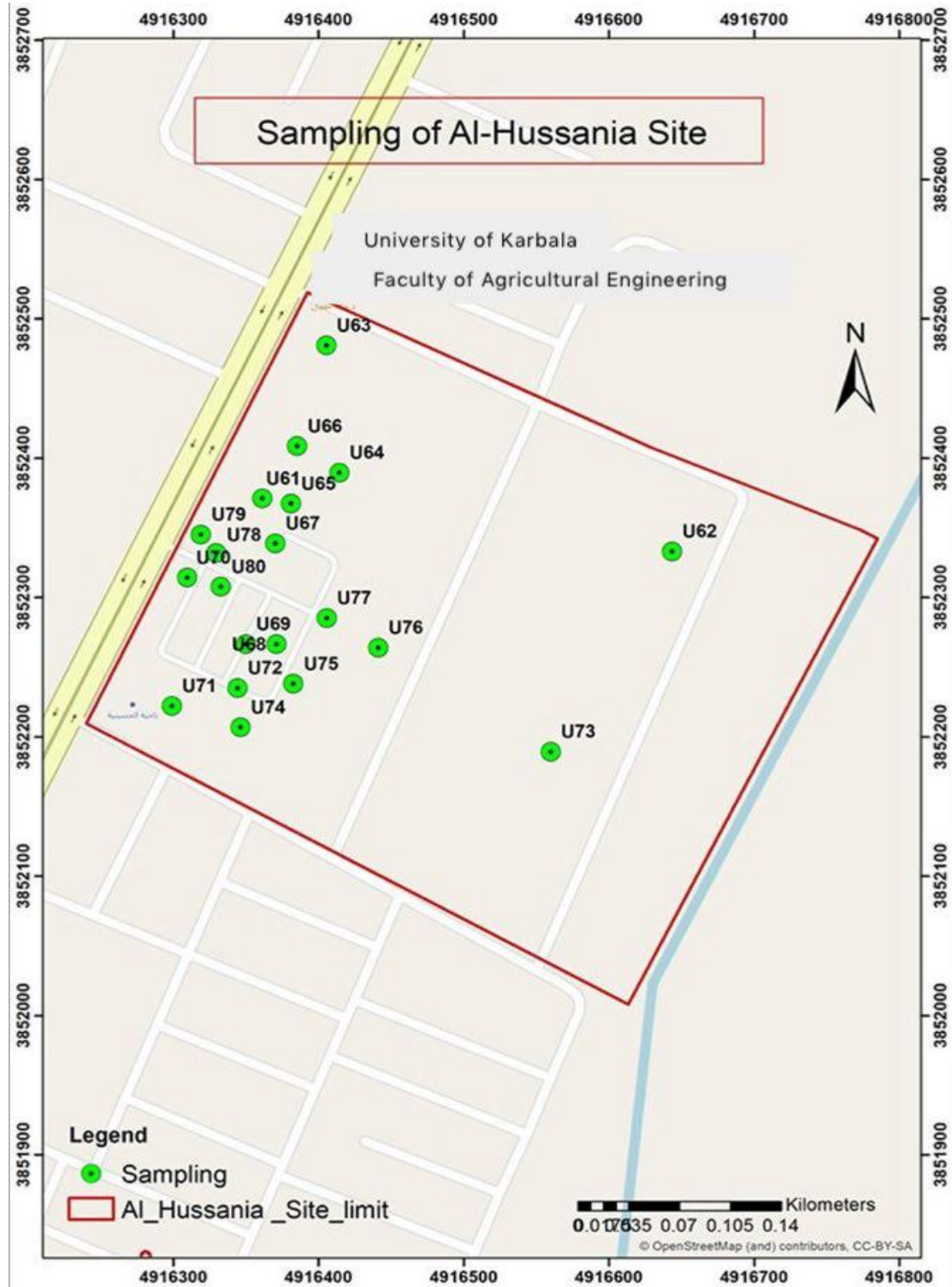


Figure (3-5): Map of location sample for Agricultural college in Al-Husseineya Site

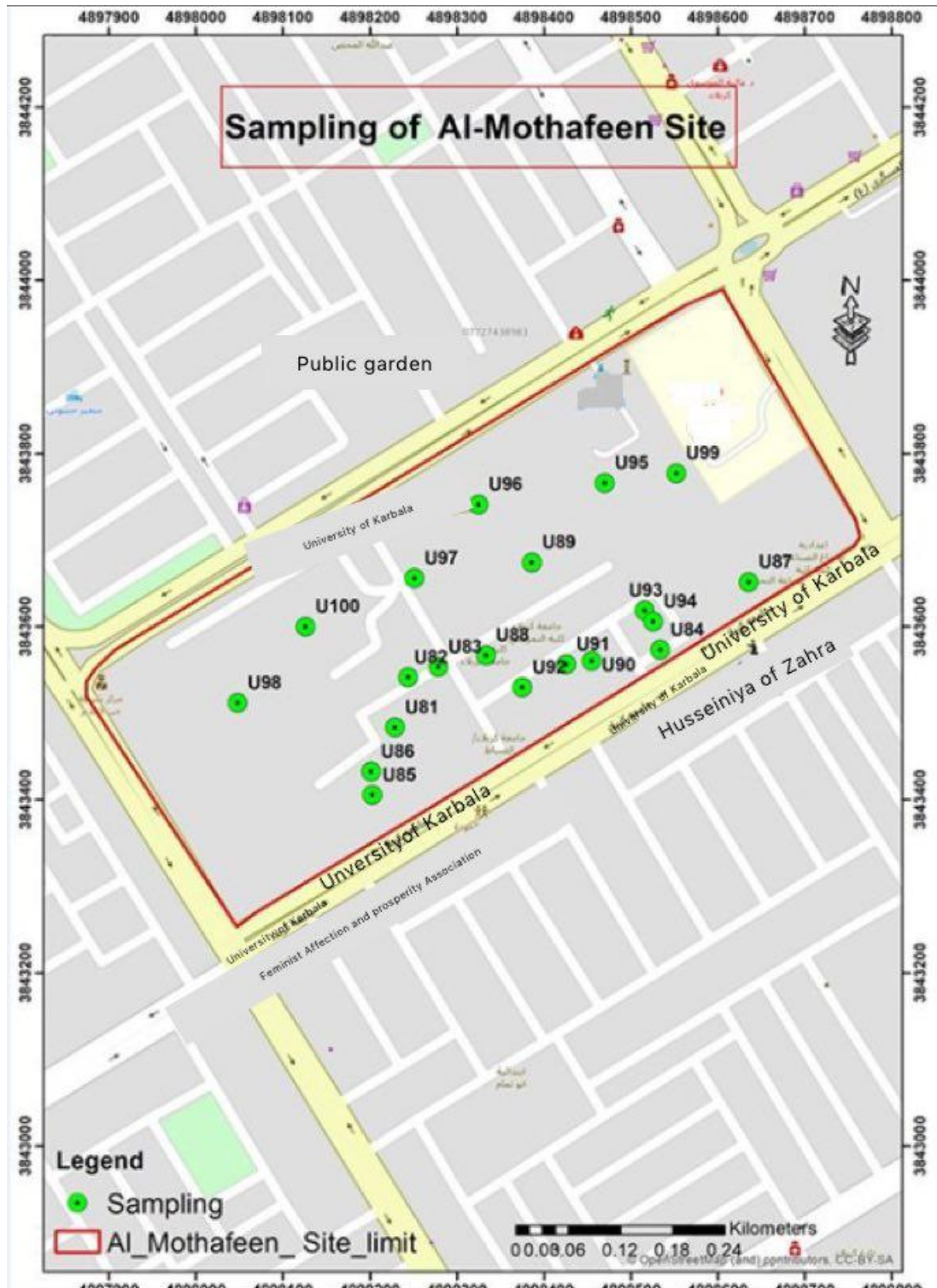


Figure (3-6): Map of location sample for Al-Mothafeen site

After collecting soil samples, they are placed in a plastic bag and marked with the sample code and symbol. Samples transfer to the laboratory of nuclear physics in the department of physics, College of Science, Kerbala university. Soil samples were cleaned, dried, and kept free from moisture before measuring in an oven for 60 minutes at a temperature of 120⁰C (shown in Figure (3-7)) in order to reach a stable weight and avoid any absorption of moisture.



Figure (3-7): Oven used in this study.

The samples were crushed using an electric grinder in Figure (3-8) to reach suitable homogeneity (the loss ratio of samples when are sieved that it is very small according to a mass of fresh samples).



Figure (3-8): Electric mill.

The samples were sieved by sieve that 0.8-mm-pore-size as Figure (3-9) to get rid of gravel and suspended plant wall and obtain homogeneous and microscopic particles that may affect the measurement process.



Figure (3-9): Sieve used in this study

Next, the sample weights were then measured using a highly sensitive digital weighing (see Figure (3-10)) that scale of $\pm 0.06\%$.



Figure (3-10): Balance used in this study.

Then the samples were filled in plastic Marinelli cups with a capacity of (1) liters to measure gamma emitters and a plastic cups with capacity (0.13) litter to measure alpha emitters. Finally, two cups were stored for about a four week before measuring to allow, a Secular equilibrium between ^{226}Ra and ^{222}Rn [30].

3.5 Systems of Measurement Used in This Study

There are two techniques used in this study, the gamma-ray spectroscopy system with scintillation detector NaI(Tl) of (3"×3") crystal dimension and solid-state nuclear track detectors (CN-85) technique, as follows:

3.5.1 NaI(Tl) System Spectroscopy

A gamma-ray spectrometer (NaI(Tl)), as shown in Figure(3-11), was used to measure the Radioactivity of the soil, which was made by (ORTEC) that consists of detector NaI(Tl) (3 "× 3") and provide multi-channel analyzer (MCA) (ORTEC-Digi Base) that contains a 1024 channel connecting the unit called ADC (Analog to Digital Converter) which helps an analyst to convert pulse next to the numbers of digital numbers and that nuclear measurements and the analyses are carried out by a computer program called MAESTRO[67]. The detection system consists of the many device, such (NaI (Tl)) detector, high voltage, preamplifier, amplifier, MCA, computer and shielding in Figure (3-12).

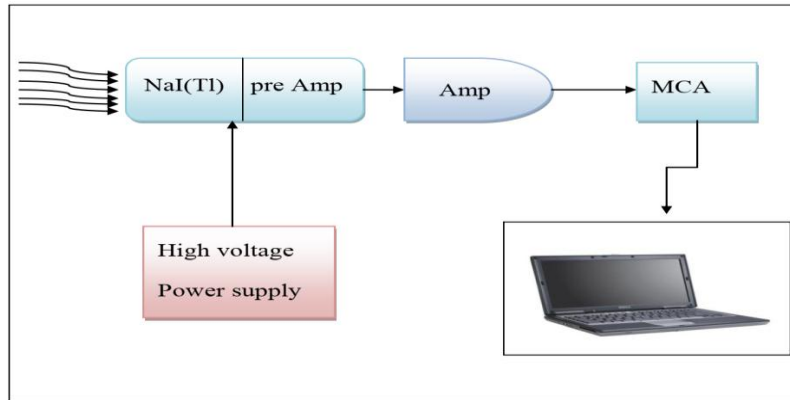


Figure (3-11): Sketch of the equipment set up of NaI(Tl) detector[67].

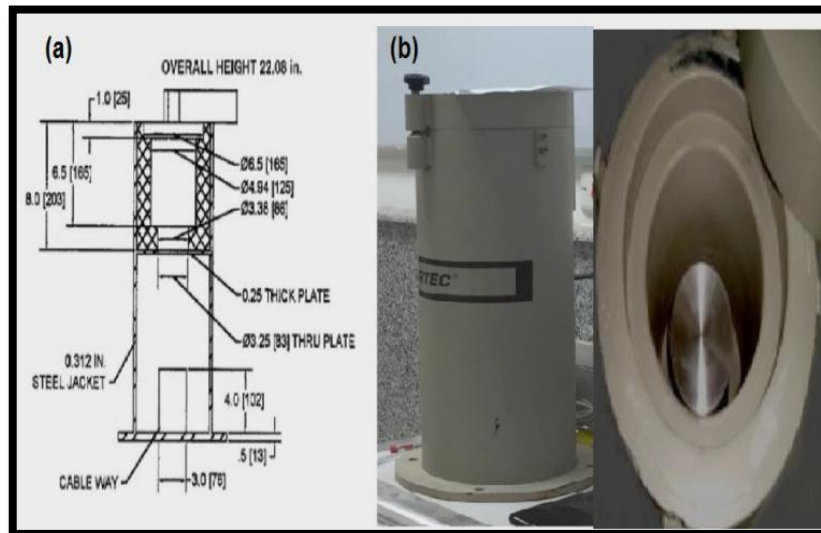


Figure (3-12): Shielding, (a) Schematic diagram of the shielding chamber and (b) Photograph of the shielding chamber with detector position[67].

3.5.2 Preparation of the NaI(Tl) detector

3.5.2.a Energy Calibration: The energy calibration is the relationship between the number of channels and the energy absorbed in the detector [89]. The energy calibration of the NaI(Tl) spectroscopy system is established by measuring the position of selected full-energy gamma-ray peaks with large peak-height to background ratios, and whose energies are known precisely[94]. An energy calibration for this detector is performed with a set of standard γ -ray sources (^{137}Cs , ^{60}Co , ^{22}Na , ^{54}Mn , and ^{152}Eu) from USNRC and State License Expert Quantities, "Gamma Source Set", Model RSS-8, as shown in Table (3.4). The energy calibration curve is shown in Figure (3-13)

Table(3.4): Properties of Radioactive Sources used in the Present Study with Compare Experimental (I_γ)[95, 96].

Isotopes	Activity (μCi)	Energy (keV)	Serial number	Production date	I_γ %
^{137}Cs	1	661.66	IRS-126	1/1/2009	85.21
^{60}Co	1	1173.24	IRS-141	1/1/2009	99.9
		1332.5			99.88
		2505.74			20
^{22}Na	1	511	IRS-139	1/2/2009	181
		1274			99.95
^{54}Mn	1	834	IRS-128	1/1/2009	100
^{152}Eu	0.9	1407	IRS-149	1/11/2009	24
		1112			16.4
		1085.8			10
		964			17.3
		778.9			15.2
		344.3			31.4
		121.8			33.2

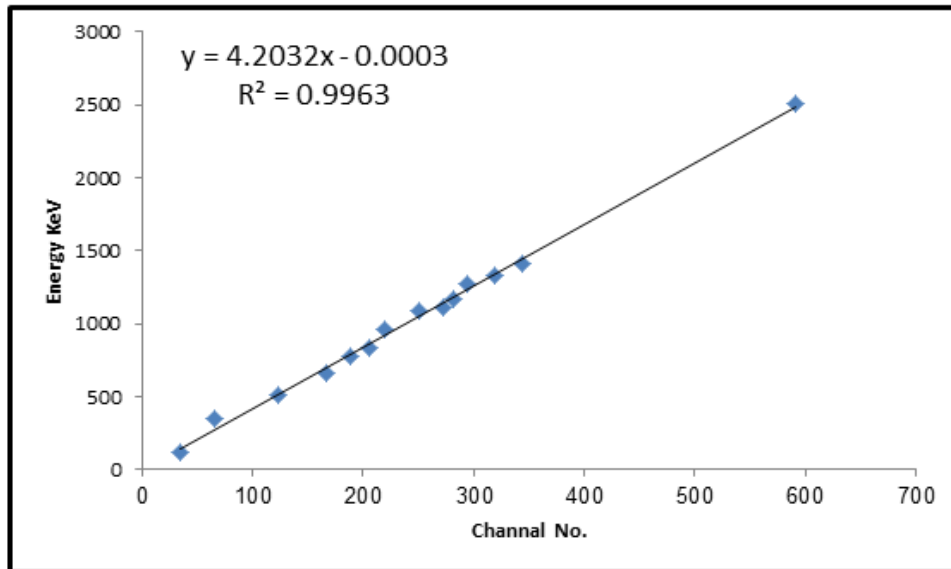


Figure (3-13): Energy Calibration Curve of NaI(Tl) 3''x3''.

From the energy calibration figure the relation between channel number and energy is linear and mathematically represented by the equation:

$$\text{Energy(keV)} = 4.203 * (\text{Channel No.}) - 0.0003 \quad \dots\dots (3.1)$$

3.5.2.b Energy Resolution

The energy resolution is the ability of the detector to recognize two peaks with a slight difference in energy [95]. Resolution can be determined from the following equation[96].

$$\text{Energy Resolution} = \left(\frac{F.W.H.M}{C} \right) \times 100\% \quad \dots\dots (3.2)$$

Where 'FWHM' is the full width at half maximum for photo peak of the spectrum of gamma rays source and C is the channel number at the midpoint of the gamma peak. In this work, the value obtained was

(7.9%)¹³⁷Cs standard source that energy 661.66 keV, as show Figure (3-14)

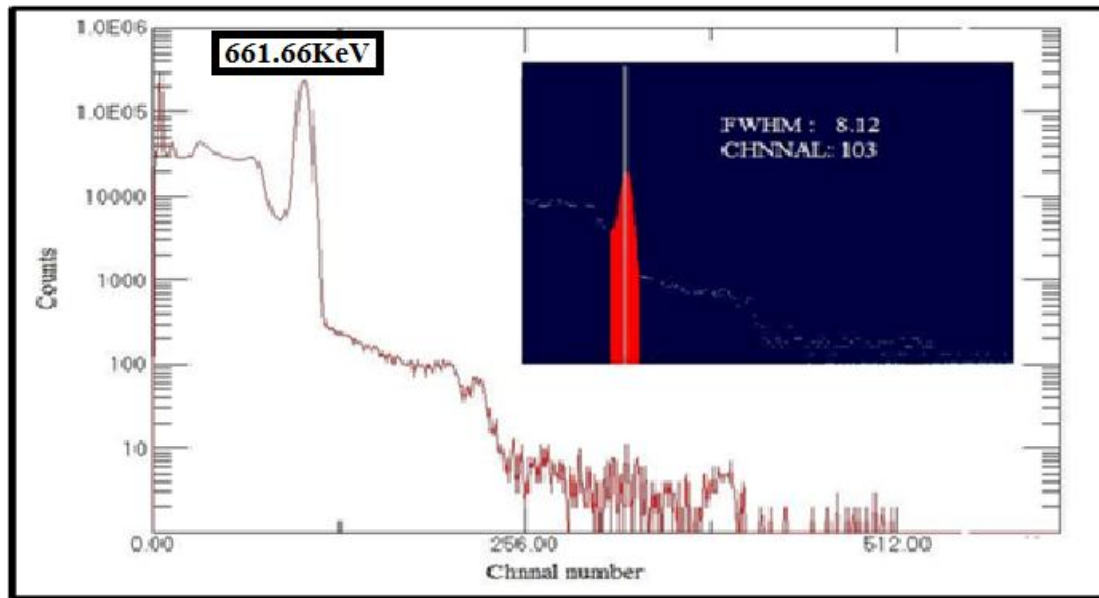


Figure (3-14): Spectrum of ¹³⁷Cs using (Maestro-32).

3.5.2.c Detector Efficiency

Detection efficiency is defined as the ratio of the number of particles or photons recorded by the detector to the number of particles emitted by the source [97]. The efficiency (ϵ) of the detector measuring system for a particular energy is calculated using the following relation[98].

$$\epsilon = \frac{C_p}{I_\gamma t.A} \times (100\%) \dots \dots (3.3)$$

where C_p is the count (area) under the specified energy peak after background subtraction, t is the time (sec) for spectrum collected, I_γ is the probability of gamma decay at energy (E) shown in table (3.4), and A is

activity sources at the time of the experiment. The activity of each standard source is corrected by using the following relation [97]:

$$A = A_0 e^{-\lambda \Delta t} \quad \dots \quad (3.4)$$

where A_0 is the initial activity (Bq) of each source at a time t_0 , A is the activity (Bq) of the source at time t , λ is the decay constant, and $\Delta t = t - t_0$ the variation in the absolute photo-peak detector efficiency with gamma-ray energy was calibrated using four sources as shown in Figure (3-15).

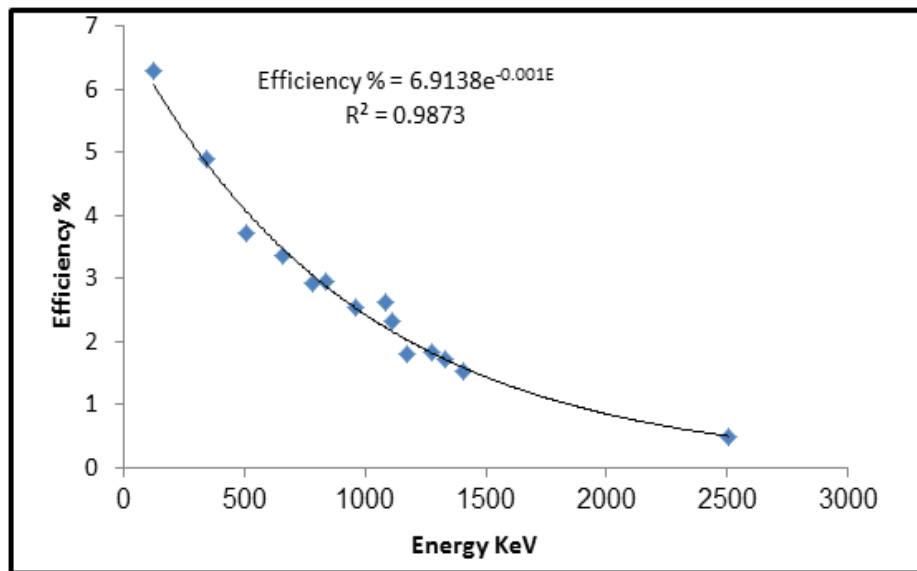


Figure (3-15): The efficiency calibration curve of NaI (TI) (3''x3'').

From Figure (3-15), the exponential relationship of correlation (98.73 %) was found follows :

$$\varepsilon = 6.9138 e^{-0.001 E(\text{keV})} \quad \dots \quad (3.5)$$

From these equation (3-5), it can be found the efficiency ^{214}Bi (^{238}U), ^{40}K and ^{208}Tl (^{232}Th).

3.5.2.d Gamma Radiation Measurement

After the end store time (a secular equilibrium between ^{226}Ra and ^{222}Rn) of soil samples in plastic Marinelli cups with a capacity of (1) liters, mass of the sample (750gm) as shown in Figure (3-16), the Marinelli was put on NaI(Tl) detector (around the detector) at time 5 hours to get the gamma-ray spectrum.

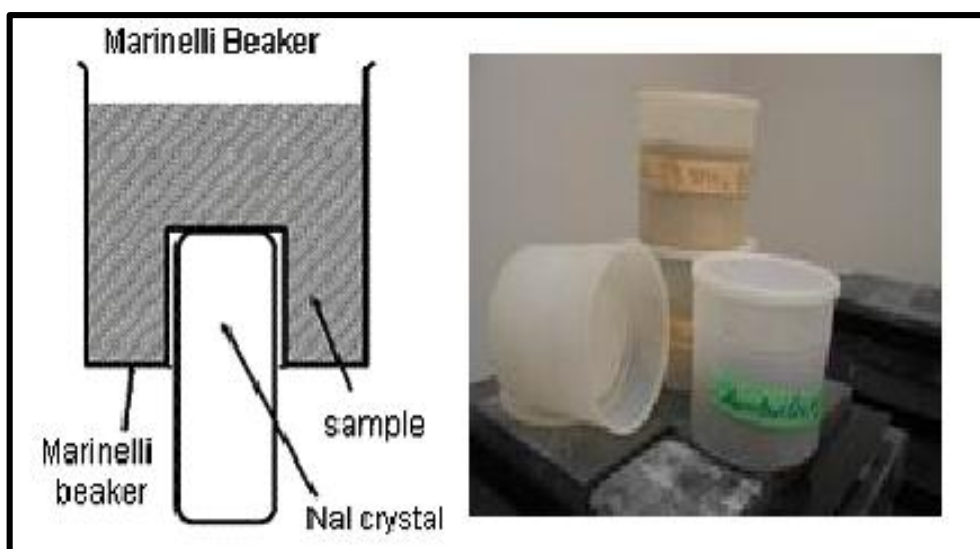


Figure (3-16): Sample of soil in marinelli beaker.

The net zone under the comparing photograph tops is determined in energy range by subtracting check because of background sources of the net zone of a specific top by utilizing the MAESTRO-32 information examination bundle. All measurement systems record background radiation due to natural radioactivity in earth materials, cosmic rays, structural materials in the system, and building materials surrounding the system. This background varies from place to place and depends on the quality, and size of the detector and also depends on the type of shield used.

The radiation background will decrease because of its interaction with the shield in the system. The background range is estimated by utilizing capacity empty (1L) polyethylene plastic Marinelli. Thanks to the poor resolution of NaI(Tl) detector, at low gamma energies which haven't well-isolated photo-peaks, containers on the indicator and checking within the meantime for the sample estimations [99]. During this manner, the measuring of the specific activity (Bq/kg) concentrations is feasible at well-separated photo-peaks high energies as that acquired in our outcomes from the gamma beams generated by the progenies of (^{232}Th) and (^{238}U), which are in common harmony with them while (^{40}K) was assessed specifically by its gamma-line of 1460 keV (^{40}Ar). Hence, the specific activity of (^{238}U) was determined using the gamma-lines 1764 keV (^{214}Bi). Similar results have been calculated of ^{232}Th were identified using the gamma-ray lines 2614 keV (^{208}Tl), as shown in Figure (3-17.a),(3-17.b),(3-17.c)

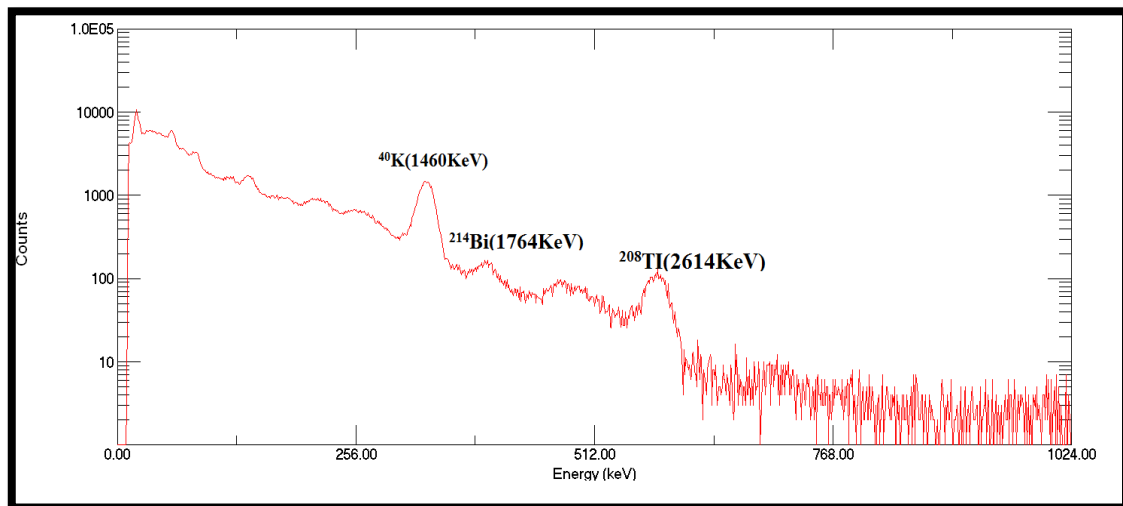


Figure (3-17. a): The spectrum of sample U2 (University of Kerbala Freiha site) in Maestro-32.

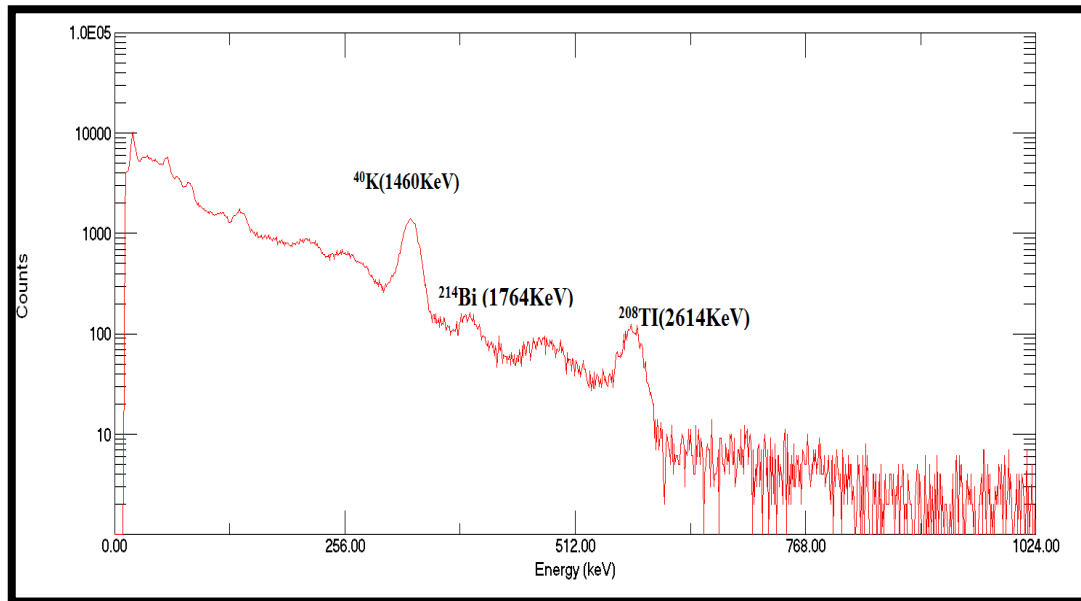


Figure (3-17. b): The spectrum of sample U65 (University of Kerbala agricultural college) in Maestro-32.

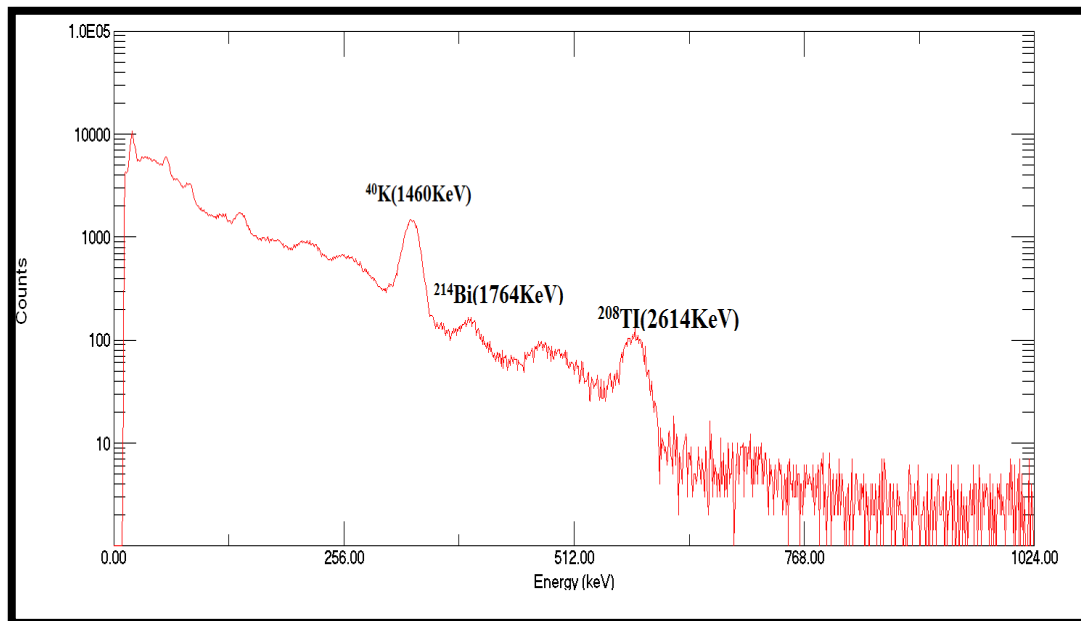


Figure (3-17.c): The spectrum of sample U85 (University of Kerbala Al-Mothafeen Site) in Maestro-32.

3.6 Experimental Part of CN-85 Detector

3.6.1 Preparation of Samples and Detectors

The technique were similar to that applied in the NaI(Tl) method. An integrated passive radon dosimeter was used to measure the concentration (^{222}Rn , ^{226}Ra , and ^{238}U) in the soil university of Kerbala. These included solid-state nuclear track (SSNTDs) detectors CN-85 has the chemical formula ($\text{C}_6\text{H}_8\text{O}_9\text{N}_2$) made by the Kodak, path, France, with thickness (12) μm . With dimensions of $1 \times 1 \text{ cm}^2$. A specific number was engraved in the upper right corner of the detector to collect information more easily and locate the detectors in different locations. The detector was fixed at the lower part of the plastic cover by a two-sided adhesive tape Point the side up with the number up, with samples. At the bottom of a closed cylindrical plastic can of bottom (5) cm and (7) cm length and, volume (92 gm) as shown in Figure (3-18). CN-85, and then sealed for exposure of (172) day.

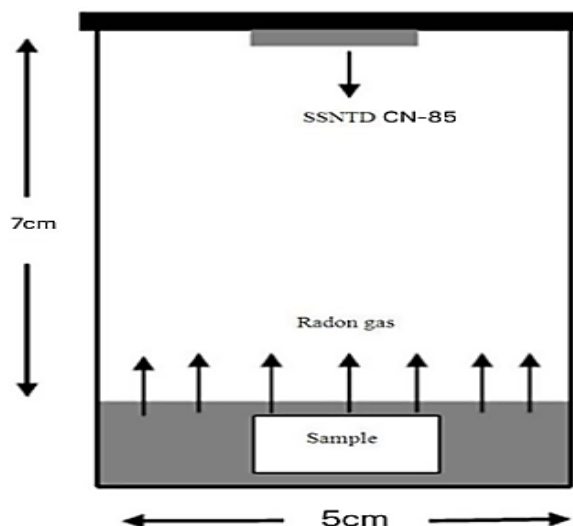


Figure (3-18): A test tube technique used in the study.

3.6.2 Process of Chemical Etching

After collecting the samples from the university soil in Karbala city and removing the detectors from dosimeters, we had installed the tracks resulted from alpha-particles emitted from radon and its progeny into the reagents material. For endorsement of the tracks, it used (NaOH) for concentration 2.5N placed in a heat-resistant glass container, in the water bath (Schwa Bach, Germany). And equipped with an electric heater as shown in Figure (3-19). At temperature $(70 \pm 0.1)C^{\circ}$ for 3 hours [59]. After that detectors were removed from the water bath and thoroughly rinsed with distilled water to remove leftover digging from the surface, then they were dried out on fine paper.



Figure (3-19): Water Bath

3.6.3 Calculation Alpha Particles Track on the Surface of Detectors

To enumerate the alpha particle tracks on the detector surface, we used an optical microscope (KRUSS-MBI 2000) as shown in figure (3-20). It was used with a magnification power(400X) to detect the soil since the viewing area for (400X) magnifications are $6.25 \times 10^{-4} \text{cm}^2$. The pathways

were counting at least (30) different sight for each detector due to radiation infers by radon decay is pure statistically radon phenomena.

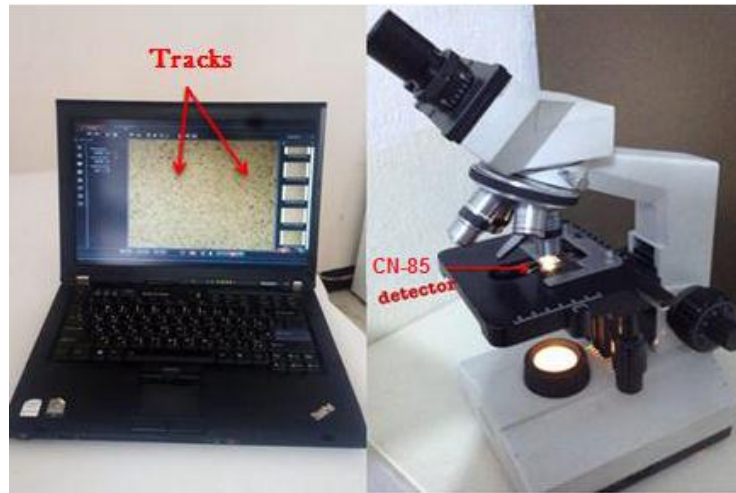


Figure (3-20): Optical microscope

3.7 Calculations

3.7.1 Gamma-Ray emitters

3.7.1.1 Specific Activity (A)

The specific activity (activity concentration) of the gamma - emitting radionuclides in the sample can be calculated from the following equation[100]:

$$A \left(\frac{\text{Bq}}{\text{kg}} \right) = \frac{N}{I_{\gamma} \varepsilon M T} \dots \dots \dots (3.6)$$

A is the specific activity of the radionuclide in the sample, N is the net area under photo peak, I_{γ} is the probability of gamma decay, ε is the efficiency of the gamma-ray detector at energy E, M is the weight of

the measured sample in kg, and T is the life time for collecting the spectrum in seconds.

3.7.1.2 Radium Equivalent Activity (Ra_{eq})

The (Ra_{eq}) is used to estimate the risk of specific activity measured unit (Bq/kg). Its activity varies according to the different soil types, and can be standardized relative to the resulting radiation exposure known as the Ra_{eq} radionuclide. It can be compared with the specific activity for the soil containing different amounts of and used the following equation[101]:

$$Ra_{eq} \left(\frac{Bq}{kg} \right) = A_U + 1.43 A_{Th} + 0.077A_K \dots \dots \dots (3.7)$$

3.7.1.3 Hazard Indices

3.7.1.3.1 External Hazard Index (H_{ex})

It is used to estimate biological hazard of radionuclides which emits natural γ -ray and, it can be calculated as following [102, 103]:

$$H_{ex} = \frac{A_U}{370} + \frac{A_{Th}}{259} + \frac{A_K}{4810} \dots \dots \dots (3.8)$$

A_U , A_{Th} and A_K are specific activity of ^{238}U , ^{232}Th and ^{40}K respectively.

3.7.1.3.2 Internal Hazard Index (H_{in})

Internal exposure means inhalation of Radon gas and its daughters, it can be calculated according to the following equation[104]:

$$H_{in} = \frac{A_U}{185} + \frac{A_{Th}}{259} + \frac{A_K}{4810} \dots \dots \dots (3.9)$$

3.7.1.3.3 Representative Level Index (I_γ)

Radiation dangers due to the predetermined, radionuclides of (^{238}U (^{226}Ra), ^{232}Th , and ^{40}K). Were evaluated by another file called (Representative level indicator) $I_{\gamma r}$, was resolved to utilizing the equation beneath [105]:

$$I_{\gamma r} = \left(\frac{1}{150}\right) A_U + \left(\frac{1}{100}\right) A_{\text{Th}} + \left(\frac{1}{1500}\right) A_K \dots \dots (3.10)$$

3.7.1.3.4 Alpha Index (I_α)

It has been created to evaluate the excess alpha radiation because of the radon inhaled breath beginning from building materials, the (alpha-index) was resolved utilizing equation beneath[103]:

$$I_\alpha = \frac{A_U}{200 \left(\frac{\text{Bq}}{\text{kg}}\right)} \dots \dots \dots (3.11)$$

3.7.1.4 Exposure Rate (X)

The rate of gamma-ray exposure in the air, measured at one meter above a thick slab that infinitely extended, due to Uranium, Thorium and Potassium, that were uniformly distributed within the material, is equal to [104, 106]:

$$\dot{X} \left(\frac{\mu\text{R}}{\text{h}}\right) = 1.90 A_U + 2.82 A_{\text{Th}} + 0.197 A_K \dots \dots \dots (3.12)$$

X is defined as the exposure rate ($\mu\text{R}/\text{h}$). Here, the concentrations of activity are usually given in pCi/g . For each radionuclide in the radioactive

series, the average values of the gamma-ray energies are described by the constants presented on the right-hand side of Eq. (3.12)

3.7.1.5 Radiological doses

3.7.1.5.1 Absorbed Dose Rate in Air (Dr)

The total percentage of air intake in terms of concentrations of the terrestrial nuclei can be calculated by the following equation [107].

$$D_r \left(\frac{\text{nGy}}{\text{h}} \right) = 0.462 A_U + 0.604 A_{Th} + 0.0417 A_K \dots \dots \dots (3.13)$$

(0.462), (0.604), (0.0417) are the conversion factors for naturally occurring radionuclides

3.7.1.5.2 Annual Gonadal Equivalent Dose (AGED)

As per UNSCEAR[108]. The gonads are viewed as organs of intrigue, the yearly gonads identical portion [AGED] for the occupants in the study region because of the particular activities of (^{238}U , ^{232}Th and ^{40}K). Was determined utilizing equation (3.14) given by Arafa as[109, 110]:

$$\text{AGED} \left(\frac{\text{mSv}}{\text{y}} \right) = 3.09 A_U + 4.18 A_{Th} + 0.314 A_K \dots \dots \dots (3.14)$$

(3.09), (4.18), (0.314) are the conversion factors for naturally occurring radionuclides

3.7.1.5.3 The Annual Effective Dose Equivalent (AEDE)

The yearly successful portion equivalent (AEDE) can be determined from the consumed portion by applying the portion transformation factor of (0.7) (Sv/Gy), with an outside inhabitation factor of (0.2)[111]:

$$AEDE_{outdoor} \left(\frac{mSv}{y} \right) = [D_r(mGy/hr) \times 8760 \text{ hr} \times 0.2 \times 0.7Sv/Gy] \times 10^{-6} \dots (3.15)$$

3.7.1.6 Excess life-time Cancer Risk (ELCR)

This factor measures the cancer probability created over a lifetime span for a given level of exposure. In this factor, (70) years is considered as the normal life-span for an individual. This risk factor can be given by [101, 112].

$$ELCR = AEDE \times DL \times RF \dots \dots (3.16)$$

where; the outdoor Annual Effective Dose Equivalent ($AEDE_{outdoor}$), the term DL is the normal Duration of Life (70 years as mentioned previously), RF is the Risk Factor (1/Sv), For the stochastic impact, generally, ICRP utilizes RF as 0.05 for people.

3.7.2 Calculations of Alpha emitters

Radon concentrations were measured in soil sample under study using solid state nuclear track detector CN-85, as well as radiological parameters due to radon concentrations also were calculated as following:

The track densities were measured using the following equation

$$\rho = \frac{\text{Average number of total pits(tracks)}}{\text{Area of field view}} \dots \dots (3.17)$$

3.7.2.1 Radon concentration

The radon concentration in the airspace of the tube (C) was calculated from following equations [113]:

$$C \left(\frac{Bq}{m^3} \right) = \frac{\rho}{K t} \dots\dots (3.18)$$

Where ρ is the number of track per (cm²) in the (CN-85) detector, and (t) represent the exposure time of our sample, K refers to calibration factor of CN-85 plastic track detector, K value equal to (0.256) Track.cm-2 /Bq.m³. day[54]. The radon concentrations in soil sample, was estimated following[114]:

$$C_{Rn} \left(\frac{Bq}{m^3} \right) = C \left(\frac{\lambda h t}{L} \right) \dots\dots (3.19)$$

where, C_{Rn} is concentrations radon gas in sample (Bq/m³), λ is decay constant of radon gas, which is equal to 0.1814 day⁻¹, h refers to thickness of the sample equal to 3.5 cm and L is distance between sample to detector.

In this analysis, radon and radium had to achieve an effective balance of about (99.4%) percent in almost (4weeks). It was as the half-life of ²²⁶Ra is 1600 y and ²²²Rn is 3.8 d, lately the auditory equilibrium has recently been achieved, radon alpha decomposition can be used to find radium activity, over time ,increased radon concentration after closing of the can following [115]:

$$C_{Rn} = C_{Ra} (1 - e^{-\lambda_{Rn}.T}) \dots\dots\dots (3.20)$$

The annual effective dose in terms of mSv/y units was obtained using the relation[116]:

$$\text{AED (m Sv/y)} = C \times F \times H \times T \times D \dots (3.21)$$

Where; F was the equilibrium factor which equal to (0.4), T was the time in hours in a year (8760 h/y), H was the occupancy factor which is equal to (0.8), and D was the dose conversion factor which equal to $[9 \times 10^{-6} \text{ (m Sv) / (Bq.h.m}^{-3}\text{)}]$ [117]:

3.7.2.2 Radium Concentration: The radium activity of the samples soil using the Can technique can be calculated by the relation[118]:

$$C_{Ra}(\text{Bq.kg}^{-1}) = \left(\frac{\rho}{k.Te} \right) \left(\frac{hA}{M} \right) \dots \dots \dots (3.22)$$

Where, C_{Ra} is the radium content of soil (Bq/kg), M is the mass of the soil sample and, A is the cross-section area of a cylindrical can in (m^2), (h) was the distance between the reagent and the soil samples. and, (T_e) was the time of actual exposure (T) the real exposure time and, λ_{Rn} the constant of decay for radon was computed following [119]:

$$Te = [T - \lambda_{Rn}^{-1} ((1 - e^{-\lambda_{Rn} \cdot T})] \dots \dots \dots (3.23)$$

3.7.2.3 Radon Exhalation Rates

mass exhalation rate : The mass exhalation rate (E_M) of the samples soil for release of the ^{222}Rn gas was calculated following [120]:

$$E_M = \frac{CV\lambda}{MT_e} \dots \dots \dots (3.24)$$

surface exhalation rate: The surface exhalation rate of (E_s) of the samples soil for release of radon gas was calculated following[120]:

$$E_s = \frac{CV\lambda}{AT_e} \dots \dots \dots (3.25)$$

3.7.2.4 Uranium Concentration: Using the law of secular equilibrium is an ideal way to find the numbers of uranium atoms (N_U) in the sample using the following equation[121]:

$$N_u \lambda_u = N_{Rn} \lambda_{Rn} \dots \dots \dots (3.26)$$

The activity of radon (A_{Rn}) can also be calculated in sample using the following equation[121]:

$$N_u \lambda_u = A_{Rn} \dots \dots \dots (3.27)$$

Where: λ_U is uranium decay constant ($4.98 \times 10^{-18} \text{ sec}^{-1}$); then W_U is uranium weight in the sample which can be calculated according to the following equation[121]:

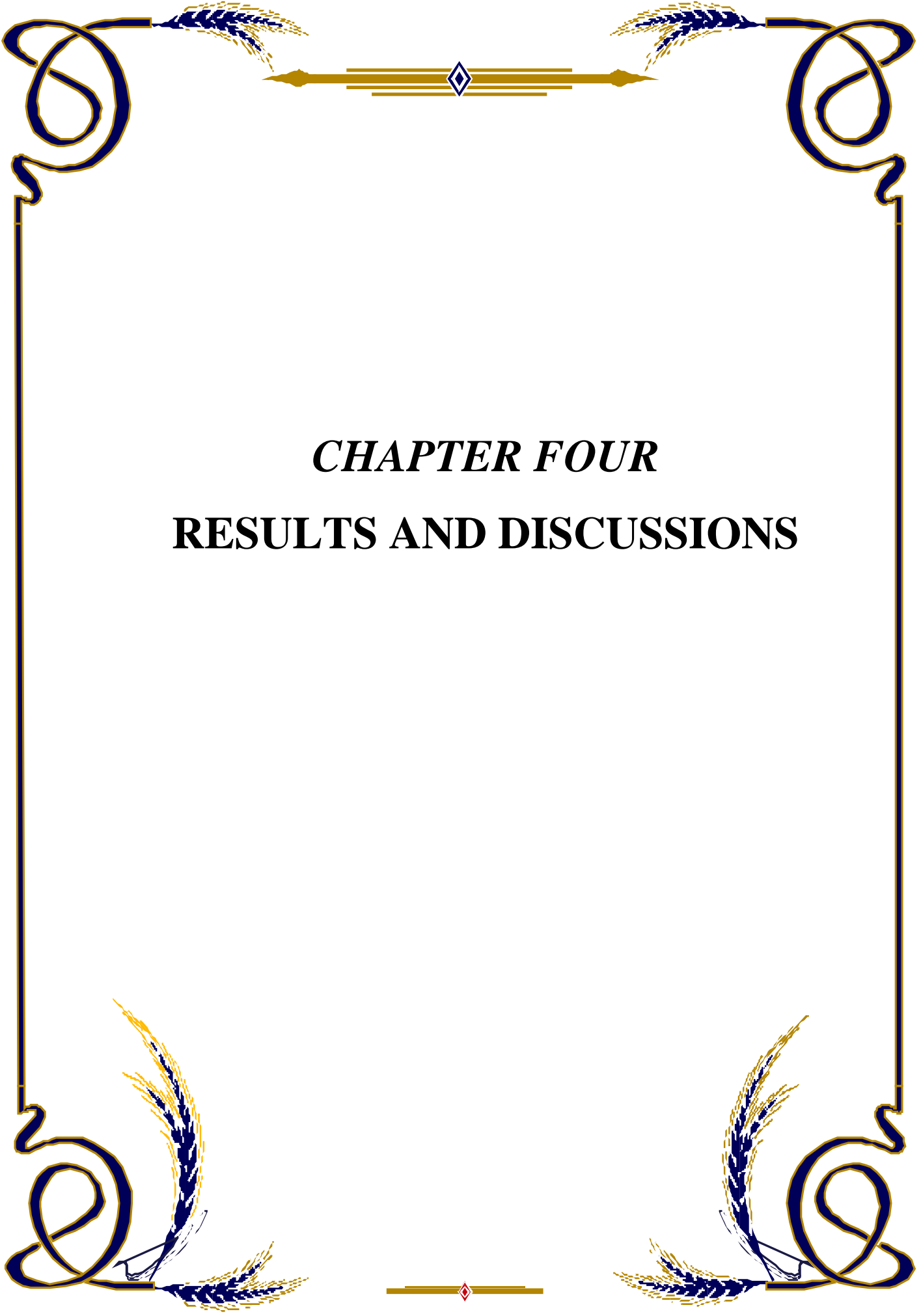
$$W_u = \frac{N_u \cdot A_u}{N_{AV}} \dots \dots \dots (3.28)$$

Where: W_{mol} is the weight of molecular uranium, N_{AV} . the number of Avogadro ($6.023 \times 10^{23} \text{ atom} \times \text{mol}^{-1}$) the activity of uranium (C_U) of soil samples, was calculated following[120]:

$$C_U (\text{ppm}) = \frac{W_U}{W_s} \dots \dots \dots (3.29)$$

Where W_U was the weight of ^{238}U in soil samples, and W_s was the weight of sample. The uranium concentration unit to activity unit in $\text{Bq} \cdot \text{kg}^{-1}$ of ^{238}U uranium[122, 123]:

$$1 \text{ ppm of Uranium} = 12.35 \text{ Bq} \cdot \text{kg}^{-1} \dots \dots \dots (3.30)$$



CHAPTER FOUR
RESULTS AND DISCUSSIONS

CHAPTER FOUR

RESULTS AND DISCUSSION

4.1 Introduction

This chapter shows the results from the two experiments conducted in this study. Gamma emitters and alpha emitters were measured in 100 samples of soil that collected from different sites of Karbala governorate university (Freiha region, Al-Husseineya region (Agricultural college), and Al-Mothafeen region). As well as, this chapter was contained the results radiological hazard index due to alpha and gamma emitters in the same samples under study. It also includes discussing the results with the global standards for gamma and alpha emitters by presenting the most important conclusions, recommendations, and proposed future actions. It will be divided the results in to gamma and alpha emitters as follows:

4.2 Gamma-Ray Emitters

4.2.1 Gamma Emitters in Freiha Site

4.2.1.1 Specific Activity

The specific activities of the ^{238}U , ^{232}Th and ^{40}K , radionuclides were measured in soil samples selected from different sites from the university of Kerbala (Freiha Site), and their radiation hazard parameters are listed in the table (4.1). From the table (4.1), the specific activity for ^{238}U ranged from 3.0 ± 0.35 Bq/kg in sample U41 to 35.3 ± 1.7 Bq/kg in sample U6 with an average value of 17.02 ± 7.70 Bq/kg. However, the specific activity for ^{232}Th varied from 2.8 ± 0.21 Bq/kg in sample U41 to 16.5 ± 0.7 Bq/kg in sample U6 with an average value of

8.22 ± 2.9 Bq/kg. In addition, the values of ^{40}K were ranged from 150.8 ± 2.8 Bq/kg in sample U4 to 447.4 ± 6.2 Bq/kg in sample U35 with an average value of 301.02 ± 77.5 Bq/kg.

Table (4.1): Results of specific activity in Kerbala university of Freiha site

No.	Sample code	specific activity in Bq/kg					
		Uranium-238		Thorium-232		Potassium-40	
		Average	\pm S.D	Average	\pm S.D	Average	\pm S.D
1	U1	19.3	1.2	13.9	0.6	310.5	5.0
2	U2	16.3	0.94	7.1	0.38	362.2	4.62
3	U3	9.8	0.8	6.9	0.4	316.9	4.9
4	U4	8.2	0.6	4.7	0.3	150.8	2.8
5	U5	23.5	1.4	8.6	0.5	416.3	6.0
6	U6	35.3	1.7	16.5	0.7	367.1	5.6
7	U7	8.6	0.66	8.4	0.39	310.8	4.09
8	U8	11.3	0.77	5.7	0.33	300.1	4.10
9	U9	17.5	1.0	10.1	0.5	349.4	4.8
10	U10	26.1	1.4	9.1	0.5	388.7	5.6
11	U11	13.9	0.9	8.3	0.4	165.5	3.2
12	U12	14.0	0.9	9.5	0.5	272.8	4.3
13	U13	7.7	0.59	3.2	0.23	274.2	3.64
14	U14	15.1	0.9	9.4	0.4	285.9	4.0
15	U15	4.3	0.47	6.7	0.35	277.1	3.91
16	U16	20.4	1.0	6.1	0.3	232.9	3.6
17	U17	20.9	1.3	8.0	0.5	378.0	5.6
18	U18	10.3	0.7	7.2	0.4	242.7	3.7
19	U19	10.9	0.7	11.2	0.4	223.1	3.2
20	U20	10.9	0.8	16.8	0.6	261.6	4.0
21	U21	9.0	0.6	8.3	0.4	273.7	3.8
22	U22	15.1	0.9	13.0	0.5	251.8	3.7
23	U23	30.6	1.4	8.8	0.5	350.3	5.1
24	U24	7.3	0.60	9.8	0.42	247.3	3.66
25	U25	23.7	1.2	7.0	0.4	287.7	4.4
26	U26	28.0	1.4	12.5	0.6	470.9	6.1
27	U27	33.5	1.6	9.2	0.5	384.8	5.7
28	U28	21.8	1.1	5.9	0.4	206.9	3.6
29	U29	23.6	1.2	5.2	0.3	345.3	4.8
30	U30	20.8	1.1	9.6	0.4	295.6	4.2
31	U31	19.9	1.0	8.4	0.4	361.9	4.5

32	U32	19.1	0.98	9.2	0.41	373.1	4.49
33	U33	25.3	1.2	11.4	0.5	164.9	3.1
34	U34	16.1	0.94	10.8	0.47	394.7	4.86
35	U35	32.7	1.6	5.6	0.4	447.4	6.2
36	U36	16.3	0.8	7.4	0.3	109.2	2.3
37	U37	28.6	1.32	10.9	0.49	440.7	5.38
38	U38	8.7	0.68	7.3	0.38	241.3	3.72
39	U39	20.8	1.3	8.7	0.5	324.1	5.1
40	U40	23.2	1.2	9.4	0.4	332.1	4.6
41	U41	3.0	0.35	2.8	0.21	160.2	2.69
42	U42	14.4	0.8	7.7	0.4	260.7	3.7
43	U43	25.7	1.3	7.7	0.4	333.1	4.9
44	U44	21.6	1.2	5.5	0.4	409.2	5.6
45	U45	13.1	0.8	11.1	0.4	352.9	4.4
46	U46	8.2	0.72	3.1	0.27	303.5	4.54
47	U47	26.7	1.3	8.1	0.4	358.9	4.8
48	U48	13.1	0.9	5.9	0.4	226.3	4.0
49	U49	16.1	1.0	6.9	0.4	296.5	4.6
50	U50	13.0	0.9	8.3	0.4	311.0	4.6
51	U51	16.8	1.0	15.6	0.6	378.2	4.8
52	U52	27.8	1.2	5.9	0.3	231.2	3.7
53	U53	4.1	0.46	3.6	0.26	253.0	3.75
54	U54	17.5	0.9	6.4	0.3	270.7	3.6
55	U55	9.6	0.7	7.2	0.3	185.0	3.0
56	U56	19.1	1.2	8.2	0.5	333.4	5.2
57	U57	16.9	1.1	5.8	0.3	378.0	5.2
58	U58	11.3	0.77	6.5	0.35	332.2	4.35
59	U59	6.3	0.50	4.3	0.25	210.8	3.01
60	U60	8.7	0.68	6.9	0.37	286.4	4.06
Maximum		35.3	1.7	16.8	0.7	447.4	6.2
Minimum		3	0.35	2.8	0.21	109.2	2.3
Average± S.D		17.02±7.70		8.22±2.9		301.02±77.5	
Worldwide average[124]		33		45		420	

The UNSCEAR (2008) recommended standard indicate that the world's average specific activity of ^{238}U , ^{232}Th , and ^{40}K are 33 Bq/kg, 45 Bq/kg, and 420 Bq/kg,

respectively[124]. From the results in Table (4.1), it was found that all values of ^{238}U the specific activities were less than the worlds average activity that recommended by UNSCEAR 2008 that the specific activities, with the exception of U6 and U27. While all values of specific activity of ^{232}Th were within the UNSCEAR 2008 report. As well as, it is clear for ^{40}K , that the specific activities, with the exception of U26, U35 U37 samples were only found to be higher than the worldwide average (420 Bq/kg). Figures (4-1), (4-2), and (4-3) were drawn by GIS technique, show the geographical distribution of the Freiha site and the amount of specific activity for uranium-238, thorium-232, and potasium-40 in the soil of this region, where different colors were used to distinguish between high, medium and low quantities.

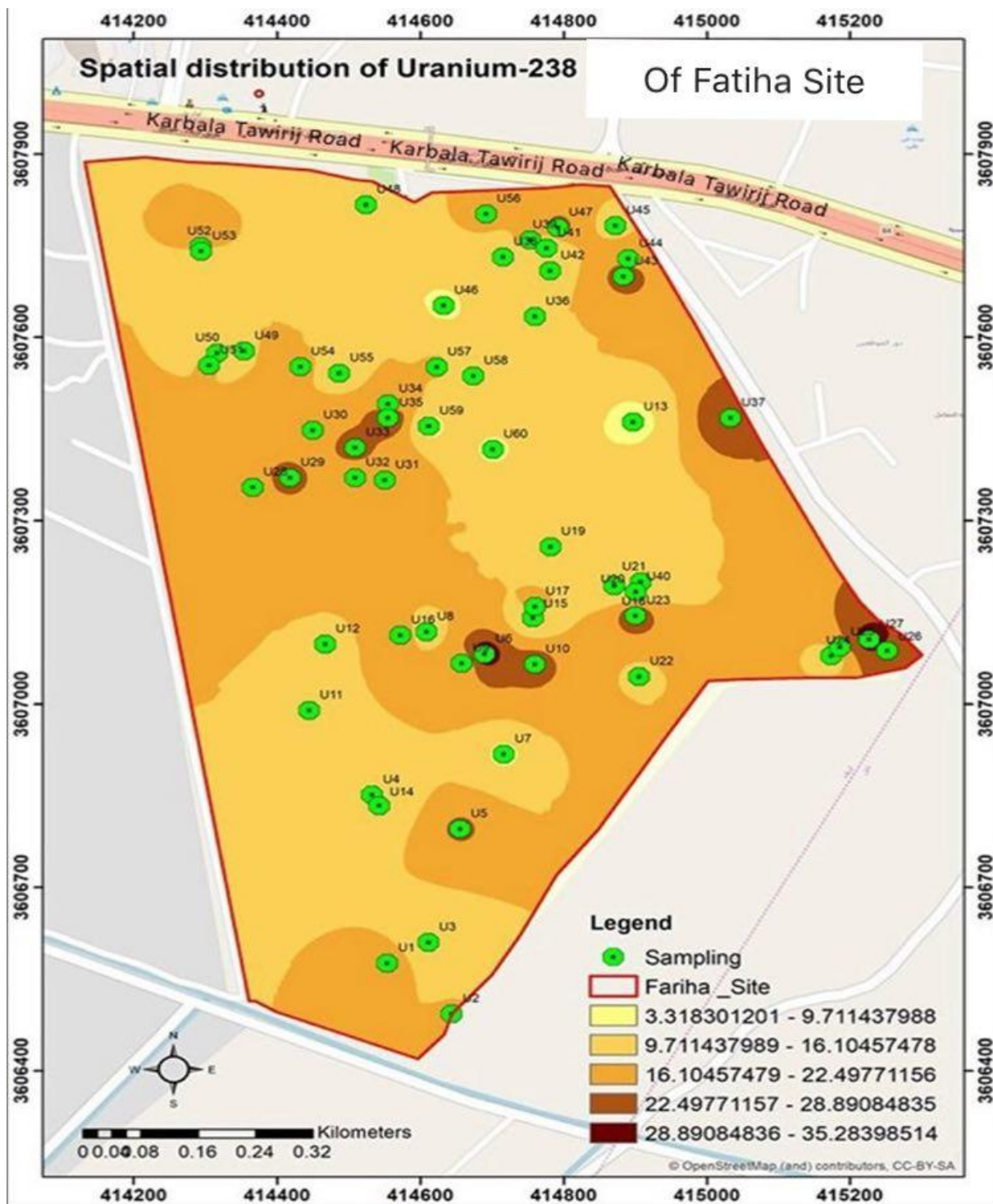


Figure (4-1): Map of the values of specific activity of ^{238}U in Kerbala university of Fatiha site

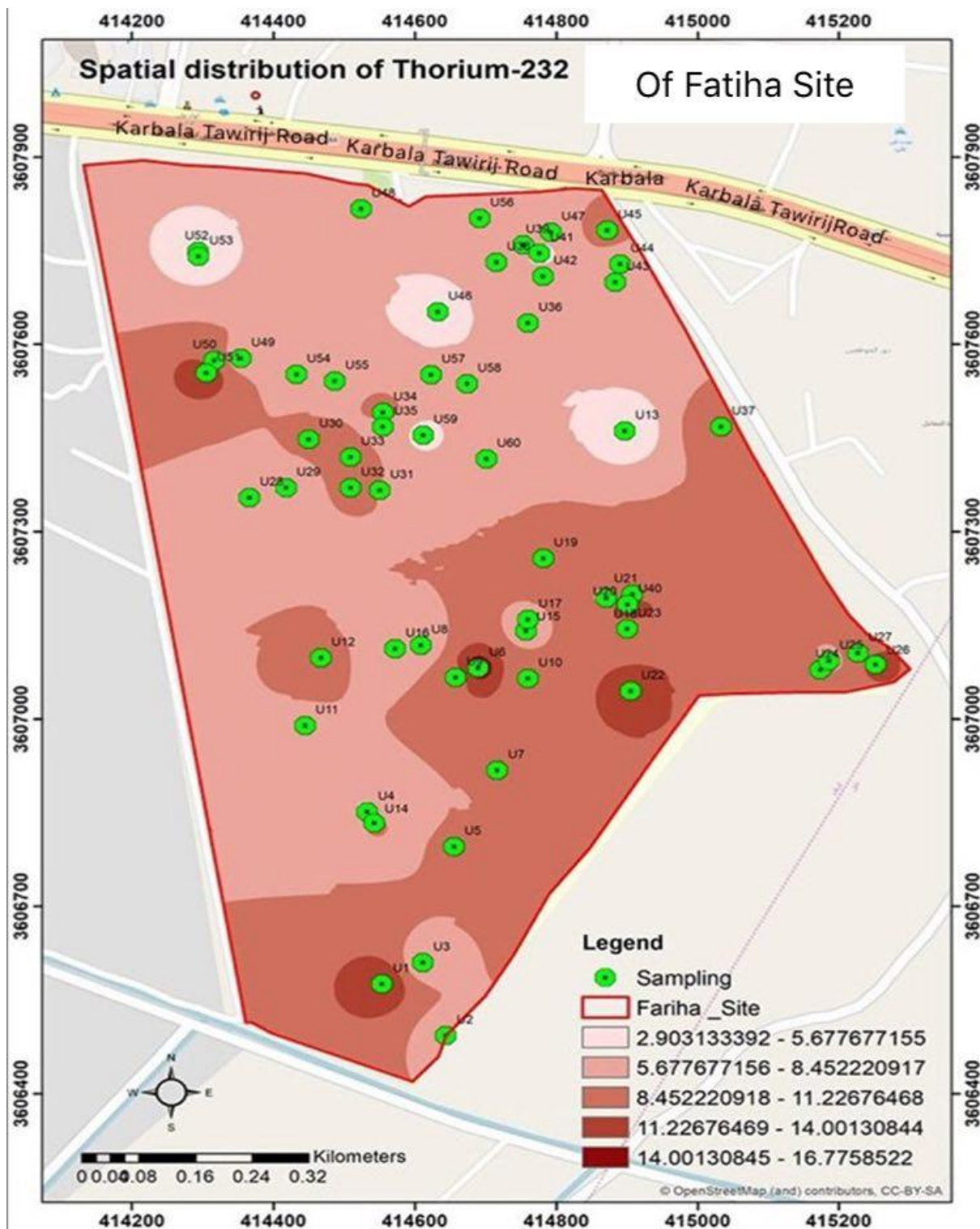


Figure (4-2): Map of the values of specific activity of ^{232}Th in Kerbala University of Freiha site.

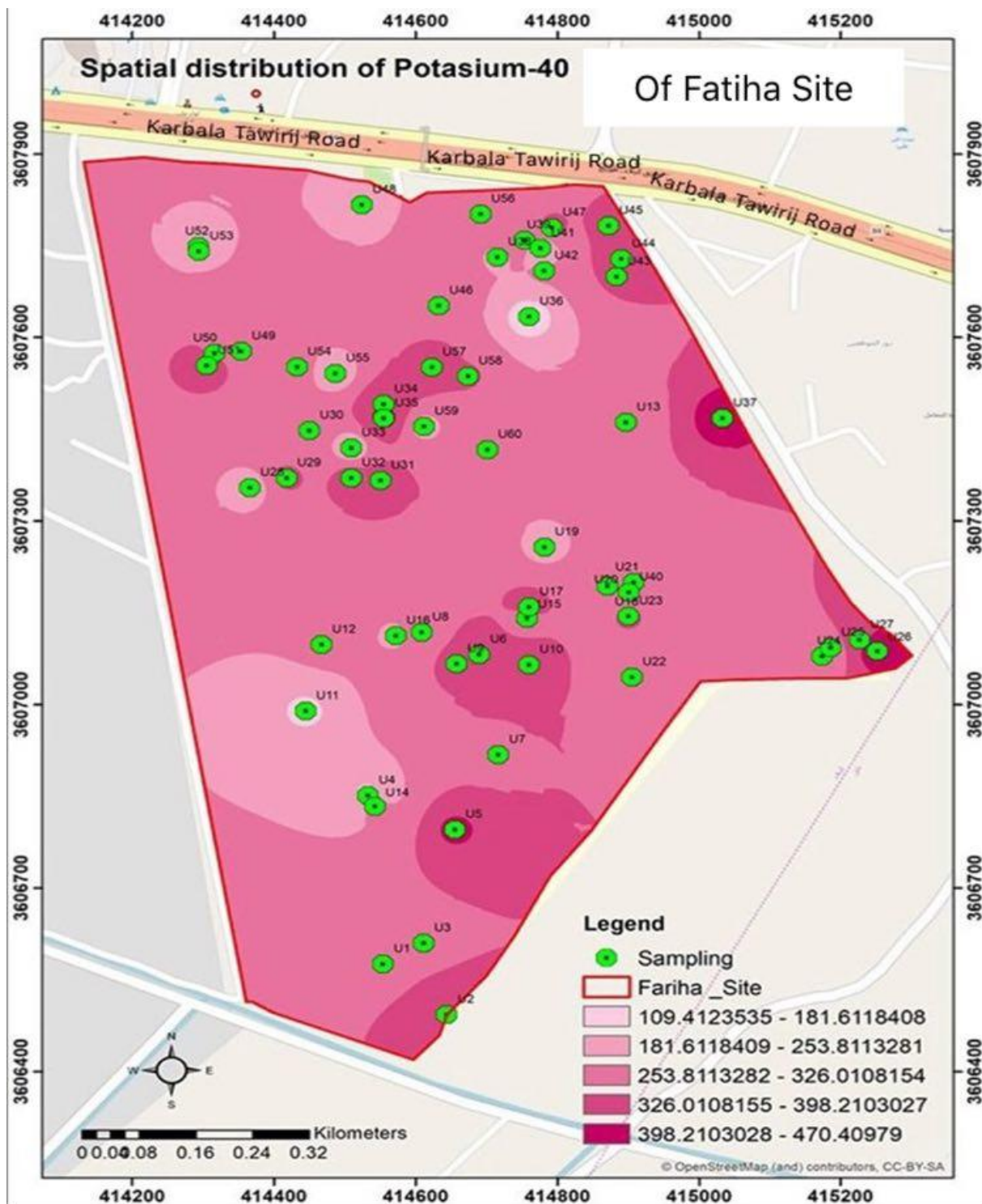


Figure (4-3): Map of the values of specific activity of ^{40}K Kerbala university of Freiha site.

4.2.1.2 Radiological Effects

The results of Ra_{eq} , H_{ex} , H_{in} , I_{yr} , I_{α} are shown in Table (4.2). which shows the values of Ra_{eq} in Bq/kg varied from 19.3 to 87.2 with an average of 51.96 ± 1.83 Bq/kg. The maximum of Ra_{eq} are less than 370 Bq/kg [125]. Results for H_{ex} , H_{in} , I_{yr} , and I_{α} see Table (4.2) were range from 0.05 to 0.20 with an average value of 0.1405 ± 0.0049 , from 0.06 to 0.33 with an average of 0.1866 ± 0.0074 , from 0.15 to 0.65 with an average of 0.01105 ± 0.0135 , and from 0.021 to 0.177 with an average of 0.0854 ± 0.0502 , respectively. The results of the risk indicators H_{ex} , H_{in} , I_{yr} , and I_{α} for all values for all samples studied during in this work are less than one which is the maximum value of the recommended permissible safety limit[126].

Table (4.2): Results of Ra_{eq} , H_{ex} , H_{in} , I_{yr} and I_{α} in Freiha site of Kerbala university

No	Sample code	Ra_{eq} (Bq/kg)	H_{ex}	H_{in}	I_{yr}	I_{α}
1	U1	63.1	0.17	0.22	0.47	0.097
2	U2	54.3	0.15	0.19	0.42	0.082
3	U3	44.1	0.12	0.15	0.35	0.049
4	U4	26.5	0.07	0.09	0.20	0.041
5	U5	67.9	0.18	0.25	0.52	0.118
6	U6	87.2	0.24	0.33	0.65	0.177
7	U7	44.5	0.12	0.14	0.35	0.043
8	U8	42.6	0.11	0.15	0.33	0.057
9	U9	58.8	0.16	0.21	0.45	0.088
10	U10	69.0	0.19	0.26	0.52	0.131
11	U11	38.5	0.10	0.14	0.29	0.070
12	U12	48.6	0.13	0.17	0.37	0.070
13	U13	33.4	0.09	0.11	0.27	0.039
14	U14	50.6	0.14	0.18	0.39	0.076
15	U15	35.2	0.10	0.11	0.28	0.022
16	U16	47.1	0.13	0.18	0.35	0.102
17	U17	61.4	0.17	0.22	0.47	0.105

18	U18	39.3	0.11	0.13	0.30	0.052
19	U19	44.1	0.12	0.15	0.33	0.055
20	U20	55.1	0.15	0.18	0.42	0.055
21	U21	41.9	0.11	0.14	0.33	0.045
22	U22	53.1	0.14	0.18	0.40	0.076
23	U23	70.2	0.19	0.27	0.53	0.153
24	U24	40.4	0.11	0.13	0.31	0.037
25	U25	55.9	0.15	0.21	0.42	0.119
26	U26	82.1	0.22	0.30	0.63	0.140
27	U27	76.3	0.21	0.30	0.57	0.168
28	U28	46.2	0.12	0.18	0.34	0.109
29	U29	57.6	0.16	0.22	0.44	0.118
30	U30	57.3	0.15	0.21	0.43	0.104
31	U31	59.8	0.16	0.22	0.46	0.100
32	U32	61.0	0.16	0.22	0.47	0.096
33	U33	54.3	0.15	0.22	0.39	0.127
34	U34	61.9	0.17	0.21	0.48	0.081
35	U35	75.2	0.20	0.29	0.57	0.164
36	U36	35.3	0.10	0.14	0.26	0.082
37	U37	78.1	0.21	0.29	0.59	0.143
38	U38	37.7	0.10	0.13	0.29	0.044
39	U39	58.2	0.16	0.21	0.44	0.104
40	U40	62.2	0.17	0.23	0.47	0.116
41	U41	19.3	0.05	0.06	0.15	0.015
42	U42	45.5	0.12	0.16	0.35	0.072
43	U43	62.4	0.17	0.24	0.47	0.129
44	U44	61.0	0.16	0.22	0.47	0.108
45	U45	56.1	0.15	0.19	0.43	0.066
46	U46	36.0	0.10	0.12	0.29	0.041
47	U47	65.9	0.18	0.25	0.50	0.134
48	U48	39.0	0.11	0.14	0.30	0.066
49	U49	48.8	0.13	0.18	0.37	0.081
50	U50	48.8	0.13	0.17	0.38	0.065
51	U51	68.2	0.18	0.23	0.52	0.084
52	U52	54.0	0.15	0.22	0.40	0.139
53	U53	28.7	0.08	0.09	0.23	0.021

54	U54	47.5	0.13	0.18	0.36	0.088
55	U55	34.1	0.09	0.12	0.26	0.048
56	U56	56.5	0.15	0.20	0.43	0.096
57	U57	54.3	0.15	0.19	0.42	0.085
58	U58	46.2	0.12	0.16	0.36	0.057
59	U59	28.7	0.08	0.09	0.23	0.032
60	U60	40.6	0.11	0.13	0.32	0.044
Maximum		87.2	0.24	0.33	0.65	0.177
Minimum		19.3	0.05	0.06	0.15	0.015
Average± S.D.		51.96±1.83	0.14±0.004	0.186±0.007	0.396±0.013	0.0854±0.050
Worldwide average		<370[125]	<1[3]	<1[3]	<1[3]	<1[3]

The results of X, D_r, AGED, AEDE outdoor, ELCR were listed in Table (4.3). From this Table, it can be seen the maximum value of X was 185.9 µR/h in sample U6, while the minimum was 45.2 µR/h in sample U41 with an average value of 114.828 ± 3.921 µR/h, the results of D_r ranges from 9.8 nGy/h to 41.6 nGy/h with an average value of 25.388±0.833 nGy/h. The values of D_r in all samples of the present study were smaller than world average value (55 nGy / h) according to UNSCEAR 2000[127]. AGED values, as shown in Table (4.3) were ranged from 71.3 mSv/y to 293.3 mSv/y with an average of 181.49±6.233 mSv. So, the values of AGED in all samples are lower when compared with the world average permissible limit of ≤ 300 mSv/y[110]. The results of AEDE outdoor in this study were ranged from 0.021mSv/y to 0.051mSv/y, with an average of 0.396±0.013 mSv/y. Since all AEDE value outdoors are less of the corresponding global values, it is 0.08 mSv /year [128]. The data of ELCR were ranged from 0.042 x 10⁻³ to 0.178 x 10⁻³ with an average of (0.108±0.003) x10⁻³. According to these results, the values of (ELCR) are very low; therefore, it has been determined that the risk of developing cancer is almost negligible. The results of the

radioactive hazard due to natural radionuclides of the studied samples were lower than the global average according to OECD [129], ICRP[130], UNSCEAR[131], and other.

Table (4.3): Results of X, D_r, AGED, AEDE_{outdoor}, ELCR in Freiha site of Kerbala university

No.	Sample code	Exposure rate (μR/h)	D _r (nGy/h)	AGED (mSv/y)	AEDE _{outdoor} (mSv/y)	ELCR× 10 ⁻³
1	U1	137.0	30.3	215.2	0.037	0.130
2	U2	122.3	26.9	193.8	0.033	0.116
3	U3	100.5	21.9	158.6	0.027	0.094
4	U4	58.5	12.9	92.3	0.016	0.055
5	U5	150.9	33.4	239.3	0.041	0.143
6	U6	185.9	41.6	293.3	0.051	0.178
7	U7	101.3	22.0	159.3	0.027	0.094
8	K8	96.7	21.2	153.0	0.026	0.091
9	U9	130.6	28.8	206.0	0.035	0.123
10	U10	151.8	33.8	240.7	0.041	0.145
11	U11	82.4	18.3	129.6	0.022	0.079
12	U12	107.1	23.6	168.6	0.029	0.101
13	U13	77.7	16.9	123.3	0.021	0.073
14	U14	111.5	24.6	175.7	0.030	0.105
15	U15	81.7	17.6	128.3	0.022	0.075
16	U16	101.8	22.8	161.7	0.028	0.098

17	U17	136.7	30.3	216.7	0.037	0.130
18	U18	87.7	19.2	138.1	0.024	0.083
19	U19	96.2	21.1	150.6	0.026	0.091
20	U20	119.6	26.1	186.0	0.032	0.112
21	U21	94.4	20.6	148.4	0.025	0.088
22	U22	115.0	25.3	180.1	0.031	0.109
23	U23	152.0	34.1	241.3	0.042	0.146
24	U24	90.2	19.6	141.2	0.024	0.084
25	U25	121.4	27.2	192.8	0.033	0.117
26	U26	181.2	40.1	286.6	0.049	0.172
27	U27	165.4	37.1	262.8	0.045	0.159
28	U28	98.8	22.3	157.0	0.027	0.096
29	U29	127.5	28.4	203.1	0.035	0.122
30	U30	124.8	27.7	197.2	0.034	0.119
31	U31	132.8	29.4	210.2	0.036	0.126
32	U32	135.7	29.9	214.6	0.037	0.129
33	U 33	112.7	25.5	177.6	0.031	0.109
34	U34	138.8	30.4	218.8	0.037	0.131
35	U35	166.1	37.1	264.9	0.046	0.159
36	U36	73.4	16.6	115.6	0.020	0.071
37	U37	171.9	38.2	272.3	0.047	0.164

38	U38	84.7	18.5	133.2	0.023	0.079
39	U39	127.9	28.4	202.4	0.035	0.122
40	U40	136.0	30.2	215.3	0.037	0.130
41	U41	45.2	9.8	71.3	0.012	0.042
42	U42	100.4	22.2	158.5	0.027	0.095
43	U43	136.2	30.4	216.2	0.037	0.131
44	U44	137.2	30.4	218.2	0.037	0.130
45	U45	125.7	27.5	197.7	0.034	0.118
46	U46	84.1	18.3	133.6	0.022	0.079
47	U47	144.3	32.2	229.1	0.039	0.138
48	U48	86.1	19.1	136.2	0.023	0.082
49	U49	108.5	24.0	171.7	0.029	0.103
50	U50	109.4	24.0	172.5	0.029	0.103
51	U51	150.4	33.0	235.9	0.040	0.141
52	U52	115.0	26.0	183.2	0.032	0.112
53	U53	67.8	14.6	107.2	0.018	0.063
54	U54	104.6	23.2	165.8	0.029	0.100
55	U55	75.0	16.5	117.9	0.020	0.071
56	U56	125.1	27.7	198.0	0.034	0.119
57	U57	122.9	27.1	195.2	0.033	0.116
58	U58	105.2	23.0	166.4	0.028	0.099

59	U59	65.6	14.3	103.6	0.018	0.061
60	U60	92.4	20.1	145.7	0.025	0.086
Maximum		185.9	41.6	293.3	0.051	0.178
Minimum		45.2	9.8	71.3	0.012	0.042
Average±S.E		114.82±3.9	25.38±0.883	181.49±6.23	0.0310±0.001	0.108±0.003
Worldwide average		55[132]	≤ 300 [110]	0.08 [128]	1×10⁻³

4.2.2 Gamma Emitters in Agricultural College

4.2.2.1 Specific Activity

specific activities of the ^{238}U , ^{232}Th and ^{40}K , radionuclides were measured in selected Soil samples from different regions from the university of Karbala (Al-Husseineya Site), and their radiation hazard parameters are listed in Table (4.4). From Table (4.4), The specific activity for ^{238}U ranged from 6.5 ± 0.6 Bq/kg in sample U61 to 35.1 ± 1.5 Bq/kg in sample U79 with an average value of 21.75 ± 7.2 Bq /kg. However, the specific activity for ^{232}Th varied from 3.1 ± 0.2 Bq/kg in sample U80 to 14.2 ± 0.5 Bq/kg in sample U61 with an average value of 9.43 ± 3.2 Bq/kg. In addition, the values of ^{40}K were ranged from 111.5 ± 2.5 Bq/kg in sample U74 to 419 ± 5.6 Bq/kg in sample U66 with an average value of 335.88 ± 82.2 Bq/kg.

Table (4.4): Results of specific activity in agricultural college of Kerbala university

No.	Sample code	Specific activity in Bq/kg					
		Uranium -238		Thorium-232		Potasium-40	
		Average	±S.D	Average	±S.D	Average	±S.D
1	U61	6.5	0.6	14.2	0.5	407.8	4.9
2	U62	25.1	1.1	13.0	0.5	383.5	4.4
3	U63	13.6	0.8	5.8	0.3	294.7	3.8
4	U64	19.9	1.0	5.4	0.3	152.4	2.9
5	U65	27.6	1.3	9.6	0.4	329.1	4.5
6	U66	15.3	1.0	9.6	0.5	419.7	5.6
7	U67	27.1	1.2	11.5	0.5	373.4	4.5
8	U68	28.3	1.4	13.1	0.6	390.8	5.2
9	U69	21.6	1.0	4.7	0.3	246.0	3.6
10	U70	17.1	1.1	8.4	0.5	308.4	4.7
11	U71	23.9	1.2	11.4	0.5	417.1	5.2
12	U72	27.7	1.4	9.3	0.5	365.3	5.2
13	U73	30.1	1.4	9.9	0.5	329.9	4.7
14	U74	24.1	1.1	3.4	0.3	111.5	2.5
15	U75	18.8	0.9	13.4	0.5	290.8	3.9
16	U76	12.1	0.8	10.9	0.4	363.5	4.3
17	U77	20.7	1.1	10.5	0.5	391.2	5.2
18	U78	11.4	0.9	12.8	0.6	417.4	5.6
19	U79	35.1	1.5	8.7	0.4	376.9	5.0
20	U80	29.0	1.1	3.1	0.2	348.3	4.1
maximum		35.1	1.5	14.2	0.5	419.7	5.6
minimum		6.5	0.6	3.1	0.2	111.5	2.5
Average±S.D		21.75±7.2		9.43±3.2		335.88±82.2	
Worldwide average[124]		33		45		420	

The A UNSCEAR 2008 recommended standard indicates that the worlds average a specific activity of ^{238}U , ^{232}Th and ^{40}K are 33 Bq/kg, 45 Bq/kg, and 420 Bq/kg, respectively [124]. From leads to a Table (4.4), it had been found that each one values of ^{238}U specific activities were less than world activities average activity that recommended by UNSCEAR 2008 that the precise activities, with the exception of U79 . While all values of the specific activity of ^{232}Th . It was included in the 2008 UNSCEAR Report. As well as, it is clear for ^{40}K , that the

specific activities, were less than the worlds average activity that recommended by UNSCEAR 2008 report. Figures (4-4), (4-5), and (4-6) were drawn by GIS technique, show the geographical distribution of the Freiha site and the amount of specific activity for uranium-238, thorium -232 and potasium-40 in the soil of this region, where different colors were used to distinguish between high, medium and low quantities.

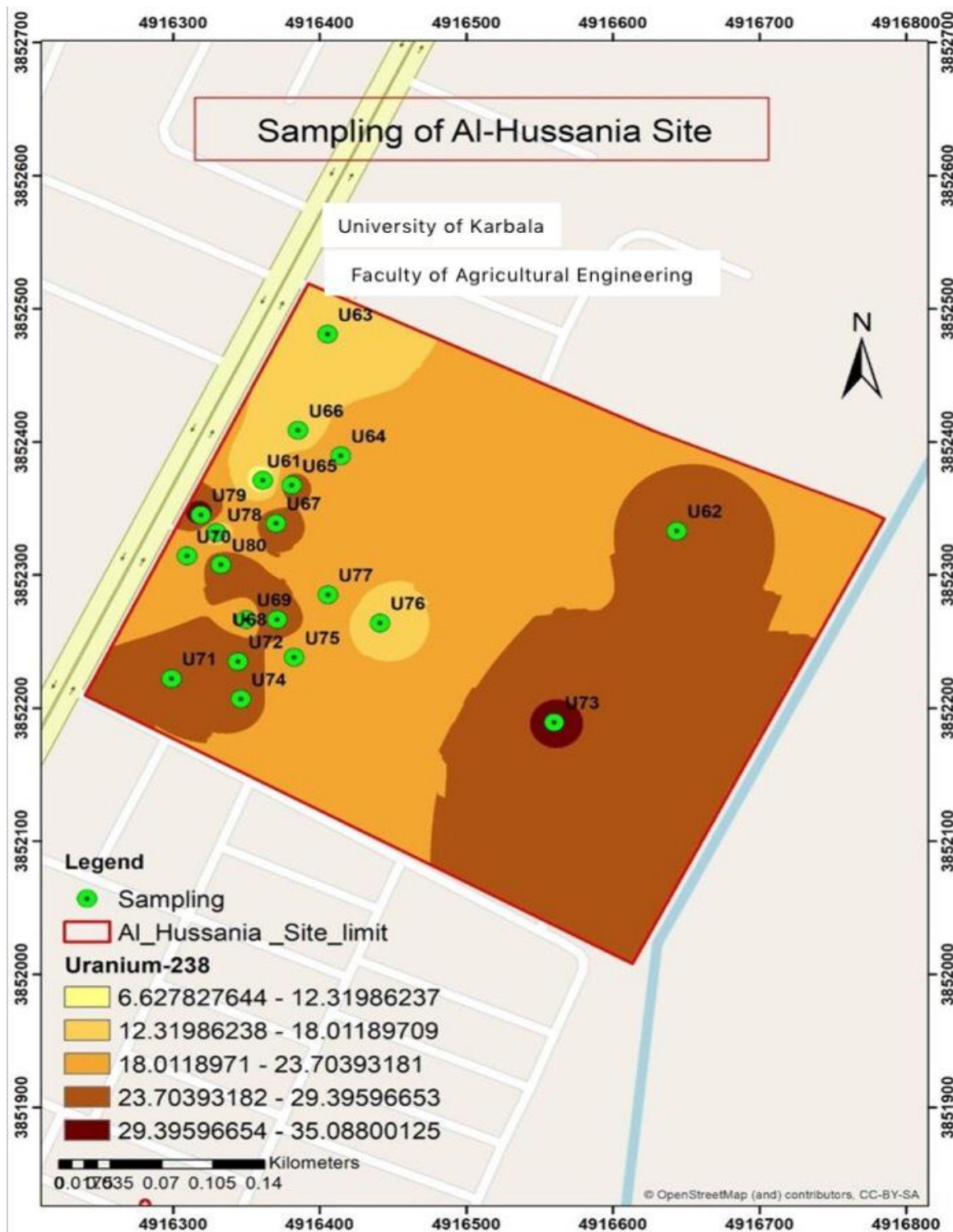


Figure (4-4): Map of the values of specific activity of ^{238}U in Agricultural College of Kerbala University

of

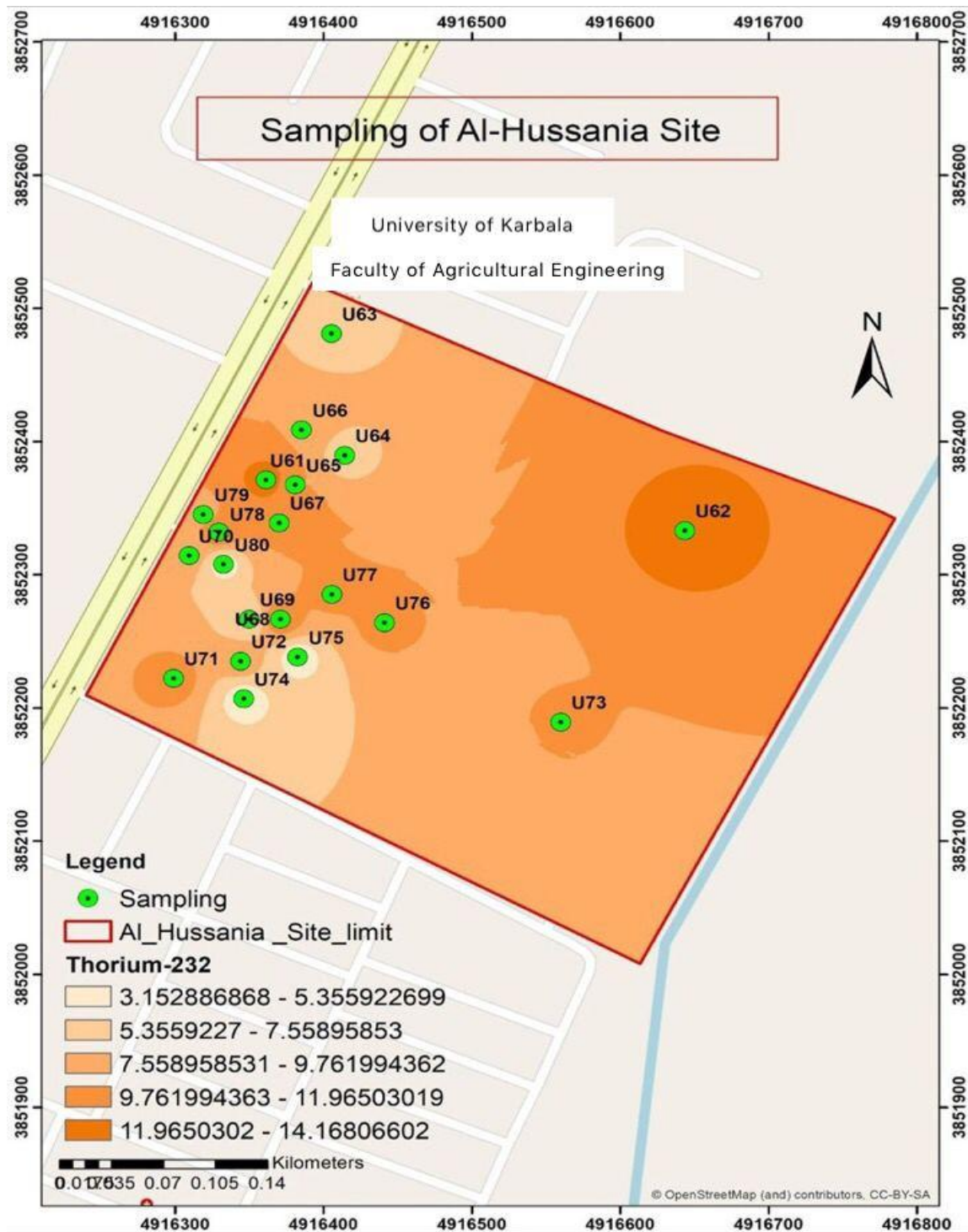


Figure (4-5): Map of the values of specific activity of ²³²Th in Agricultural College of Kerbala university

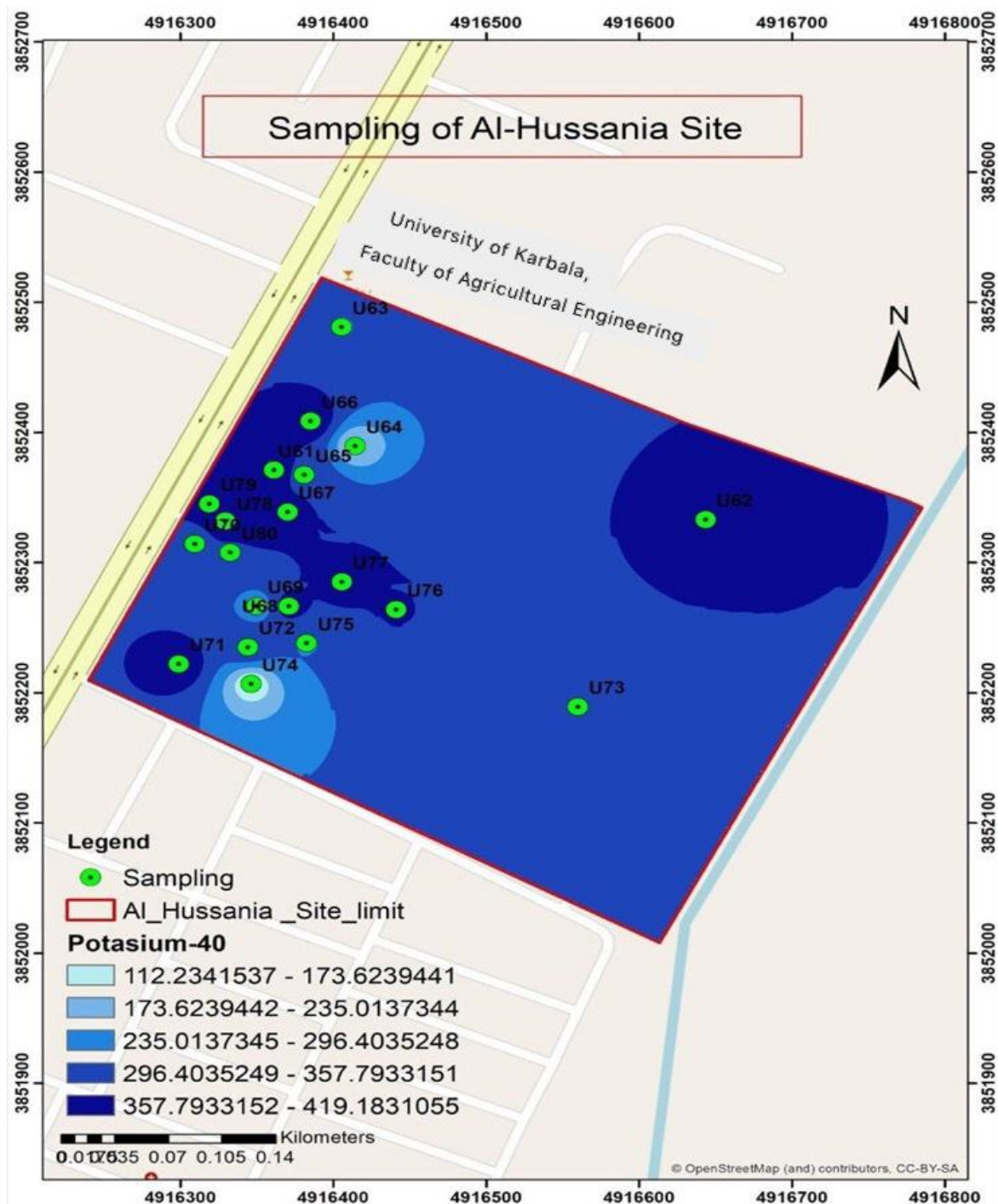


Figure (4-6): Map of the values of specific activity of ^{40}K in agricultural college of Kerbala University

4.2.2.2 Radiological Effects

The results of Ra_{eq} , H_{ex} , H_{in} , $I_{\gamma r}$, I_{α} are shown in Table (4.5). As can be seen from Table (4.5), the values of Ra_{eq} in Bq/kg varied from 37.5 to 77.1 Bq / kg with an average of 61.11 ± 2.589 Bq/kg. The maximum of Ra_{eq} are less than 370 Bq/kg[125]. Results for H_{ex} , H_{in} , $I_{\gamma r}$, and I_{α} (as shown in Table (4.5)) were range from 0.101 to 0.208 with an average value of 0.165 ± 0.0070 , from 0.157 to 0.302 with an average of 0.224 ± 0.009 , from 0.58 to 0.269 with an average of 0.463 ± 0.019 , and from 0.0325 to 0.1755 with an average of 0.108 ± 0.0080 , respectively. The results of the risk indicators H_{ex} , H_{in} , $I_{\gamma r}$, and I_{α} for all values for all samples studied during this work are but one which is that the maximum value of the recommended permissible safety limit[126, 133].

Table (4.5): Results of Ra_{eq} , H_{ex} , H_{in} , $I_{\gamma r}$ and I_{α} in Agricultural College of Kerbala university

NO.	Sample code	Ra_{eq} (Bq/kg)	H_{ex}	H_{in}	$I_{\gamma r}$	I_{α}
61	U61	58.2	0.157	0.175	0.457	0.0325
62	U62	73.2	0.198	0.266	0.553	0.1255
63	U63	44.6	0.120	0.157	0.345	0.068
64	U64	39.4	0.106	0.160	0.288	0.0995
65	U65	66.7	0.180	0.255	0.499	0.138
66	U66	61.3	0.166	0.207	0.478	0.0765
67	U67	72.3	0.195	0.269	0.545	0.1355
68	U68	77.1	0.208	0.285	0.580	0.1415

69	U69	47.3	0.128	0.186	0.355	0.108
70	U70	52.9	0.143	0.189	0.404	0.0855
71	U71	72.3	0.195	0.260	0.551	0.1195
72	U72	69.1	0.187	0.262	0.521	0.1385
73	U73	69.7	0.188	0.270	0.520	0.1505
74	U74	37.5	0.101	0.167	0.269	0.1205
75	U75	60.4	0.163	0.214	0.453	0.094
76	U76	55.7	0.150	0.183	0.432	0.0605
77	U77	65.8	0.178	0.234	0.504	0.1035
78	U78	61.8	0.167	0.198	0.482	0.057
79	U79	76.6	0.207	0.302	0.572	0.1755
80	U80	60.3	0.163	0.241	0.457	0.145
Maximum		77.1	0.208	0.302	0.269	0.1755
Minimum		37.5	0.101	0.157	0.58	0.0325
Avarege± S.E.		61.11±2.589	0.165±0.0070	0.224±0.009	0.46±0.019	0.108±0.0080
Worldwide mean		<370[125]	<1[3]	<1[3]	<1[3]	<1[3]

The results of X, Dr, AGED, AEDE outdoor, ELCR were listed in Table (4.6). From this Table, it can be seen the maximum value of X was 167.7 $\mu\text{R/h}$ in sample U68, while the minimum was 77.3 $\mu\text{R/h}$ in sample U74, with an average value of $134.1 \pm 5.735 \mu\text{R/h}$, the results of D_r ranges from from 17.8 nGy / h to 37.3 nGy/h with an average value of $29.745 \pm 1.259 \text{ nGy/h}$. The values of D_r in all samples

of the present study were smaller than world average value (55 nGy / h) according to UNSCEAR 2000[127]. The values of AGED, as shown in Table (4.6) were ranged from 123.7mSv / y to 264.9mSv / y with an average of 212.115 ± 9.031 mSv/y. So, the values of AGED in all samples are lower when compared with the world average Permissible limit ≤ 300 mSv / y [110]. The results of AEDE outdoor in this study were ranged from 0.022 mSv / y to 0.046 mSv / y, with an average of 0.0365 ± 0.0015 mSv / y. As all AEDE outdoor values are lower than the corresponding universal values of , they are 0.08 mSv/y[128]. The data of ELCR were ranged from 0.077×10^{-3} to 0.16×10^{-3} with an average of $(0.12775 \pm 0.0053) \times 10^{-3}$. According to these results, the (ELCR) values are very low; therefore, it has been determined, that the risk of developing cancer is negligible. The results of the radioactive hazard due to natural radionuclides of the studied samples were lower than the global average according to OECD [129], ICRP[130], UNSCEAR[131], and others.

Table (4.6): Results of X, Dr, AGED, AEDE_{outdoor}, ELCR in Agricultural College of Kerbala university

No .	Sample code	Exposure rate(μ R/h)	Dr (nGy/h)	AGED(mSv/y)	AEDE _{outdoor} (mSv/y)	ELCR $\times 10^{-3}$
1	U61	132.7	28.6	207.5	0.035	0.123
2	U62	159.9	35.4	252.3	0.043	0.152
3	U63	100.3	22.1	158.8	0.027	0.095
4	U64	83.1	18.8	131.9	0.023	0.081
5	U65	144.3	32.3	228.7	0.040	0.139
6	U66	138.8	30.4	219.2	0.037	0.130
7	U67	157.5	35.0	249.1	0.043	0.150
8	U68	167.7	37.3	264.9	0.046	0.160
9	U69	102.8	23.1	163.6	0.028	0.099
10	U70	116.9	25.8	184.8	0.032	0.111
11	U71	159.7	35.3	252.5	0.043	0.152
12	U72	150.8	33.6	239.2	0.041	0.144
13	U73	150.1	33.6	238.0	0.041	0.144
14	U74	77.3	17.8	123.7	0.022	0.077
15	U75	130.8	28.9	205.4	0.035	0.124
16	U76	125.3	27.3	197.1	0.034	0.117
17	U77	146.0	32.2	230.7	0.040	0.138
18	U78	140.0	30.4	219.8	0.037	0.131
19	U79	165.5	37.2	263.2	0.046	0.160
20	U80	132.5	29.8	211.9	0.037	0.128
Maximum		167.7	37.3	264.9	0.046	0.160
Minimum		77.3	17.8	123.7	0.022	0.077
Average\pmSD		134.1\pm5.7	29.74\pm1.2	212.11\pm9.03	0.036\pm0.0015	0.12\pm0.005
Worldwide mean		-----	55[132]	≤ 300 [110]	0.08 [128]	1×10^{-3}

4.2.3 Gamma Emitters in Al-Mothafeen Site

4.2.3.1 Specific Activity

The specific activities of the ^{238}U , ^{232}Th and ^{40}K , radionuclides were measured in selected soil samples from different locations from, the university of Karbala (Al-Mothafeen Site), and their radiation hazard parameters are listed in Table

(4.7). From Table (4.7), The specific activity for ^{238}U ranged from 11.0 ± 0.7 Bq/kg in sample U98 to 41.5 ± 1.4 Bq/kg in sample U94 with an average value of 22.4 ± 8.8 Bq/kg, however the specific activity for ^{232}Th varied from 6.1 ± 0.3 Bq/kg in sample U88 to 17.3 ± 0.5 Bq/kg in sample U95 with an average value of 11.19 ± 3.3 Bq/kg. In addition, the values of ^{40}K were ranged from 207.1 ± 3.2 Bq/kg in sample U95 to 448.4 ± 6.0 Bq/kg in sample U87 with an average value of 333.11 ± 70.7 Bq/kg.

Table (4.7): Results of specific activity in Al-Mothafeen Site of Kerbala university

No.	Sample code	Specific activity in Bq/kg					
		Uranium-238		Thorium-232		Potassium-40	
		Average	\pm S.D	Average	\pm S.D	Average	\pm S.D
1	U81	16.3	0.9	11.0	0.5	403.6	4.8
2	U82	14.5	0.9	6.7	0.4	249.5	3.8
3	U83	16.3	1.0	6.1	0.4	360.9	4.8
4	U84	17.6	1.0	11.9	0.5	397.5	5.1
5	U85	37.2	1.5	12.1	0.5	373.7	4.9
6	U86	17.5	1.0	13.0	0.5	313.9	4.6
7	U87	25.1	1.4	17.2	0.7	448.4	6.0
8	U88	17.7	1.0	6.1	0.3	374.4	4.7
9	U89	27.3	1.5	10.5	0.6	314.1	5.3
10	U90	31.4	1.5	10.5	0.5	424.7	5.6
11	U91	32.2	1.2	10.1	0.4	240.4	3.3
12	U92	30.1	1.4	16.8	0.6	340.5	5.0
13	U93	31.1	1.4	14.7	0.6	216.1	3.9
14	U94	41.5	1.4	10.8	0.4	290.5	3.9
15	U95	13.1	0.8	17.3	0.5	207.1	3.2
16	U96	12.4	0.8	10.9	0.4	313.0	4.1
17	U97	12.9	0.8	6.6	0.3	244.6	3.6
18	U98	11.0	0.7	11.2	0.5	348.7	4.4
19	U99	24.4	1.3	10.4	0.5	396.9	5.2
20	U100	18.4	0.9	9.9	0.4	403.7	4.4
	maximum	41.5	1.4	17.3	0.5	448.4	6.0
	minimum	11.0	0.7	6.1	0.3	207.1	3.2
	Average \pm S.D	22.4 \pm 8.8		11.19 \pm 3.3		333.11 \pm 70.7	
	Worldwide average[124]	33		45		420	

The UNSCEAR 2008 recommended standard indicate that the worlds average specific activity of ^{238}U , ^{232}Th and ^{40}K are 33 Bq/kg, 45 Bq/kg, and 420 Bq/kg, respectively[124]. From leads to Table (4.7), it had been found that each one values of ^{238}U specific activities were less than the worlds average activity that recommended by UNSCEAR 2008 that the precise activities, with the exception of U85and U94. While all values of the specific activity of ^{232}Th were within the UNSCEAR 2008 report. Also as, it's is clear for ^{40}K , that the precise activities, with the exception U26, U35 U37 and samples were only found to be above worldwide average (420 Bq/kg). Figures (4-7), (4-8), and (4-9) were drawn by GIS technique, show the geographical distribution of the Freiha site and therefore the amount of the specific activity for uranium-238, thorium -232 and potassium-40 within the soil of this region, where different colors were wont to distinguish between high, medium and low quantities.

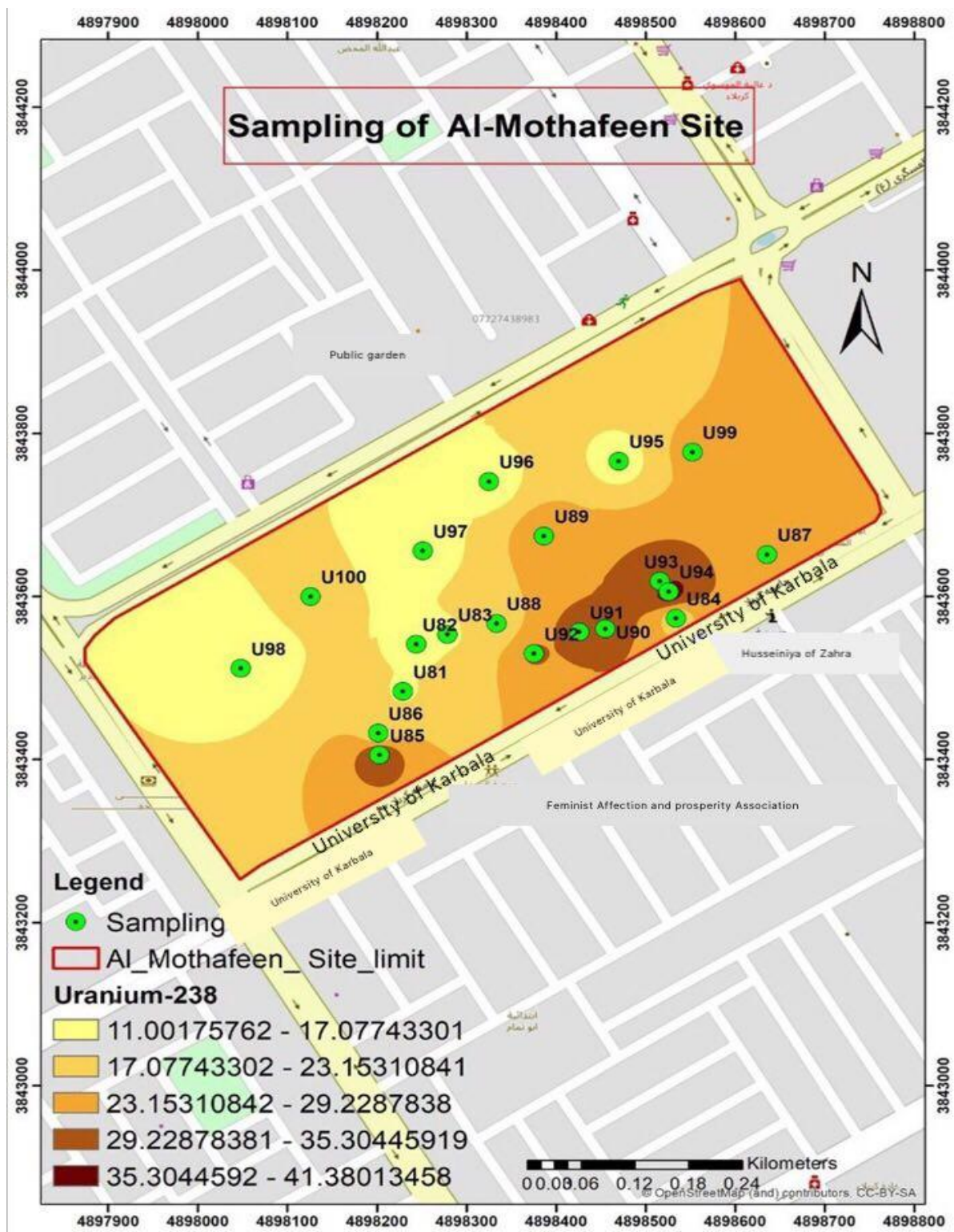


Figure (4-7): Map of the values of specific activity of ^{238}U in Al-Mothafeen Site of Kerbala university

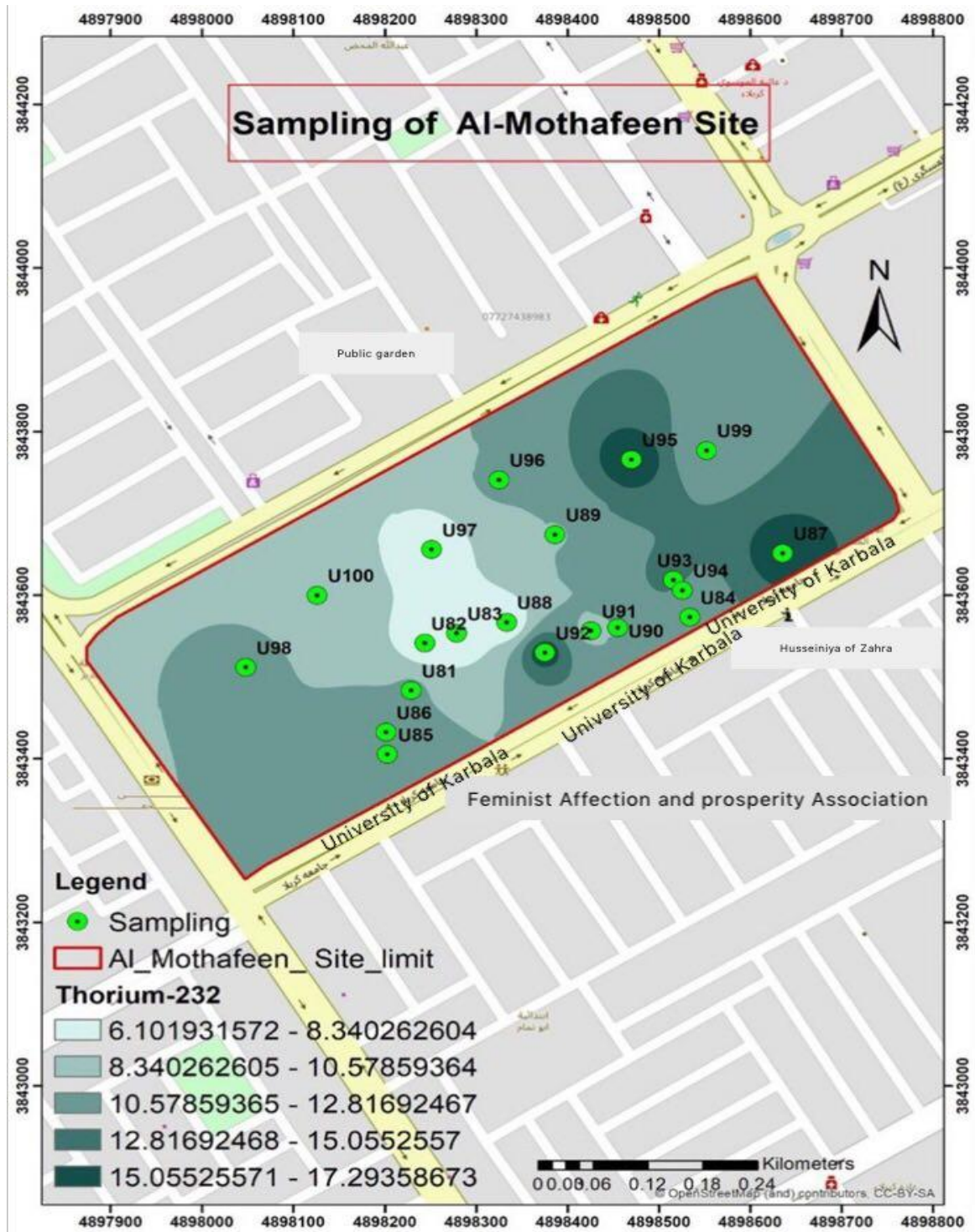


Figure (4-8): Map of the values of specific activity of ^{232}Th in Al-Mothafeen Site of Kerbala university

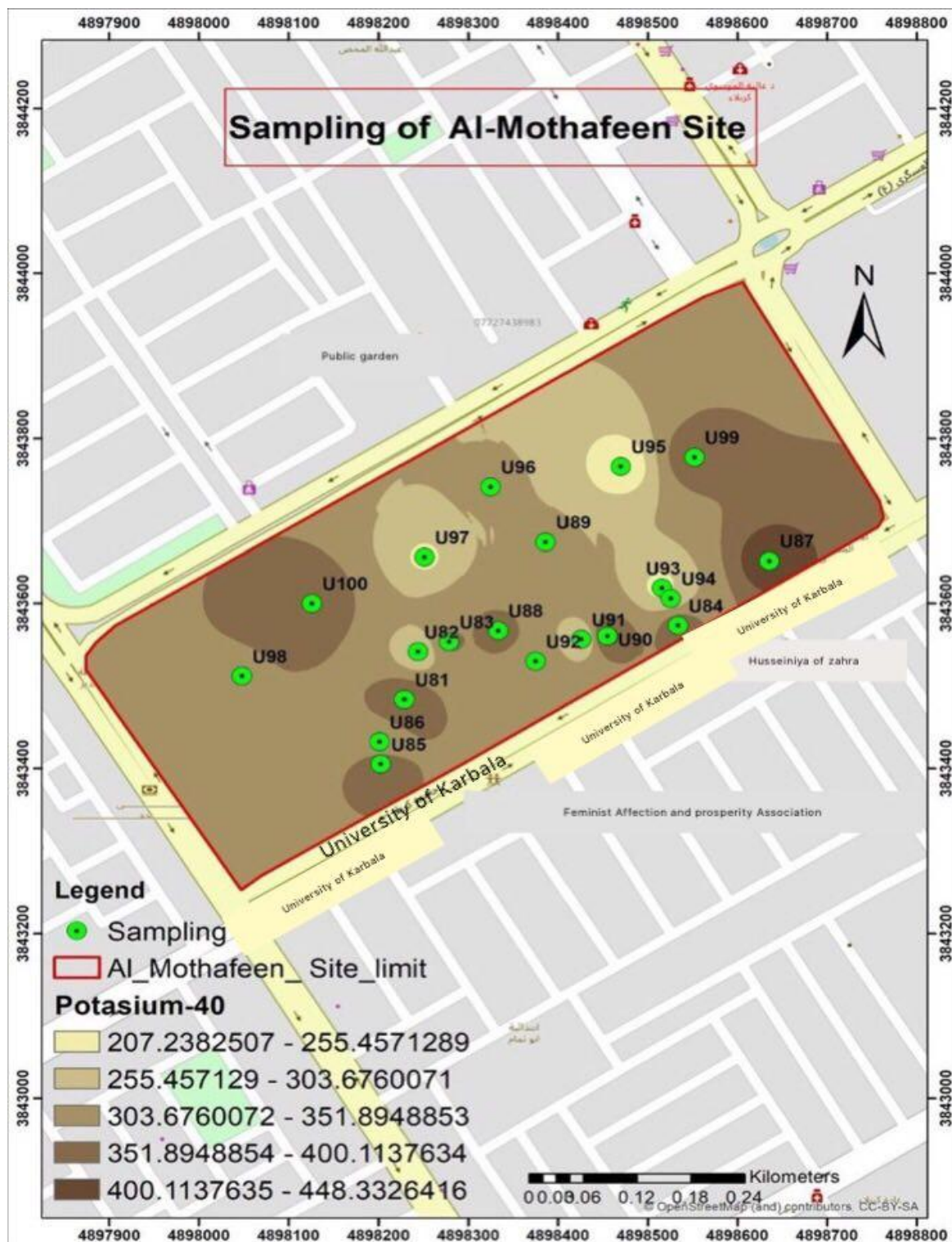


Figure (4-9): Map of the values of specific activity of ^{40}K in Al-Mothafeen Site of Kerbala university

4.2.3.3 Radiological Effects

The results of Ra_{eq} , H_{ex} , H_{in} , I_{yr} , I_{α} are shown in Table (4.8). which shows the values of Ra_{eq} in Bq/kg varied from 41.2 to 84.2 Bq/kg with an average of 64.055 ± 2.777 Bq/kg. The maximum of Ra_{eq} are less than 370 Bq/kg [125]. Results for H_{ex} , H_{in} , I_{yr} , and I_{α} see Table (4.8) were range from 0.111 to 0.227 with an average value of 0.173 ± 0.0075 , from 0.146 to 0.326 with an average of 0.2335 ± 0.0122 , from 0.315 to 0.638 with an average of 0.4832 ± 0.0199 , and from 0.055 to 0.2075 with an average of 0.112 ± 0.0098 , respectively. The results of the risk indicators H_{ex} , H_{in} , I_{yr} , and I_{α} for all values for all samples studied in this work are less than one, which is the maximum recommended safety limit value [126].

Table (4.8): Results of Ra_{eq} , H_{ex} , H_{in} , I_{yr} and I_{α} in Mothafeen Site of Kerbala university

No	Sample code	Ra_{eq} (Bq/kg)	H_{ex}	H_{in}	I_{yr}	I_{α}
1	U61	58.2	0.157	0.175	0.457	0.0325
2	U62	73.2	0.198	0.266	0.553	0.1255
3	U63	44.6	0.120	0.157	0.345	0.068
4	U64	39.4	0.106	0.160	0.288	0.0995
5	U65	66.7	0.180	0.255	0.499	0.138
6	U66	61.3	0.166	0.207	0.478	0.0765
7	U67	72.3	0.195	0.269	0.545	0.1355
8	U68	77.1	0.208	0.285	0.580	0.1415
9	U69	47.3	0.128	0.186	0.355	0.108
10	U70	52.9	0.143	0.189	0.404	0.0855
11	U71	72.3	0.195	0.260	0.551	0.1195
12	U72	69.1	0.187	0.262	0.521	0.1385
13	U73	69.7	0.188	0.270	0.520	0.1505
14	U74	37.5	0.101	0.167	0.269	0.1205
15	U75	60.4	0.163	0.214	0.453	0.094
16	U76	55.7	0.150	0.183	0.432	0.0605
17	U77	65.8	0.178	0.234	0.504	0.1035
18	U78	61.8	0.167	0.198	0.482	0.057
19	U79	76.6	0.207	0.302	0.572	0.1755
20	U80	60.3	0.163	0.241	0.457	0.145
Maximum		84.2	0.227	0.326	0.638	0.2075

Minimum	41.2	0.111	0.146	0.315	0.055
Average \pmS.D	64.05\pm2.77	0.17\pm0.007	0.23\pm0.012	0.483\pm0.019	0.112\pm0.0098
Worldwide mean	<370[125]	<1[126]	<1[3]	<1[3]	<1[3]

The results of X, Dr, AGED, AEDE outdoor, ELCR were listed in Table (4.9). from this table, it can be seen the maximum value of X was 184.5 μ R/h in sample U87, while the minimum was 91.3 μ R/h in sample U97, with an average value of 139.73 \pm 5.734 μ R/h, the results of D_r ranges from 20.1 to 40.7 nGy / h with an average value of 31.005 \pm 1.313 nGy/h. The values of D_r in all samples of present study were smaller than value of the world average which equals (55 nGy /hour) according to UNSCEAR 2000[127]. AGED values, as shown in Table (4.9) were ranged from 144.3 mSv/yt to 290.3 mSv /y with an average of 220.60 \pm 9.119 mSv/y. So, the values of AGED in all samples are lower when compared with the world average permissible limit of \leq 300 mSv/y[110] The results of AEDE outdoor in this study were ranged from 0.025 mSv/y to 0.05 mSv/y, with an average of 0.038 \pm 0.0015 mSv /y. Since all external AEDE values are lower than their corresponding global values, it is 0.08 mSv / y [134]. The data of ELCR were ranged from 0.086 $\times 10^{-3}$ to 0.175 $\times 10^{-3}$ with an average of (0.1330 \pm 0.0056) $\times 10^{-3}$. According to these results, the values of ELCR are very low; therefore, it has been determined that the risk of developing cancer is negligible. The results of the radioactive hazard due to natural radionuclides of the studied samples were less than the global average according to OECD [129], ICRP[130], UNSCEAR[131]], and other.

Table (4.9): Results of X, Dr, AGED, AEDE_{outdoor}, ELCR in Al-Mothafeen Site of Kerbala university

No	Sample code	Exposure rate ($\mu\text{R/h}$)	Dr (nGy/h)	AGED (mSv/y)	AEDE _{outdr} (mSv/y)	ELCR $\times 10^{-3}$
1	U61	132.7	28.6	207.5	0.035	0.123
2	U62	159.9	35.4	252.3	0.043	0.152
3	U63	100.3	22.1	158.8	0.027	0.095
4	U64	83.1	18.8	131.9	0.023	0.081
5	U65	144.3	32.3	228.7	0.040	0.139
6	U66	138.8	30.4	219.2	0.037	0.130
7	U67	157.5	35.0	249.1	0.043	0.150
8	U68	167.7	37.3	264.9	0.046	0.160
9	U69	102.8	23.1	163.6	0.028	0.099
10	U70	116.9	25.8	184.8	0.032	0.111
11	U71	159.7	35.3	252.5	0.043	0.152
12	U72	150.8	33.6	239.2	0.041	0.144
13	U73	150.1	33.6	238.0	0.041	0.144
14	U74	77.3	17.8	123.7	0.022	0.077
15	U75	130.8	28.9	205.4	0.035	0.124
16	U76	125.3	27.3	197.1	0.034	0.117
17	U77	146.0	32.2	230.7	0.040	0.138
18	U78	140.0	30.4	219.8	0.037	0.131
19	U79	165.5	37.2	263.2	0.046	0.160
20	U80	132.5	29.8	211.9	0.037	0.128
Maximum		184.5	40.7	290.3	0.05	0.175
Minimum		91.3	20.1	144.3	0.025	0.086
Average \pmS.D		139.73\pm5.73	31.005\pm1.31	220.60\pm9.119	0.03\pm0.001	0.13\pm0.05
Worldwide mean		-----	55[132]	≤ 300 [110]	0.08 [128]	1×10^{-3}

4.2.4 Compare The Results of Gamma Emitters between Sites in present Study

A summary of the average of the specific activity for ^{238}U , ^{232}Th , and ^{40}K inside three locations University of Kerbala (Al-Frariha, Al-Hussania, Al-Mothafeen) were shown in Tables (4.1), (4.4) and (4.7). While the average of radiological hazard index in the same three locations university of Kerbala were shown in Tables (4.2), (4.3), (4.5), (4.6), (4.8), and (4.9). The highest average of specific activity of uranium-238 and thorium-232 were found in Al-Mothafeen site, while the highest average of specific activity potassium-40 was in Al-Hussania site, and the average of specific activity in all area under study within global average limit according to UNSCEAR 2008, as shown in Figures (4-10), (4-11), and (4-12). Also the highest average value of radiological effects were found in the Al-Mothafeen side. The result in the soil samples in the current study were below the recommended procedure level according to UNSCEAR, OCDE, and ICRP, as shown in Figure (4-13).

From the above results of the normal radioactivity, it is found that the difference between the values of ^{238}U , ^{232}Th , and ^{40}K . These differences are attributable thanks to soil type during this location which is sandy and clay soils. Also, it are often see that the precise activity of uranium is above thorium altogether samples. It's also observed that the measured specific activity of ^{40}K exceeds markedly the values of both uranium and thorium, because it is that the most abundant radioactive element under concentration. Moreover, the excessive use of the potassium-containing fertilizers within the area adjacent to the sampling sites may contribute to the upper values of ^{40}K activity. The decrease or increase of the recorded values is thanks to several factors like soil type, the geological

nature of the world, the region selected (agricultural or industrial), or could also be exposed to other external factors.

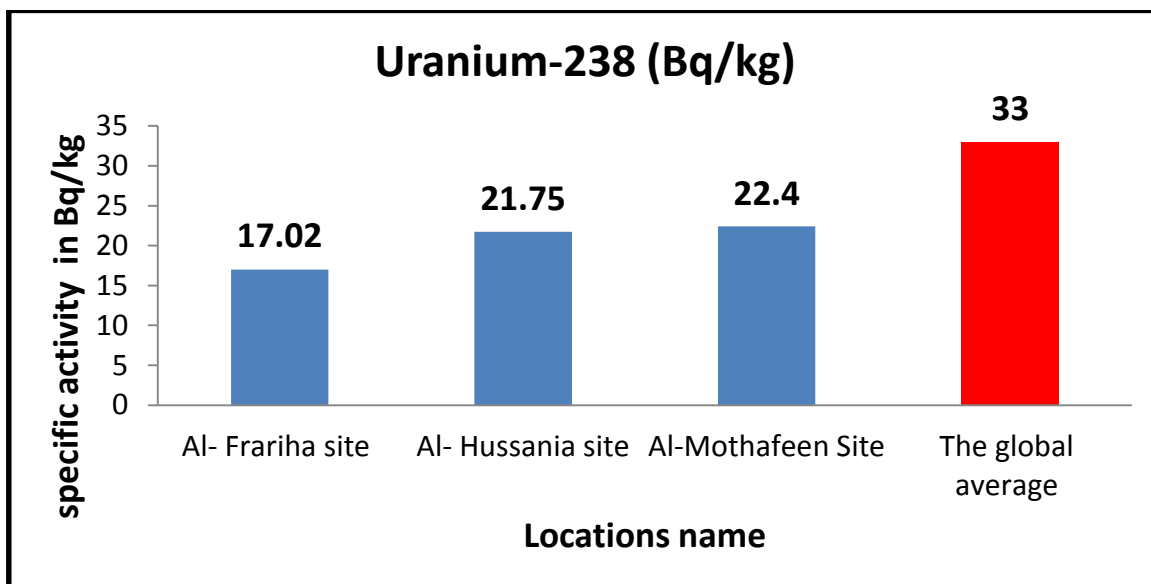


Figure (4-10): Comparing of specific activity for ²³⁸U in all locations under study.

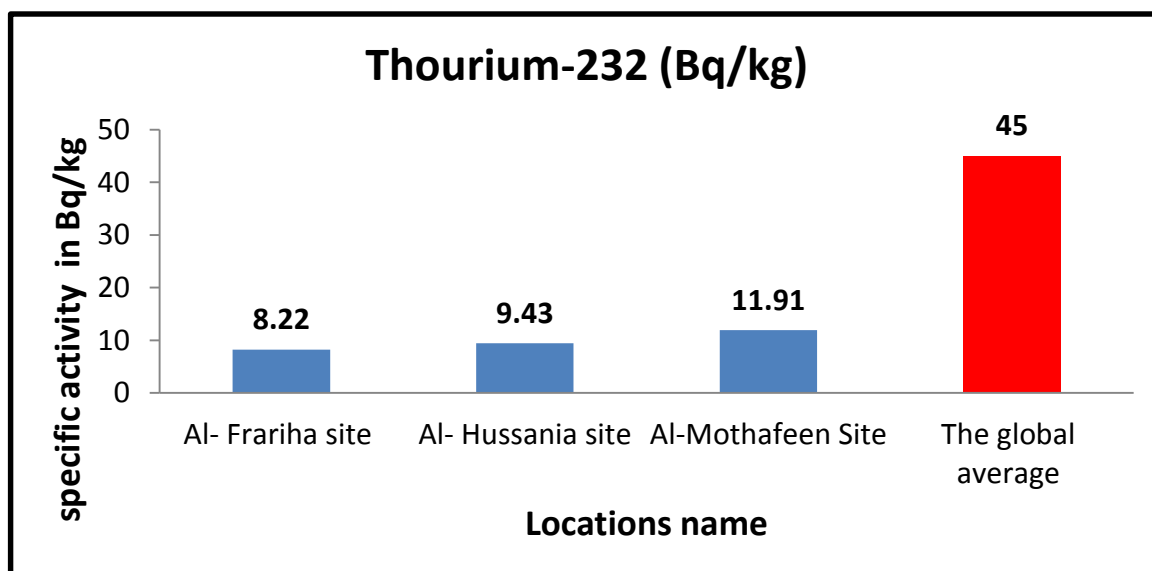


Figure (4-11): Comparing of specific activity for ²³²Th in all locations under study.

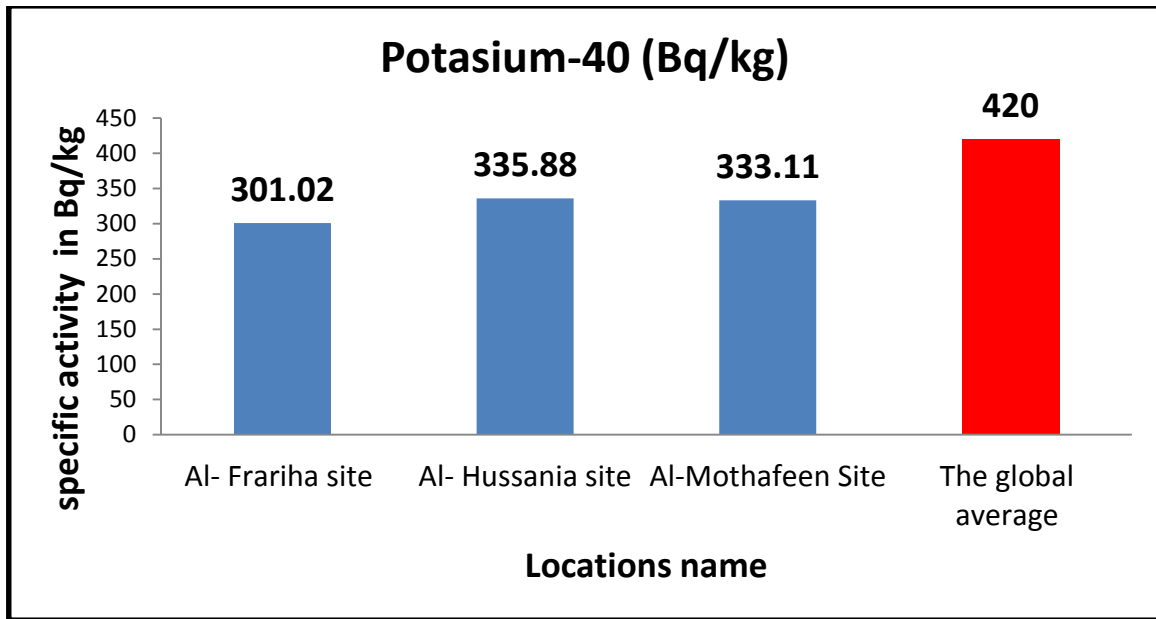


Figure (4-12): Comparing of specific activity for ⁴⁰K in all locations under study.

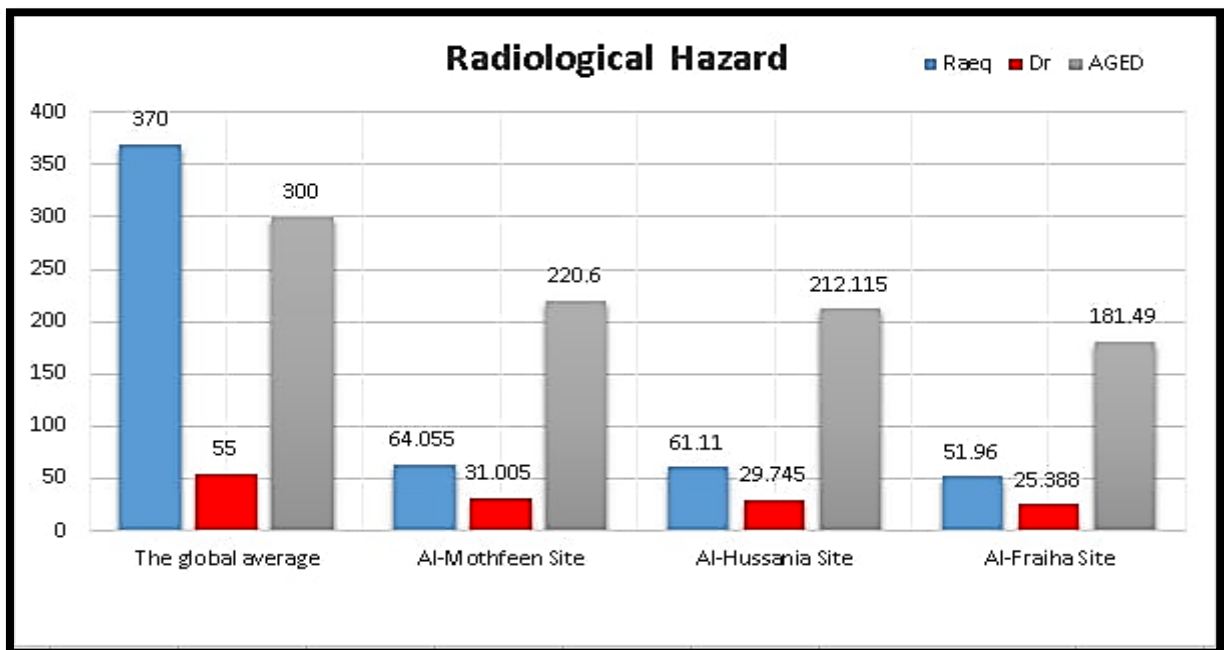


Figure (4-13): Comparing of radiological hazard due to gamma emitters in all locations under study.

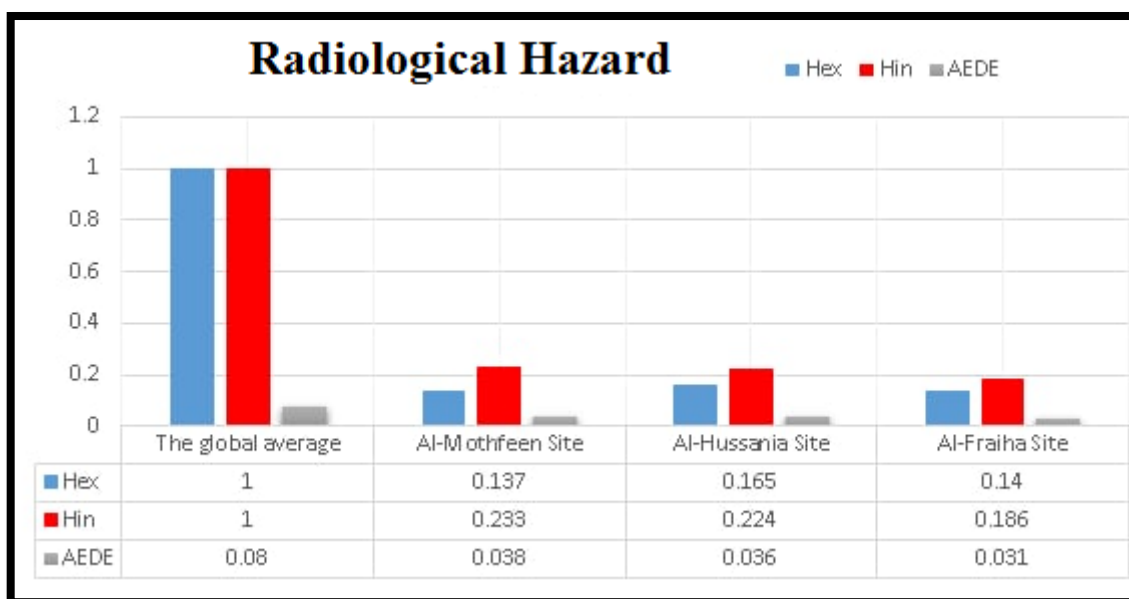


Figure (4-14): Comparing of radiological hazard due to gamma emitters in all locations under study.

4.2.5 Compare the Results of Gamma Emitters with other Study

When the results of the specified activity average for ^{238}U , ^{232}Th , and ^{40}K obtained from the current study are compared with the results recorded in different countries (out Iraq and in Iraq) as shown in Tables (4.10) and (4.11) respectively. It is found that the activity specified for ^{238}U is higher than Saudi Arabia, Turkey, Serbia, but it is less of the values recorded in Jordan, Thailand, Nigeria, Iran and Qatar, Spain, as shown in Table (4.10). The average value of specific activities for ^{232}Th in this study was less than the values specified in Thailand, Nigeria, Jordan, Spain, Nigeria, Serbia, Saudi Arabia, Iran, Turkey and higher from Qatar. The average activities specified for ^{40}K in this research were lower than Spain, Thailand, Iran, Saudi Arabia, Nigeria, and higher from Jordan, Serbia, Qatar, Turkey.

The results of the average values of the specific activities for ^{238}U in this study correspond to lower values from Maysan and Kurdistan, and higher than, Babylon, Najaf, Babylon and Karbala. The average value for specific activities for the ^{232}Th is lower than Karbala, Babylon, Maysan, Kurdistan, and Babel and is very close to the value recorded in Najaf. Finally, the activities identified for ^{40}K in the current study correspond to lower values than, Babylon and Maysan, and higher from Karbala, Najaf and Kurdistan. As shown in Table (4.11).

Table (4.10): Comparison of the Present Study Results in Soil with Different Countries.

NO.	Countries	Specific Activity in Bq/kg			Reference
		^{238}U	^{232}Th	^{40}K	
1	Qatar	25.5	7.7	165.8	[26]
2	Spain	25.2	28.9	384.4	[31]
3	Serbia	2.52	9.40	1.60	[24]
4	Saudi Arabia	14.22	14	968.19	[37]
5	Jordan	49	70	291	[23]
6	Iran	23	31	453	[36]
7	Turkey	7.4	9.5	35.7	[35]
8	Thailand	64.48	67.04	447.7	[25]
9	Nigeria	76	204.48	755.6	[38]
	Iraq (Karbala)	19.04	9.06	314.41	Present study

Table (4.11): Comparison of the Results of the Current Study in Soil with Different Sites in Iraq.

NO.	Governorate	Specific Activity in Bq/kg			Reference
		^{238}U	^{232}Th	^{40}K	
1	Babylon	14.07	12.32	416.65	[28]
2	Missan	21.19	9.72	453.91	[30]
3	Karbala	19.45	24.47	245.1	[32]
4	Babylon	16.07	9.60	271.42	[29]
5	Najaf	17.48	8.59	298.31	[33]
6	Sulaimany	83.337	19.147	284.86	[27]
Karbala (University)		19.04	9.06	314.41	Present study

4.3 Alpha Particles Emitters

4.3.1 Alpha Emitters in Freiha site

Table (4.12) shows nuclear track densities (ρ) on surface of detector CN-85, the radon concentration in air space (C), the radon concentration in samples (C_{Rn}), and annual effective dose (AED) respectively, Table (4.13) shows radium concentration (C_{Ra}), mass exhalation rate (E_m), surface exhalation rates (E_s), uranium concentration (C_U), and uranium concentration unit in Bq.kg^{-1} of uranium (C_U).

4.3.1.1 Radon Concentration and Annual Effective Dose

Shown in table (4.12) the results of C were ranged between $228.92 \pm 1.68 \text{ Bq/m}^3$ in U27 sample to $21.802 \pm 0.51 \text{ Bq/m}^3$ in U41 sample to with an average value of $120.82 \pm 1.19 \text{ Bq/m}^3$. C_{Rn} were ranged between $680.25 \pm 2.89 \text{ Bq/m}^3$ in U27 sample to $7142.62 \pm 9.39 \text{ Bq/m}^3$ in U41 sample to with an average value of $3769.718 \pm 6.678583 \text{ Bq/m}^3$, the ^{222}Rn concentration in soil samples of the area was less than the world average soil radon concentration (7400 Bq/m^3) [135]. Also from Table (4.12) and Figure (4-15), it is found that the AED was between $0.55 \pm 0.08 \mu\text{Sv/y}$ in U27 sample and $5.77 \pm 0.26 \mu\text{Sv/y}$ in U41 sample to with an average value of $3.02 \pm 0.18 \mu\text{Sv/y}$. The values of AED for all soil samples obtained from Freiha site were lower than the range of acceptable level (3-10) mSv/y that recommended by ICRP (1993)[136]. Figure (4-16) was drawn by GIS technique, show the geographical distribution of C_{Rn} , in the Freiha site, where different colors were used to distinguish between high, medium and low quantities.

4.3.1.2 Radium Concentration and Exhalation Rates

Shown in table (4.13) the values of C_{Ra} were ranged from $0.177 \pm 0.04 \text{ Bq/kg}$ to $0.017 \pm 0.014 \text{ Bq/kg}$ with an average value of $0.093 \pm 0.03 \text{ Bq/kg}$. The observed the values of C_{Ra} in all soil samples of the present study were lower than the recommended action level (370 Bq/kg) [137]. It is also below the global average value of 35 Bq/kg [138]. Figure (4-17) which was drawn by GIS technique, shows the geographical distribution of C_{Ra} , in the Freiha site, where different colors were used to distinguish between high, medium and low quantities. Also from Table (4.13), the values of E_M (mBq/kg.h) and E_S ($\text{mBq/m}^2.\text{h}$) were ranged from 0.12 ± 0.04 in U27 sample to 1.33 ± 0.12 in U41 sample to with an average value of 0.70 ± 0.09 and from 5.95 ± 0.27 in U27 sample to 62.56 ± 0.87 in U41 sample to

with an average value of 30.93 ± 0.62 . The values observed for radon exhalation rate in this study were below the global average (0.016) $\text{Bqm}^{-2}\text{s}^{-1}$ ($57.6 \text{ Bqm}^{-2}\text{h}^{-1}$) [138]. The values of exhalation rates of soil samples vary from one sample to a different this variation is thanks to the content of uranium and radium and to the porosity of the soil samples.

4.3.1.3 Uranium Concentration

Table (4.13) shows the values of C_U in unit ppm were ranged from 0.040 ± 0.02 in U27 sample to 0.423 ± 0.07 in U41 sample to with an average value of 0.22 ± 0.05 , but C_U in unit Bq/kg were ranged from 0.498 ± 0.07 in U27 sample to 5.22 ± 0.25 in U41 sample to with an average 2.75 ± 0.18 . Hence, it is found that, in all of the sites, the C_U is lower than 11 mg/kg (ppm) that was published by UNSCEAR (1994) [111]. And the specific activities of uranium in soil samples are less than the allowed limit (40 Bq/kg) from UNSCEAR [139]. Figure (4-18) and fig (4-19) was drawn by GIS technique, show the geographical distribution of C_U , C_U in the Freiha site, where different colors were used to distinguish between high, medium and low quantities.

Table (4.12) Results of track density(ρ), radon concentration (C), concentration of radon in samples(C_{Rn}), annual effective dose(AED) in Freiha Site of Kerbala university

Sample	ρ (Track/cm ²)	C (Bq/m ³)	C_{Rn} (Bq/m ³)	AED (mSv/y)
U1	6080±8.66	138.08 ± 1.30	4308.25 ±7.29	3.48 ± 0.20
U2	4640± 7.56	105.37 ±1.14	3287.87±6.37	2.65± 0.18
U3	3680±5.96	83.57± 0.89	2607.62± 5.01	2.109± 0.14
U4	2880±6.74	65.40±1.01	2040.75±5.67	1.65±0.16
U5	6720±9.10	152.61±1.37	4761.75 ±7.66	3.85±0.21
U6	9759±10.97	221.65±1.65	6915.87± 9.24	5.59±0.26
U7	4160 ±7.16	94.47±1.08	2947.75± 6.03	2.38 ±0.17
U8	5280±8.07	119.91±1.21	3741.37±6.79	3.02±0.19
U9	4960±7.82	112.64 ±1.17	3514.62±6.58	2.84±0.18
U10	8960 ±10.51	203.48±1.58	6349± 8.85	5.13±0.25
U11	5600± 8.31	127.18±1.25	3968.12± 6.99	3.20±0.19
U12	4800 ±7.69	109.01 ± 1.16	3401.25 ± 6.48	2.75±0.184
U13	2400±5.44	54.50±0.82	1700.62 ± 4.58	1.37±0.13
U14	4800 ±7.69	109.01± 1.16	3401.25±6.48	2.75±0.18
U15	1600 ±4.44	36.33 ±0.67	1133.75 ±3.74	0.91±0.10
U16	5600± 8.31	127.18 ± 1.25	3968.12±6.99	3.20±0.19
U17	6080 ± 8.66	138.08± 1.30	4308.25±7.29	3.48±0.20
U18	3520 ±6.59	79.94 ± 0.99	2494.25±5.54	2.01±0.15
U19	3680 ±6.74	83.57±1.01	2607.62±5.67	2.10±0.16
U20	3200±6.28	72.67± 0.94	2267.50 ±5.29	1.83±0.15
U21	5280±8.07	119.91±1.21	3741.37±6.79	3.02±0.19
U22	5760 ± 8.43	130.81 ± 1.27	4081.50±7.09	3.30±0.20
U23	7680 ±9.73	174.41± 1.46	5442 ± 8.19	4.40 ±0.23
U24	3360 ±6.44	76.30±0.97	2380.87±5.42	1.92±0.15
U25	8480±10.23	192.58±1.54	6008.87±8.61	4.85 ±0.24
U26	7520±9.63	170.78± 1.45	5328.62± 8.11	4.30±0.23
U27	10080 ±11.15	228.92± 1.68	7142.62± 9.39	5.77±0.26
U28	6400± 8.88	145.34±1.34	4535 ± 7.48	3.66±0.21
U29	6560 ±8.99	148.98±1.35	4648.37±7.57	3.75±0.21
U30	4640±7.56	105.37±1.14	3287.87±6.37	2.65±0.18
U31	5440±8.19	123.54 ± 1.23	3854.75±6.89	3.11±0.19
U32	6079.99±8.66	138.08±1.30	4308.24±7.29	3.48 ±0.20
U33	6880±9.21	156.25±1.38	4875.12± 7.75	3.94± 0.22
U34	5600 ±8.31	127.18±1.25	3968.12 ±6.99	3.20±0.19
U35	7680± 9.73	174.41±1.46	5442± 8.19	4.40±0.23
U36	6880 ±9.21	156.25±1.38	4875.12±7.75	3.94 ±0.22
U37	8480 ±10.23	192.58±1.54	6008.87±8.61	4.85±0.24
U38	3040±6.12	69.041± 0.92	2154.12± 5.15	1.74± 0.14
U39	6400 ± 8.88	145.34± 1.34	4535± 7.48	3.66±0.21

U40	6880±9.21	156.25±1.38	4875.12±7.75	3.94± 0.22
U41	960±3.44	21.80±0.51	680.25±2.89	0.55±0.08
U42	4480±7.43	101.74±1.12	3174.50± 6.26	2.56±0.17
U43	6880± 9.21	156.25± 1.38	4875.12±7.75	3.94±0.22
U44	6080± 8.66	138.08±1.30	4308.25±7.29	3.48±0.20
U45	5760± 8.43	130.81±1.27	4081.50±7.09	3.30±0.20
U46	3040 ± 6.12	69.04±0.92	2154.12± 5.15	1.74±0.14
U47	8000 ± 9.93	181.68±1.49	5668.75±8.36	4.58±0.23
U48	6400±8.88	145.34±1.34	4535± 7.48	3.66±0.21
U49	4800± 7.69	109.01±1.16	3401.25±6.48	2.75± 0.18
U50	6080±8.66	138.08±1.30	4308.25± 7.29	3.48±0.20
U51	4320±7.30	98.11±1.10	3061.12±6.14	2.47±0.175
U52	5600±8.31	127.18±1.25	3968.12±6.99	3.20±0.19
U53	1280±3.97	29.07±0.59	907±3.34	0.73±0.09
U54	7360±9.53	167.15±1.43	5215.25±8.02	4.21±0.22
U55	2400±5.44	54.50± 0.82	1700.62±4.58	1.37±0.13
U56	4480 ±7.43	101.74±1.12	3174.5±6.26	2.56 ±0.17
U57	4800±7.69	109.01±1.16	3401.25±6.48	2.75±0.18
U58	4000±7.02	90.84±1.059	2834.37±5.91	2.29±0.16
U59	2080±5.06	47.23±0.76	1473.87± 4.26	1.19±0.12
U60	2880 ± 5.96	65.40±0.89	2040.75±5.01	1.65± 0.14
Max	10080±11.15	228.92±1.68	7142.62±9.39	5.77±0.26
Min	960±3.44	21.80±0.51	680.25±2.89	0.55 ±0.08
Average±S.D	5320±7.93	120.82±1.19	3769.71 ±6.67	3.02± 0.18
Worldwide mean	200-300[140]	7400[135].	3-10[136]

Table (4.13) Results of effective radium concentration (C_{Ra}), surface (E_s) and mass (E_M) exhalation rates. Uranium concentration (C_U) and uranium concentration (C_U) in unit Bq/kg in Freiha Site of Kerbala university

Sample	C_{Ra} (Bq/kg)	E_M (mBq/kg.h)	E_s (mBq/m ² .h)	C_U (ppm)	C_U (Bq/kg)
U1	0.107 ±0.03	0.80 ±0.10	37.73±0.68	0.25±0.05	3.15 ±0.19
U2	0.081 ± 0.03	0.61±0.08	28.80±0.59	0.19±0.04	2.40±0.17
U3	0.064±0.02	0.48± 0.06	22.84±0.47	0.15±0.03	1.90± 0.13
U4	0.050±0.02	0.38 ±0.078	17.87± 0.53	0.12±0.04	1.49±0.15
U5	0.118±0.03	0.89± 0.10	41.71±0.71	0.28±0.05	3.48±0.20
U6	0.171±0.04	1.29± 0.12	60.57±0.86	0.41±0.07	5.05± 0.25
U7	0.073 ±0.03	0.55 ±0.08	25.82±0.56	0.17±0.04	2.15±0.16
U8	0.093±0.03	0.69 ±0.09	32.77 ±0.63	0.22±0.05	2.73±.184
U9	0.087 ±0.03	0.65 ±0.09	30.78± 0.61	0.20±0.05	2.57 ±0.17
U10	0.157± 0.04	1.18±0.12	55.61±0.82	0.37±0.06	4.64±0.23
U11	0.098 ±0 .03	0.74±0.09	34.75± 0.65	0.23±0.05	2.90±0.18
U12	0.084±0.03	0.63±0.08	29.79±0.60	0.20±0.05	2.48±0.17
U13	0.042 ±0.02	0.31±0.06	14.89 ±0.42	0.10±0.03	1.24±0.12
U14	0.084± 0.03	0.63±0.08	29.79±0.60	0.20±0.05	2.48±0.17
U15	0.02±0.01	0.21± 0.05	9.93±0.35	0.06±0.02	0.82±0.10
U16	0.098±0.03	0.74± 0.09	34.75±0.65	0.23±0.05	2.90±0.19
U17	0.107± 0.03	0.80±0.10	37.73 ±0.68	0.25±0.05	3.15±0.19
U18	0.06± 0.02	0.46±0.07	21.84±0.51	0.14±0.04	1.82±0.15
U19	0.064± 0.02	0.48 ±0.07	22.84±0 .53	0.15±0.04	1.90± 0.15
U20	0.056± 0.02	0.42±0.07	19.86 ± 0.49	0.13±0.04	1.65±0.14
U21	0.093 ±0.03	0.69±0.09	32.77±0.636	0.22±0.05	2.73±0.18
U22	0.101 ±0.03	0.76± 0.09	35.75±0.66	0.24±0.05	2.98±0.19
U23	0.135 ±0.04	1.01± 0.11	47.66±0.76	0.32±0.06	3.98±0.22
U24	0.059±0.02	0.44±0.07	20.85±0.50	0.14±0.04	1.74±0.14
U25	0.149±0.04	1.12±0.11	52.63±0.80	0.35±0.06	4.39± 0.23
U26	0.132±0.04	0.99±0.11	46.67± 0.75	0.31±0.06	3.89±0.21
U27	0.17±0.04	1.33±0.12	62.56±0.87	0.42±0.07	5.22±0.25
U28	0.112±0.03	0.84±0.10	39.72±0.70	0.26±0.05	3.31±0.20
U29	0.115 ±0.03	0.86±0.10	40.71±0.709	0.27±0.05	3.40±0.20
U30	0.081±0.03	0.61±0.08	28.80± 0.59	0.19±0.04	2.40±0.17
U31	0.095 ±0.03	0.72±0.09	33.76±0.64	0.22±0.05	2.82±0.18
U32	0.107± 0.03	0.80±0.10	37.73± 0.68	0.25±0.05	3.15±0.19
U33	0.121±0.03	0.91± 0.10	42.70 ±0.72	0.28±0.06	3.56±0.21
U34	0.098±0.035	0.74±0.09	34.75±0.65	0.23±0.05	2.90±0.18
U35	0.135±0.041	1.01±0 .11	47.66±0.76	0.32±0.06	3.98±0.22
U36	0.121 ±0.03	0.91±0.10	42.70±0.72	0.28±0.06	3.56±0.21
U37	0.149±0 .04	1.12±0.11	52.63 ±0.80	0.35±0.06	4.39±0.23
U38	0.053 ± 0.02	0.40±0.07	18.86±0.48	0.12±0.04	1.57±0.13

U39	0.112±0.03	0.84±0.10	39.72±0.70	0.26±0.05	3.31±0.20
U40	0.121±0.03	0.91±0.10	42.70 ±0.72	0.28±0.06	3.56±0.21
U41	0.017±0.01	0.127±0.04	5.95±0.27	0.04±0.02	0.49 ±0.07
U42	0.079±0.03	0.593±0.08	27.80±0.58	0.18±0.04	2.32±0.16
U43	0.121±0.03	0.91± 0.10	42.70±0.72	0.28±0.06	3.56±0 .21
U44	0.107±0.03	0.80±0.10	37.73±0.68	0.25±0.05	3.15±0.19
U45	0.101±0.03	0.76±0.09	35.75±0.66	0.24±0.05	2.98±0.19
U46	0.053±0.02	0.40±0.07	18.86±0.48	0.12±0.04	1.57±0.13
U47	0.140±0.04	1.06±0.11	49.65±0.78	0.33±0.06	4.14±0.22
U48	0.112±0.03	0.84±0.10	39.72±0.70	0.26±0.05	3.31±0.20
U49	0.084 ±0.03	0.63±0.08	29.79±0.60	0.20±0.05	2.48±0.17
U50	0.107±0 .03	0.80±0.10	37.73±0.683	0.25±0.05	3.15±0.19
U51	0.076±0.03	0.57±0.08	26.81±0.57	0.18±0.04	2.23±0.16
U52	0.098±0.03	0.74±0.09	34.75±0.65	0.23±0.05	2.90±0.18
U53	0.022±0.01	0.17±0.04	7.94 ±0.31	0.05±0.02	0.66± 0.09
U54	0.129±0.04	0.97±0.11	45.68 ±0.75	0.30±0.06	3.81±0.21
U55	0.042±0.02	0.31 ±0.06	14.89±0.42	0.10±0.03	1.24±0.12
U56	0.079±0.03	0.59±0.08	27.80±0.58	0.18±0.04	2.32± 0.16
U57	0.084±0.03	0.63±0.08	29.79 ±0.60	0.20±0.05	2.48±0.17
U58	0.070 ±0.02	0.53±0.08	24.82±0.55	0.16±0.04	2.07±0.16
U59	0.036±0.02	0.27±0.05	12.91±0.39	0.08±0.03	1.07 ±0.11
U60	0.050 ±0.02	0.38±0.06	17.87± 0.47	0.12±0.03	1.49±0.13
Maximum	0.177± 0.04	1.33±0.12	62.56±0.87	0.42±0.07	5.22±0.25
Minimum	0.017±0.01	0.12±0.04	5.95±0.27	0.04±0.02	0.49±0.07
Average±S.D	0.093±.033	0.70±0.09	30.93±0.62	0.22±0.05	2.75±0.18
Worldwide mean	35[138]	57.6 [138]	57.6 [138]	11[111]	40[139]

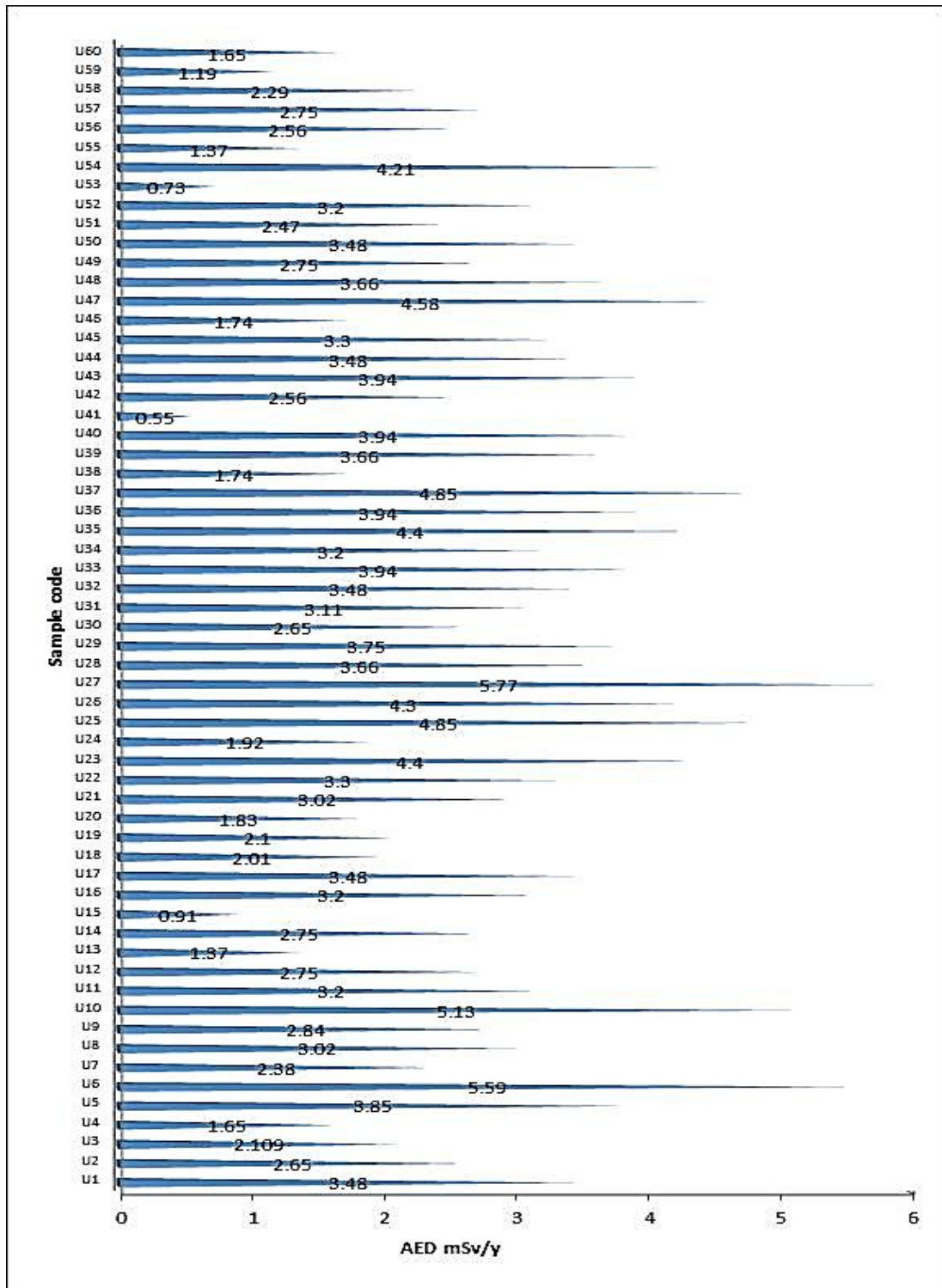


Figure (4-15): AED of radon for soil samples collected from Kerbala university of Freiha Site

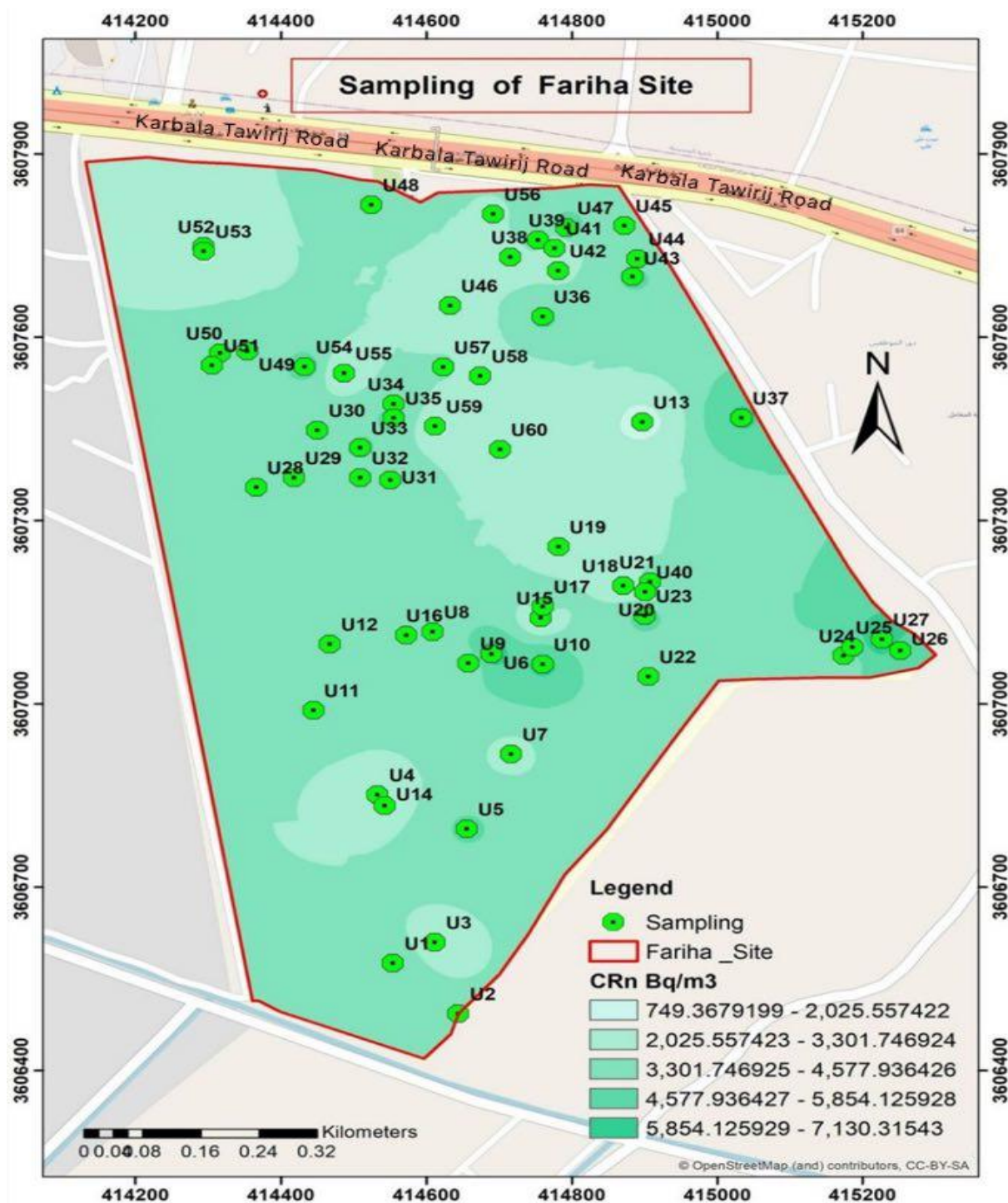


Figure (4-16): Map of the values of C_{Rn} in Fariha Site of Kerbala university

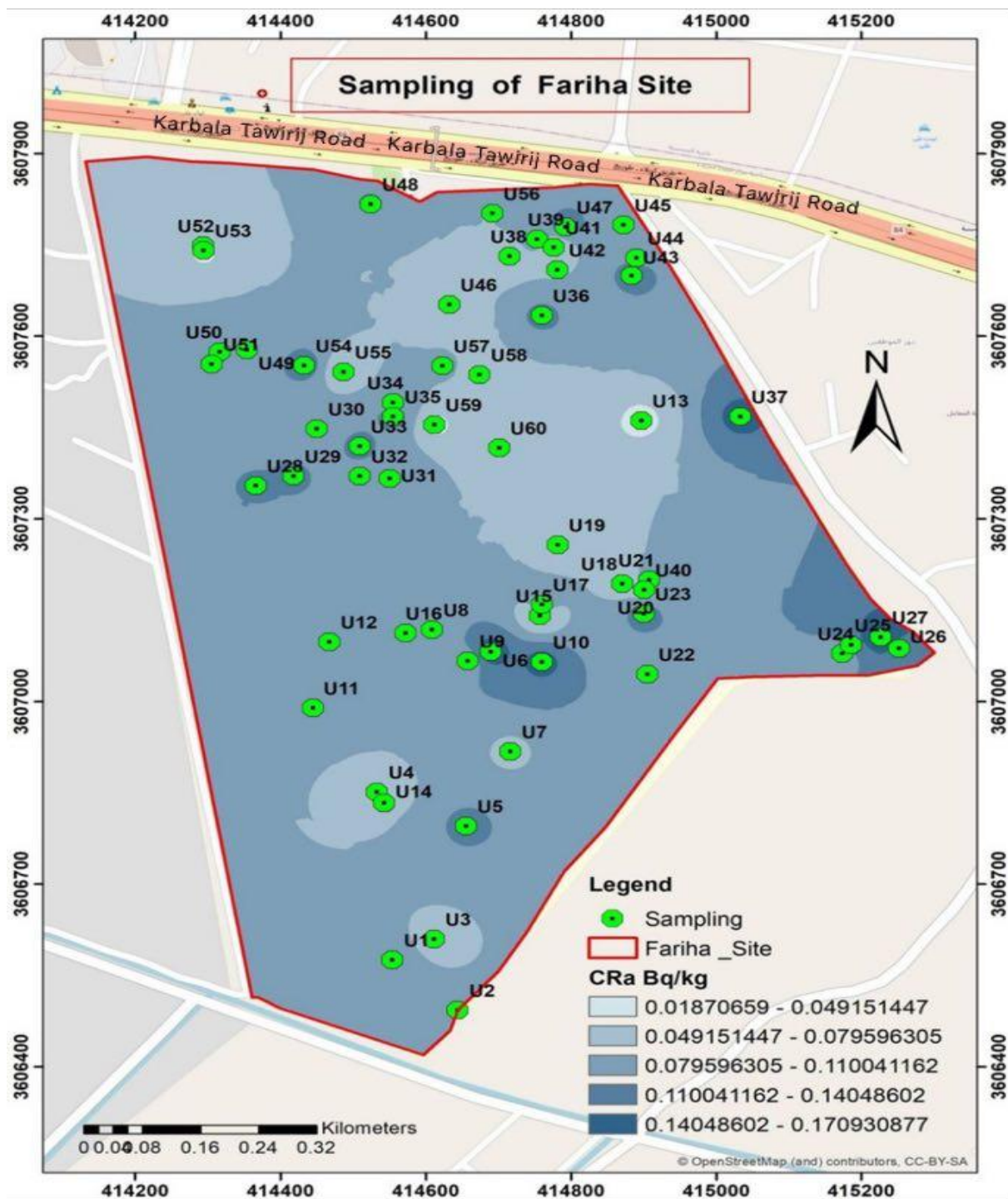


Figure (4-17): Map of the values of C_{Ra} in Fariha site of Kerbala university

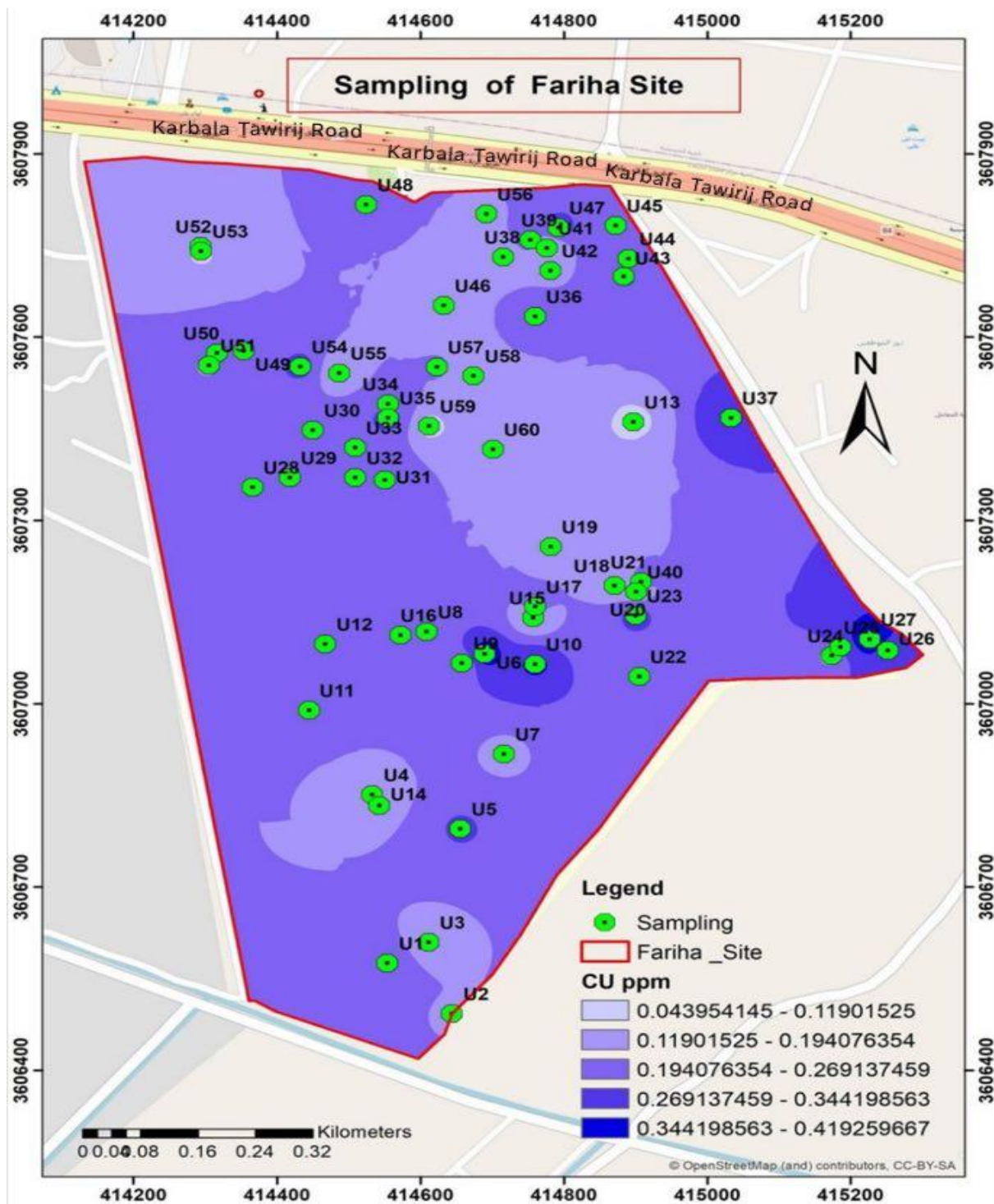


Figure (4-18): Map of the values of C_U in Fariha site of Kerbala university

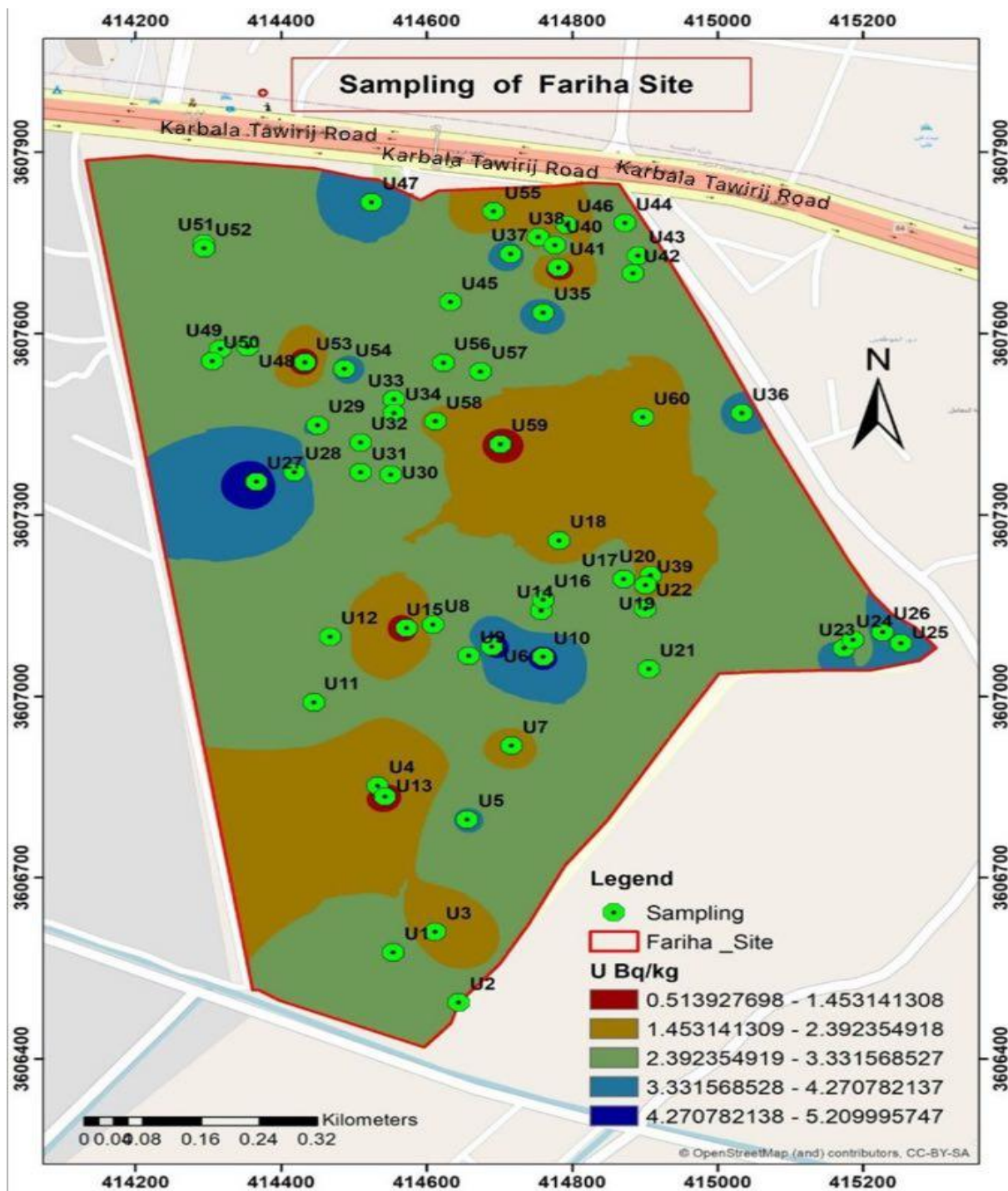


Figure (4-19): Map of the values of C_U in Fariha Site of Kerbala university

4.3.2 Alpha Emitters in Agricultural College

Table (4-14) shows nuclear track densities (ρ) on surface of detector CN-85, the radon concentration in air space (C), the radon concentration in samples (C_{Rn}), and annual effective dose (AED). respectively, Table (4-15) shows effective radium concentration (C_{Ra}), mass exhalation rates (E_m), surface exhalation rates (E_s), uranium concentration (C_U), and uranium concentration unit in $Bq.kg^{-1}$ of uranium (C_U).

4.3.2.1 Radon Concentration and Annual effective dose

Shown in table (4.14) the results of C were ranged between $243.45 \pm 1.73 Bq/m^3$ in U79 sample to $32.70 \pm 0.635 Bq/m^3$ in U61 sample to with an average value of $138.08 \pm 1.28 Bq/m^3$. C_{Rn} were ranged between $1020.37 \pm 3.54 Bq/m^3$ in U79 sample to $7596.12 \pm 9.68 Bq/m^3$ in U61 sample to with an average value of $4308.25 \pm 7.17 Bq/m^3$. The radon concentration in the soil samples in the region was lower than the global average radon concentration in the soil ($7400 Bq/m^3$) with the exception of U79 [135]. Also from Table (4.14) and Figure (4-20), it is found that the AED was between $0.82 \pm 0.10 \mu Sv/y$ in U79 sample and $6.14 \pm 0.27 \mu Sv/y$ in U61 sample to with an average value of $3.48 \pm 0.20 \mu Sv/y$. Also, the values of AED for all soil samples obtained from Freiha site were lower than the range of acceptable level (3-10) mSv/y Recommended by ICRP ICRP (1993) [136]. Figure (4-21) was drawn by GIS technique, show the geographical distribution of C_{Rn} in the Freiha site, the concentrations of radon were classified in to six range of color according to radon concentrations, where different colors were used to differentiate between high, medium, and low concentrations.

4.3.2.2 Radium concentration and Radon Exhalation Rates

Table (4.21) shows the values of C_{Ra} were ranged from 0.18 ± 0.04 Bq/kg in U79 sample to 0.02 ± 0.01 Bq/kg in U61 sample to with an average value of 0.106 ± 0.03 Bq/kg. The observed the values of C_{Ra} in all soil samples of the present study were less than the recommended action level 370 Bq/kg [137]. It is also below the global average value of 35 Bq/kg [138]. Figure (4-22) was drawn by GIS technique, show the geographical distribution of C_{Ra} in the Freiha site, the concentrations of radon were classified in to six range of color according to radon concentrations, where different colors were used to differentiate between high, medium, and low concentrations.

Also from Table (4.15), the values of E_M (mBq/kg.h) and E_S (mBq/m².h) were ranged from 0.19 ± 0.04 in U79 sample to 1.42 ± 0.13 in U61 sample to with an average value of 0.80 ± 0.0981 and from 8.93 ± 0.33 in U79 sample to 66.53 ± 0.90 in U61 sample to with an average value of 35.70 ± 0.67 . The observed values of radon exhalation rate in this study were lower than the global average of $0.016 \text{ Bq m}^{-2} \text{ s}^{-1}$ ($57.6 \text{ Bq m}^{-2} \text{ h}^{-1}$) [138]. The values of expiratory rates of soil samples differ from one sample to another, and this difference is due to the radium and uranium content and the porosity of the soil samples.

4.3.2.3 Uranium Concentration

Table (4.15) shows the values of C_U in unit ppm were ranged from (0.06 ± 0.02) ppm in U79 Sample to (0.45 ± 0.07) ppm in U61 Sample with an average value of (0.25 ± 0.05) ppm. but C_U in unit Bq/kg were ranged from in 0.74 ± 0.09 U79 sample to in 5.55 ± 0.26 U61 sample to with an average 3.15 ± 0.18 . Hence, the A_U at all sites was found to be less than 11 mg / kg (ppm) published by UNSCEAR (1994) [111]. And the specific activities the ²³⁸U in the soil samples are lower than

the allowed limit (40 Bq/kg) from UNSCEAR[139]. Figure (4-23) and fig (4-24) was drawn by GIS technique, show the geographical distribution of ^{238}U in the Agricultural College in unit of ppm and Bq/kg respectively, the concentrations of radon were classified in to six range of color according to radon concentrations, where different colors were used to differentiate between high, medium, and low concentrations.

Table (4.14) Results of track density(ρ), radon concentration (C), concentration of radon in samples(C_{Rn}), annual effective dose(AED) in Agricultural college of Kerbala university

Sample	$\rho(\text{Track}/\text{cm}^2)$	C (Bq/m ³)	C_{Rn} (Bq/m ³)	AED mSv/y
U61	1440 \pm 4.21	32.70 \pm 0.63	1020.37 \pm 3.54	0.82 \pm 0.10
U62	6400 \pm 8.8	145.34 \pm 1.34	4535 \pm 7.48	3.66 \pm 0.21
U63	4000 \pm 7.02	90.84 \pm 1.05	2834.37 \pm 5.91	2.29 \pm 0.16
U64	4640 \pm 7.56	105.37 \pm 1.14	3287.87 \pm 6.37	2.65 \pm 0.18
U65	7520 \pm 9.63	170.78 \pm 1.45	5328.62 \pm 8.11	4.30 \pm 0.23
U66	5440 \pm 8.19	123.54 \pm 1.23	3854.75 \pm 6.89	3.11 \pm 0.19
U67	8000 \pm 9.93	181.68 \pm 1.49	5668.75 \pm 8.36	4.58 \pm 0.23
U68	7040 \pm 9.32	159.88 \pm 1.40	4988.50 \pm 7.84	4.03 \pm 0.22
U69	6560 \pm 8.99	148.98 \pm 1.35	4648.37 \pm 7.57	3.75 \pm 0.21
U70	4800 \pm 7.69	109.01 \pm 1.16	3401.25 \pm 6.48	2.75 \pm 0.18
U71	8160 \pm 10.03	185.32 \pm 1.51	5782.12 \pm 8.44	4.67 \pm 0.24
U72	4640 \pm 7.56	105.37 \pm 1.14	3287.87 \pm 6.37	2.65 \pm 0.18
U73	7680 \pm 9.73	174.41 \pm 1.46	5442 \pm 8.19	4.40 \pm 0.23
U74	6400 \pm 8.88	145.34 \pm 1.34	4535 \pm 7.48	3.66 \pm 0.21

U75	5760±8.43	130.81±1.27	4081.50±7.09	3.30±0.20
U76	3840±6.88	87.20± 1.03	2721 ±5.79	2.20±0.16
U77	6560±8.99	148.98±1.35	4648.37±7.57	3.75±0.21
U78	3680±6.74	83.57± 1.01	2607.62±5.67	2.10 ±0.16
U79	10720±11.50	243.45± 1.73	7596.12±9.68	6.14±0.27
U80	8320±10.13	188.95±1.52	5895.50±8.53	4.76±0.24
Maximum	10720±11.50	243.45±1.73	7596.12 ±9.68	6.14±0.27
Minimum	1440±4.21	32.70± 0.635	1020.37± 3.54	0.82±0.10
Average±S.D	6080±85.208	138.08±1.28	4308.25±7.17	3.48±0.20
Worldwide mean	200-300[140]	7400[135].	3-10[136]

Table (4.15) Results of effective radium concentration (C_{Ra}), surface (E_s) and mass (E_M) exhalation rates. Uranium Concentration (C_U) and uranium Concentration in unit Bq/kg (C_U) in agricultural college of Kerbala university

Sample	C_{Ra} Bq/kg	E_M mBq/kg.h	E_s mBq/m².h	C_U ppm	C_U Bq/kg
U61	0.025 ±0.01	0.19±0.04	8.93±0.332	0.06±0.02	0.74±0.09
U62	0.112± 0.03	0.84±0.10	39.72± 0.70	0.26±0.05	3.31±0.20
U63	0.07 ±0.02	0.53±0.08	24.82±0.55	0.16±0.04	2.07±0.16
U64	0.081±0.03	0.61±0.08	28.80±0.59	0.19±0.04	2.40±0.17
U65	0.132± 0.04	0.99±0.11	46.67± 0.75	0.31±0.06	3.89±0.21
U66	0.095± 0.03	0.72±0.09	33.76±0.64	0.22 ±0.05	2.82±0.18
U67	0.140±0.04	1.06±0.11	49.65±0.78	0.33±0.06	4.14±0.22
U68	0.123±0.03	0.93±0 .10	43.69±0.73	0.29±0.06	3.64±0.21
U69	0.115±0.03	0.86±0.10	40.71±0.70	0.27±0.05	3.40±0.20

U70	0.084±0.03	0.63±0.08	29.79± 0.60	0.20±0.05	2.48±0.17
U71	0.143±0.04	1.08±0.11	50.64 ±0.79	0.34±0.06	4.23± 0.22
U72	0.081± 0.03	0.61±0.08	28.80±0.59	0.19±0.04	2.40±0.17
U73	0.135±0.04	1.01±0.11	47.66±0 .76	0.32±0.06	3.98±0.22
U74	0.112±0.03	0.84±0.10	39.72 ±0.70	0.26±0.05	3.31±0.20
U75	0.101±0.03	0.763±0.09	35.75±0.66	0.24±0.05	2.98±0.19
U76	0.06±0.02	0.50±0.07	23.83 ±0.54	0.16±0.04	1.99±0.15
U77	0.115±0.03	0.86±0.10	40.71±0.70	0.27±0.05	3.40±0.20
U78	0.064±0.02	0.48±0.07	22.84±0.53	0.15±0.04	1.90±0.15
U79	0.18±0.04	1.42±0.13	66.53±0.90	0.45±0.07	5.55±0.26
U80	0.146±0.04	1.10±0.11	51.64±0.79	0.34±0.06	4.31±0.23
Maximum	0.18 ± 0.04	1.42 ±0.13	66.53±0.90	0.45±0.07	5.55±0.26
Minimum	0.02 ±0 .01	0.19±0.04	8.93±0.33	0.06 ±0.02	0.74±0.09
Average ±S.D	0.106±0.03	0.80±0.0981	35.70±0.67	0.25±0.05	3.15±0.18
Worldwide mean	35[138]	57.6[138]	57.6[138]	11[111]	40[139]

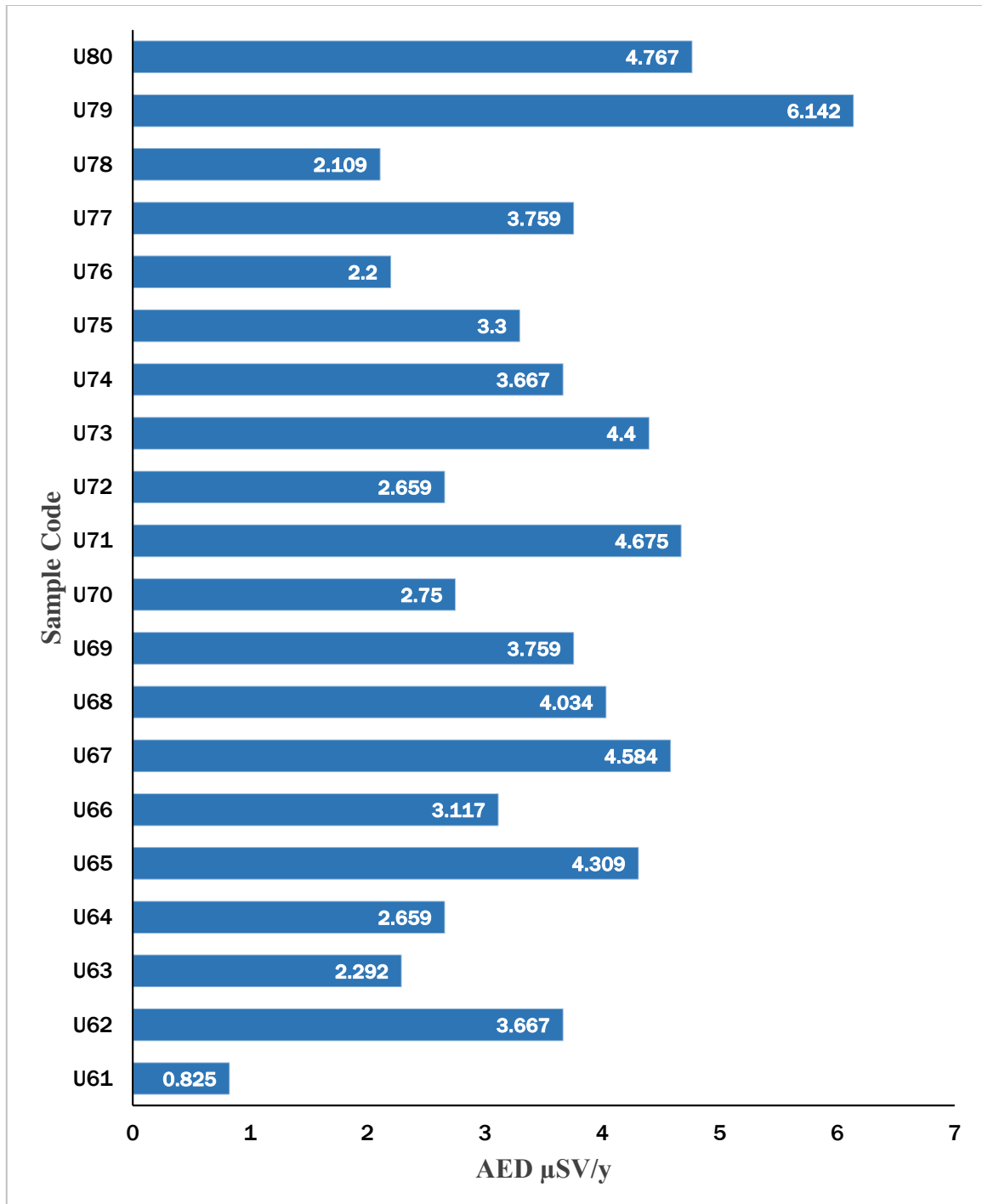


Figure (4-20): AED of radon for soil samples collected from Kerbala university of (Agricultural college)

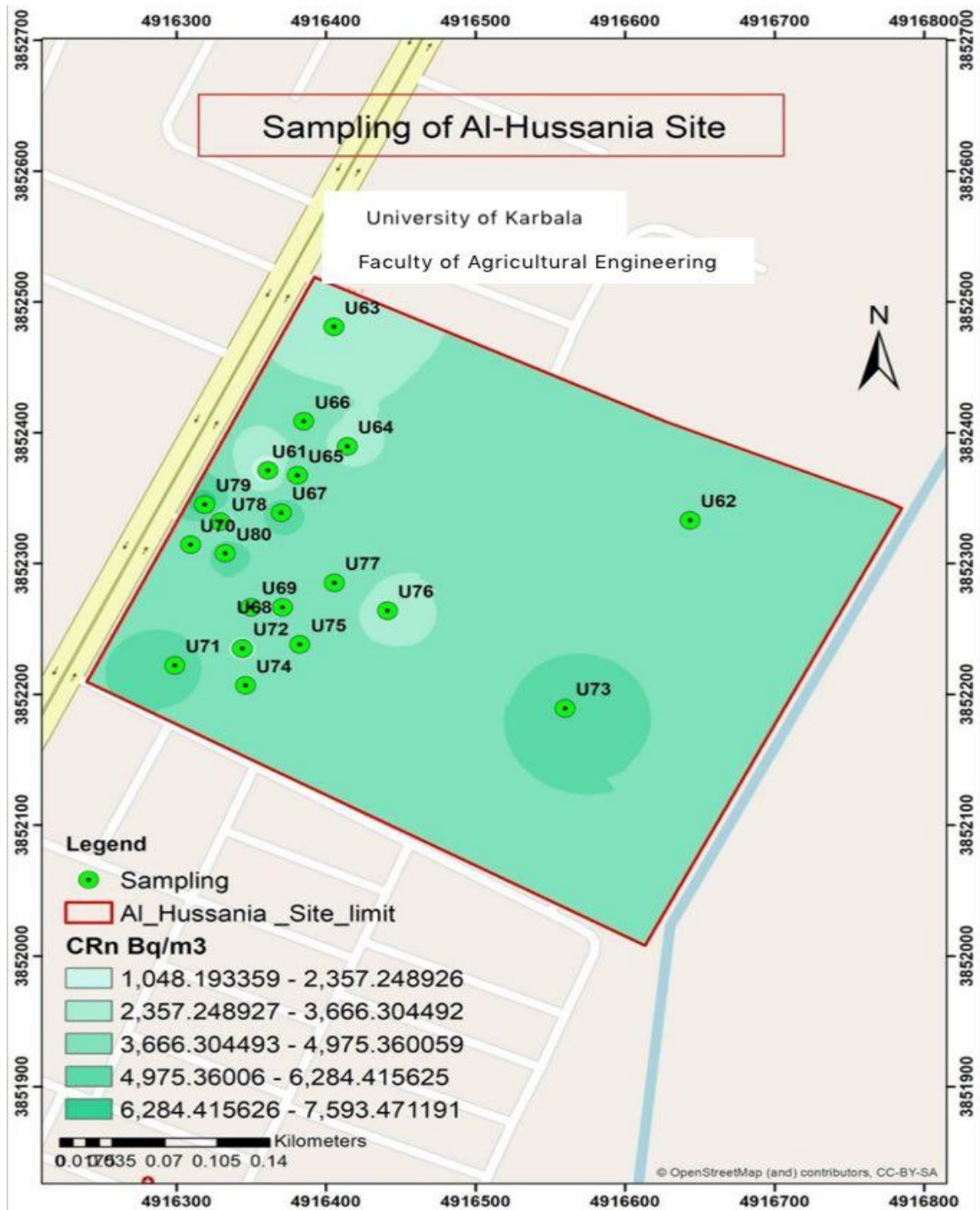


Figure (4-21): Map of the values of C_{Rn} in Agricultural college of Kerbala university

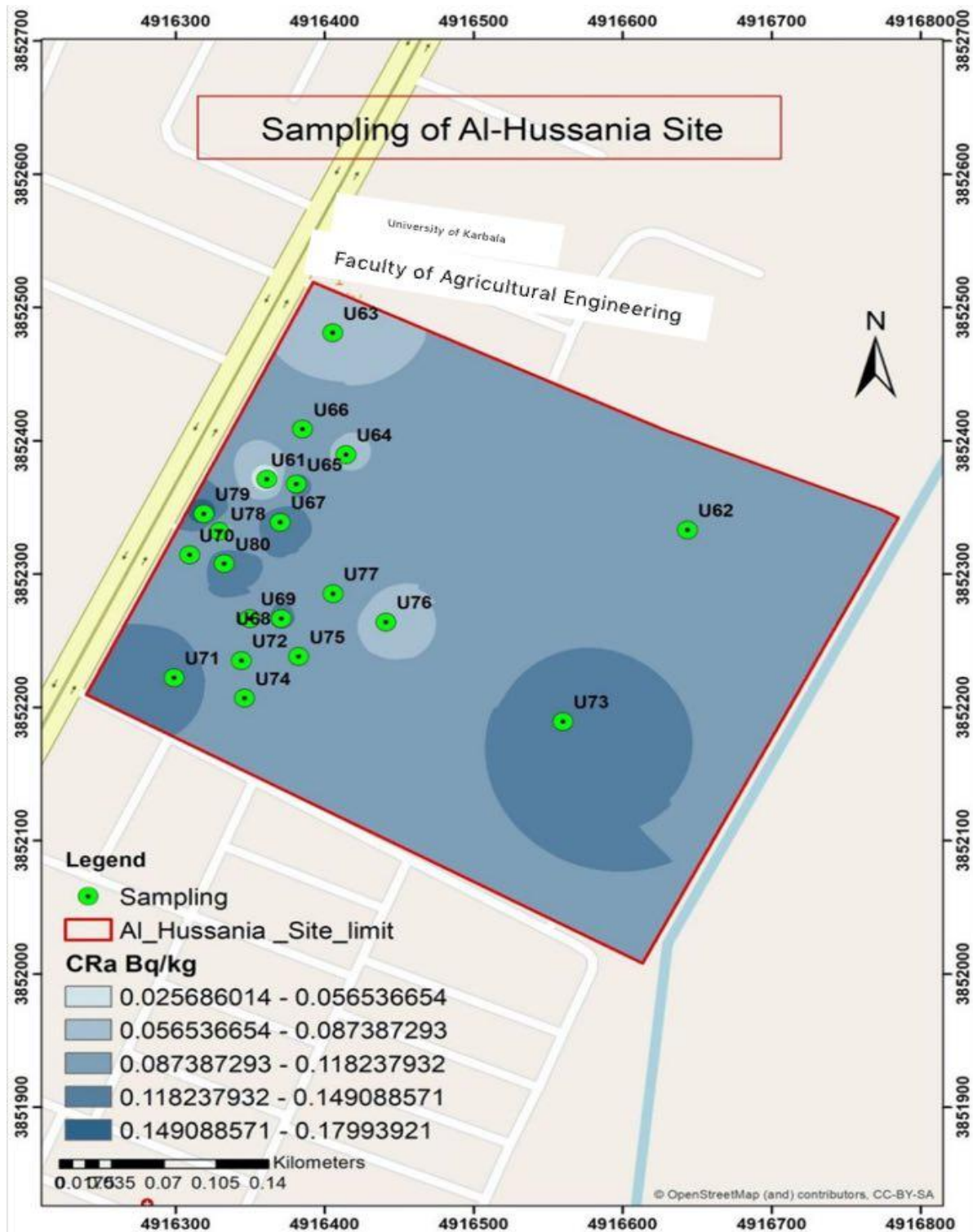


Figure (4-22): Map of the values of CR_a in Agricultural college of Kerbala university

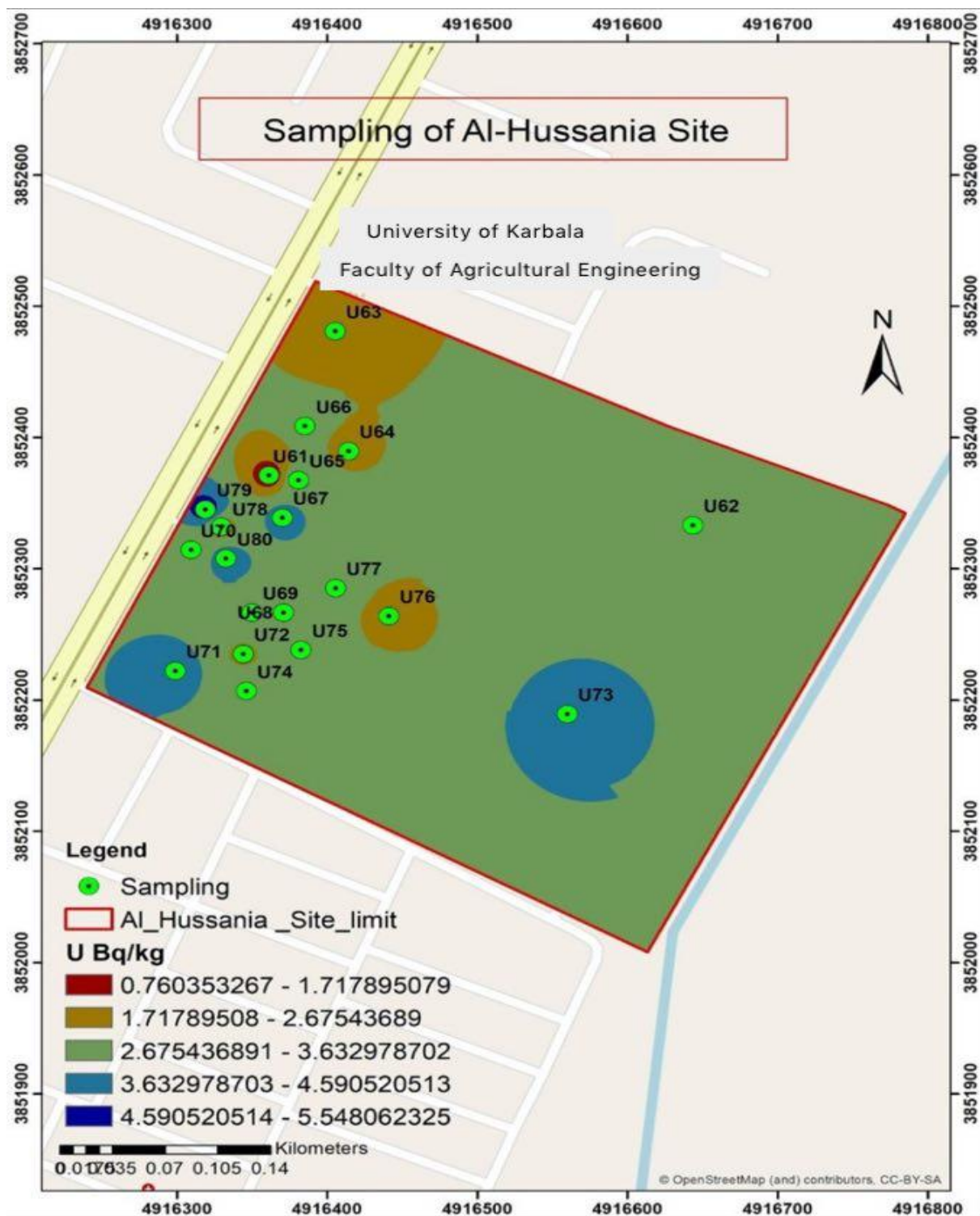


Figure (4-24): Map of the values of C_U in Agricultural college of Kerbala university

4.3.3 Alpha Emitters in-Mothafeen Site

Table (4.16) shows nuclear track densities (ρ) on surface of detector CN-85, the radon concentration in air space (C), the radon concentration in samples (C_{Rn}), and annual effective dose (AED) respectively, Table (4-15) shows effective radium concentration (C_{Ra}), mass exhalation rates (E_m), surface exhalation rates (E_s), uranium concentration (C_U), and uranium concentration unit in $Bq.kg^{-1}$ of uranium (C_U).

4.3.3.1 Radon Concentration and Annual Effective Dose

shown in table (4.16) the results of C were ranged between (406.97 ± 2.24) Bq/m^3 in U94 sample to (83.57 ± 1.01) Bq/m^3 in U98 sample to with a mean value of (163.15 ± 3.37) Bq/m^3 C_{Rn} were ranged between $2607.62 \pm 5.67 Bq/m^3$ in U94 sample to $12698 \pm 12.52 Bq/m^3$ in U98 sample to with an average value of $5090.54 \pm 155.31 Bq/m^3$ the soil radon concentration in the area was lower than the world average soil radon concentration (7400) Bq/m^3 [135]. Also from Table (4.16) and Figure (4-25), it is found that the AED was between (2.10 ± 0.16) $\mu Sv/y$ in U94 sample to (10.26 ± 0.35) $\mu Sv/y$ in U98 sample to with a mean value of (4.1162 ± 0.22075) $\mu Sv/y$ the latter indices values are found to be slightly smaller than the levels of $(3-10)$ mSv/y recommended by ICRP (1993)[130]. Figure (4-26) was drawn by GIS technique, show the geographical distribution of C_{Rn} , in the Mothafeen Sit, the concentrations of radon were classified in to six range of color according to radon concentrations, where different colors were used to differentiate between high, medium, and low concentrations.

4.3.3.2 Radium Concentration and Radon Exhalation Rates

Table (4.17) shows The values of C_{Ra} were ranged from 0.31 ± 0.06 Bq/kg U94 sample to 0.06 ± 0.02 Bq/kg in U98 sample to with an average value of 0.125 ± 0.03 Bq/kg. The observed the values of. The observed the values of C_{Ra} in all soil samples of the present study were less than the recommended action level 370 Bq/kg [137]. And also lower than the average global value of 35 Bq/kg [138]. Figure (4-27) was drawn by GIS technique, show the geographical distribution of C_{Ra} , in the Mothafeen Sit the concentrations of radon were classified in to six range of color according to radon concentrations, where different colors were used to differentiate between high, medium, and low concentrations .

Also from Table (4.17), the values of E_M (mBq/kg.h) and E_S (mBq/m².h) were ranged from 0.48 ± 0.07 in U94 sample to 2.37 ± 0.17 in U98 sample to with an average value of 0.95 ± 8.64 and from 22.84 ± 0.53 in U94 sample to 111.22 ± 1.17 in U98 sample to with an average value of 44.59 ± 0.79 . The observed values of radon exhalation rate in the present study are were below the world average of $0.016 \text{ Bqm}^{-2}\text{s}^{-1}$ ($57.6 \text{ Bqm}^{-2}\text{h}^{-1}$) [138]. The values of exhalation rates of soil samples vary from one sample to another this variation is due to the content of uranium and radium and to the porosity of the soil samples

4.3.3.3 Uranium Concentration

Table (4.17) shows the values of C_U in unit ppm were ranged from the values of C_U in unit ppm were ranged from 0.15 ± 0.04 in U94 sample to 0.75 ± 0.09 in U98 sample to with an average value of 0.30 ± 0.05 , but C_U in unit Bq/kg were ranged from 1.90 ± 0.15 in U98 sample to 9.29 ± 0.33 in U94 sample to with an average 3.72 ± 0.21 hence, it is found that, in all of the sites, the C_U is lower than 11

mg/kg (ppm) that was published by UNSCEAR (1994) [111]. And The specific activities of uranium in soil samples are less than the allowed limit (40 Bq/kg) from UNSCEAR[139]. Figure (4-28) and Figure(4-29) were drawn by GIS technique, show the geographical distribution of C_U, C_U in the Mothafeen Site the concentrations of radon were classified in to six range of color according to radon concentrations, where different colors were used to differentiate between high, medium, and low concentrations.

Table (4.16) Results of track density(ρ), radon concentration (C), concentration of radon in samples(C_{Rn}), annual effective dose (AED) in Al-Mothafeen Site of Kerbala university

Sample	ρ (Track/cm ²)	C (Bq/m ³)	C_{Rn} (Bq/m ³)	AED (mSv/y)
U81	5280±8.07	119.91±1.21	3741.37±6.79	3.02±0.19
U82	4800±7.69	109.01±1.16	3401.25±6.48	2.75±0.18
U83	6080±8.66	138.08 ±1.30	4308.25±7.29	3.48±0.20
U84	5120 ±7.95	116.27±1.19	3628±6.69	2.93±0.19
U85	11360±11.84	257.99 ±1.78	8049.62±9.96	6.50±0.28
U86	7200±9.42	163.51±1.42	5101.87 ±7.93	4.12±0.22
U87	7200± 9.42	163.51±1.42	5101.87±7.93	4.12±0.22
U88	5120 ±7.95	116.27±1.19	3628±6.69	2.93±0.19
U89	7200 ±9.42	163.51±1.42	5101.87±7.93	4.12±0.22
U90	7680±9.73	174.41±1.46	5442±8.19	4.40±0.23
U91	10400±11.33	236.19±1.70	7369.37±9.53	5.95±0.27
U92	9120 ±10.61	207.12±1.59	6462.37±8.93	5.22±0.25
U93	9440±10.79	214.39±1.62	6689.12±9.08	5.40±0.25
U94	17920±14.87	406.97±2.24	12698±12.52	10.26±0.35
U95	3840±6.88	87.20±1.03	2721±5.796	2.20±0.16
U96	4480± 7.43	101.74±1.12	3174.50±6.26	2.56±0.17
U97	5760±8.43	130.81 ±1.27	4081.50±7.09	3.30±0.20
U98	3680±6.74	83.57±1.01	2607.62±5.67	2.10±0.16
U99	6400±8.88	145.34±1.34	4535 ±7.48	3.66±0.21
U100	5600 ±8.31	127.18 ±1.25	3968.12±6.99	3.20 ±0.19
Maximum	17920 ±14.87	406.97 ±2.24	12698 ±12.52	10.26±0.35
Minimum	3680±6.74	83.57±1.01	2607.62 ±5.67	2.10±0.16
Average±S.D	7184±8.75	163.15±3.37	5090.54±155.31	4.11±0.22
Worldwide	200-300[140]	7400[135].	3-10[136]

Table (4.17) Results of effective radium concentration (C_{Ra}), surface (E_s) and mass (E_m) exhalation rates. Uranium Concentration (C_U) and uranium Concentration in unit Bq/kg (C_U) in Al-Mothafeen Site of Kerbala university

Sample	C_{Ra} Bq/kg	E_{mm} Bq/kg.h	E_{sm} Bq/m ² .h	C_U ppm	C_U Bq/kg
U81	0.093± 0.03	0.69±0.09	32.77±0.63	0.22±0.05	2.73.±0.18
U82	0.084 ± 0.03	0.63±0.08	29.79 ±0.60	0.20±0.05	2.48±0.17
U83	0.107±0.03	0.80±0.10	37.73±0.68	0.25±0.05	3.15±0.19
U84	0.090 ±0.03	0.67±0.09	31.77±0.62	0.21±0.05	2.65±0.18
U85	0.199 ±0.05	1.50±0.13	70.51±0.93	0.47±0.07	5.88±0.27
U86	0.126 ± 0.03	0.95± 0.10	44.68±0.74	0.30±0.06	3.73±0.21
U87	0.126±0.03	0.95± 0.10	44.68± 0.74	0.30±0.06	3.73±0.21
U88	0.090 ±0.03	0.67 ± 0.09	31.77±0.62	0.21±0.05	2.65±0.18
U89	0.126 ±0.03	0.95 ±0.10	44.68±0.74	0.30±0.06	3.73±0.21
U90	0.135± 0.04	1.01±0.11	47.66± 0.76	0.32±0.06	3.98±0.22
U91	0.182 ±0.04	1.37± 0.13	64.55± 0.89	0.43±0.07	5.39±0.25
U92	0.160±0.04	1.20 ±0.12	56.60 ±0.83	0.38±0.06	4.72±0.24
U93	0.165±0.04	1.25 ± 0.12	58.59± 0.85	0.39±0.07	4.89±0.24
U94	0.314±0.06	2.37±0.17	111.2±1.17	0.75±0.09	9.29±.33
U95	0.067±0.02	0.50± 0.07	23.83±0.54	0.16±0.04	1.99±0.15
U96	0.079± 0.03	0.59±0.08	27.80± 0.58	0.18±0.04	2.32±0.16
U97	0.101± 0.03	0.76 ±0 .09	35.7±2.66	0.24±0.05	2.98±0.19
U98	0.064 ±0.02	0.48±0.07	22.84± 0.53	0.15±0.04	1.9± 0.15
U99	0.112 ±0.03	0.84±0.10	39.72±0.70	0.26±0.05	3.31±0.20
U100	0.098 ±0.03	0.74 ±0.09	34.75± 0.65	0.23±0.05	2.90±0.18
Maximum	0.31±0.06	2.37 ±0.17	111.22±1.17	0.75±0.09	9.29±0.33
Minimum	0.06 ±0.02	0.48±0.07	22.84±0.53	0.15±0.04	1.90±0.15
Average±S.D	0.125±0.03	0.95±8.64	44.59±0.79	0.30±0.05	3.72±0.21
Worldwide mean	35[138]	57.6 [138]	57.6 [138]	11[111]	40[139]

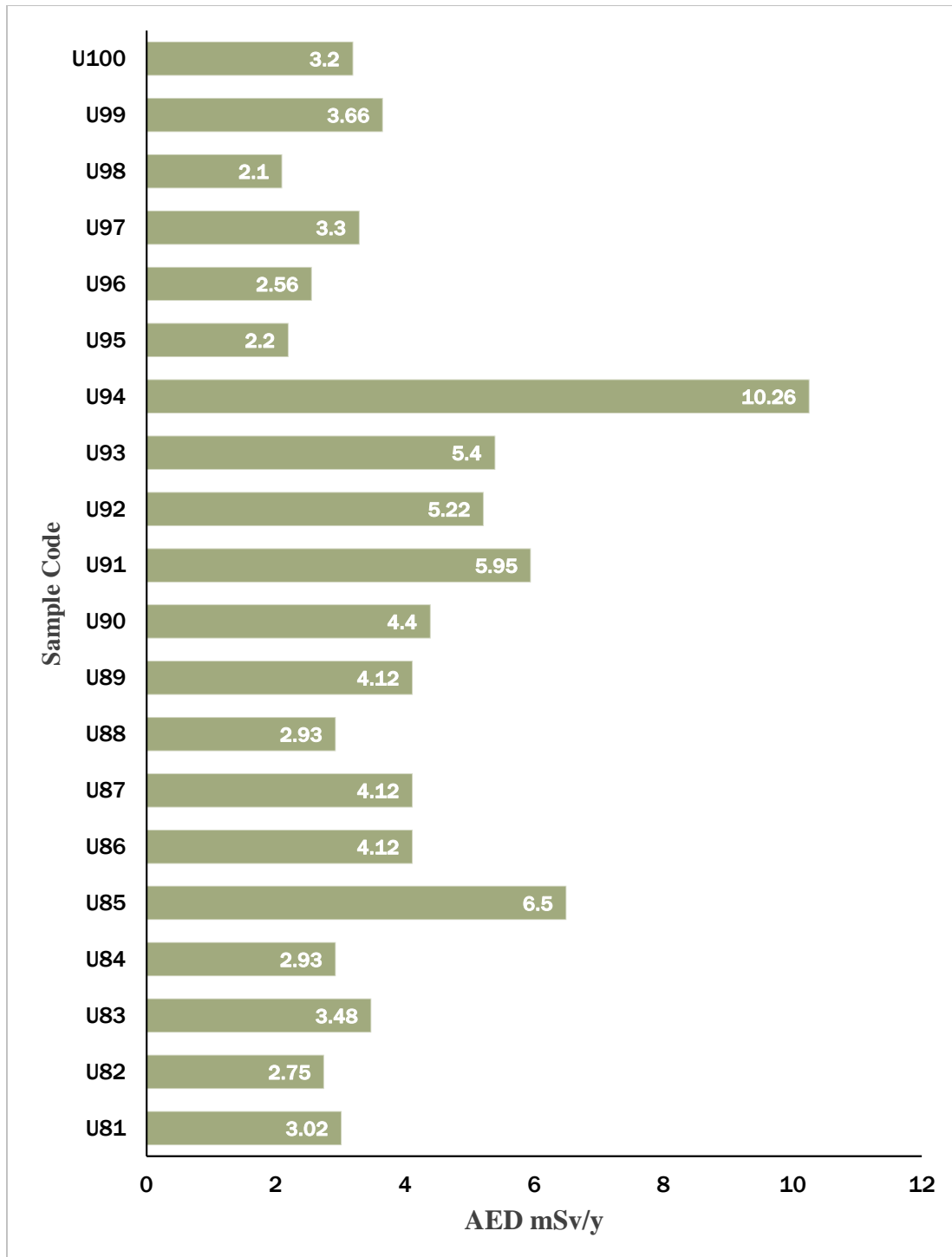


Figure (4-25): AED of radon for soil samples collected from Kerbala university of Al-Mothafeen site

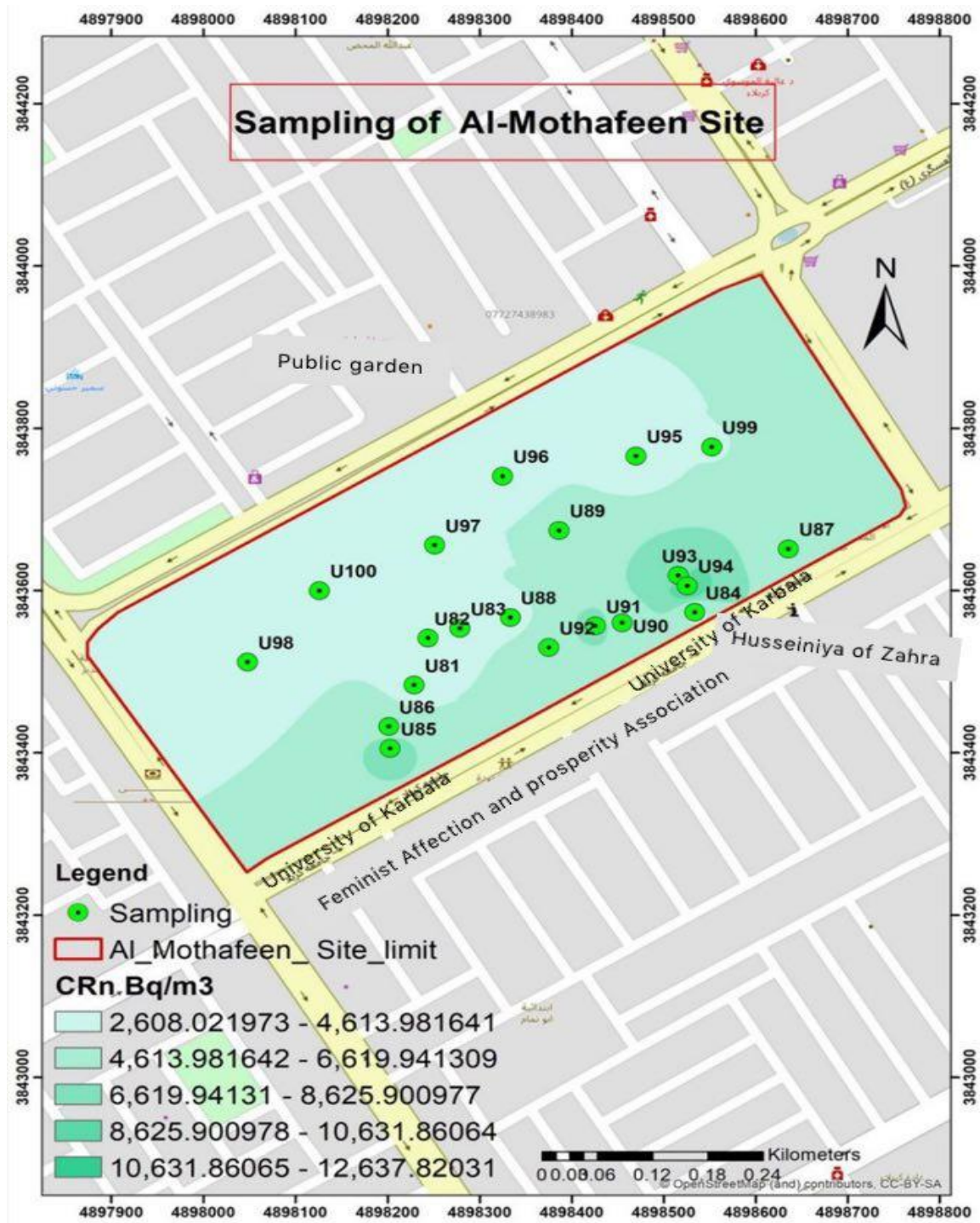


Figure (4-26): Map of the values of C_{Rn} in Al-Mothafeen Site of Kerbala university

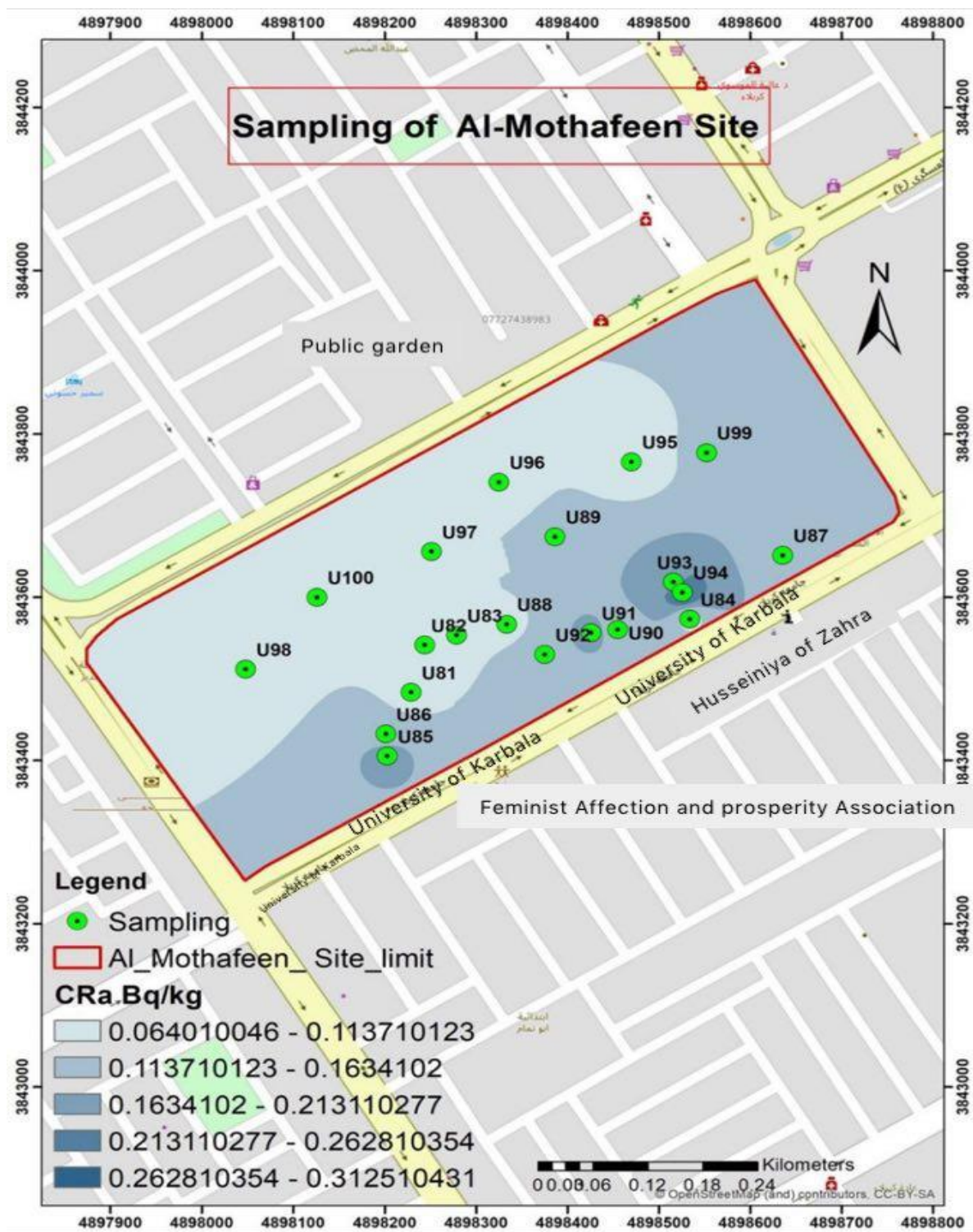


Figure (4-27): Map of the values of C_{Ra} in Al-Mothafeen Site of Kerbala university

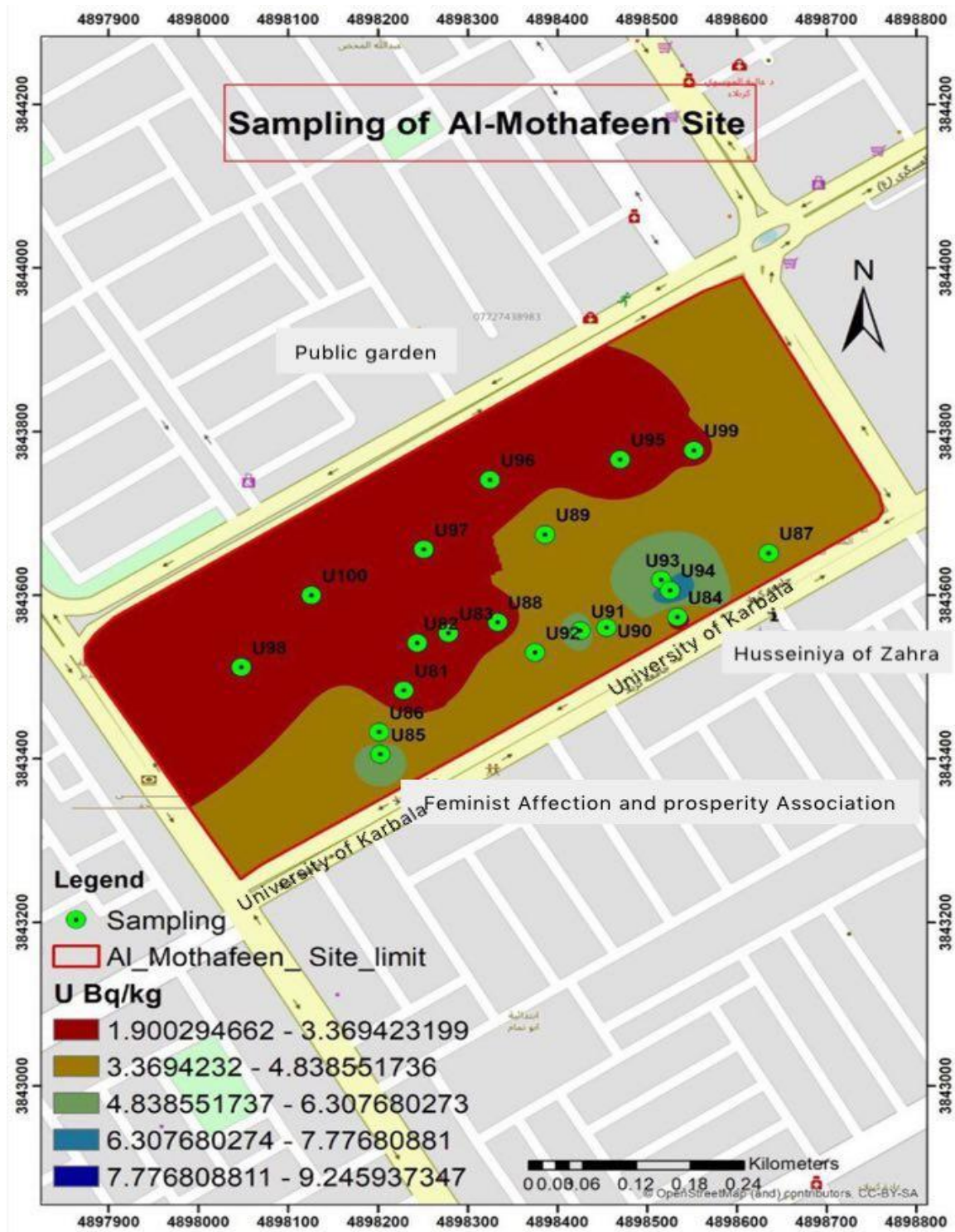


Figure (4-29): Map of the values of C_U in Al-Mothafeen Site of Kerbala university

4.3.4 Compare the Results of Alpha Emitters Between Sites in Present Study

A summary of the average of the C_{Rn} , C_{Ra} and C_U as well as radiological hazard index such as AED, E_M and E_s inside three locations in university of Karbala (Freiha, Al-Husseineya, Al-Mothafeen) were shown in tables from (4.13) to (4.17). The highest average of C_{Rn} , C_{Ra} and C_U were found in Al-Mothafeen site, and still all the average in the study area within global average limit [111]. As shown in Figure (4-30). Also, the highest average value of AED, E_M and E_s were found in Al-Mothafeen side as shown in Figure (4-31). This result is still within normal limits [138] .

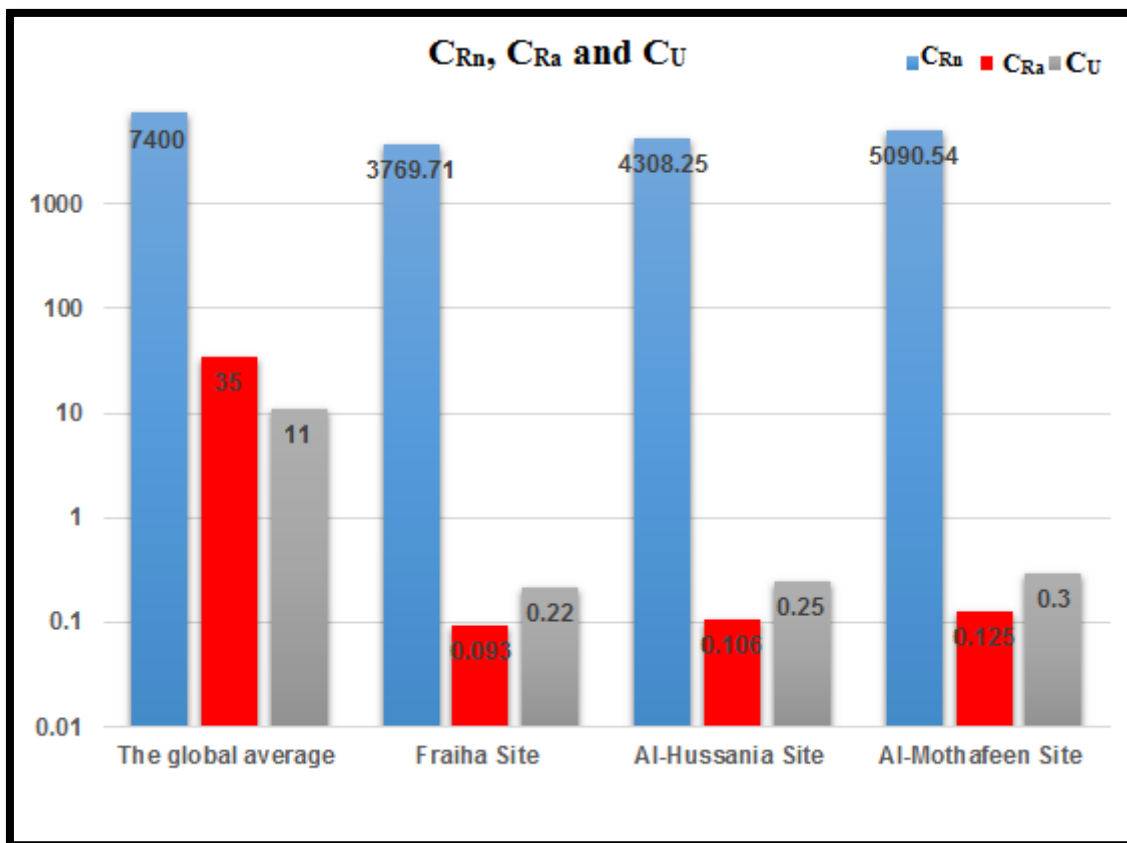


Figure (4-29): Comparing of C_{Rn} , C_{Ra} and C_U in all locations under study.

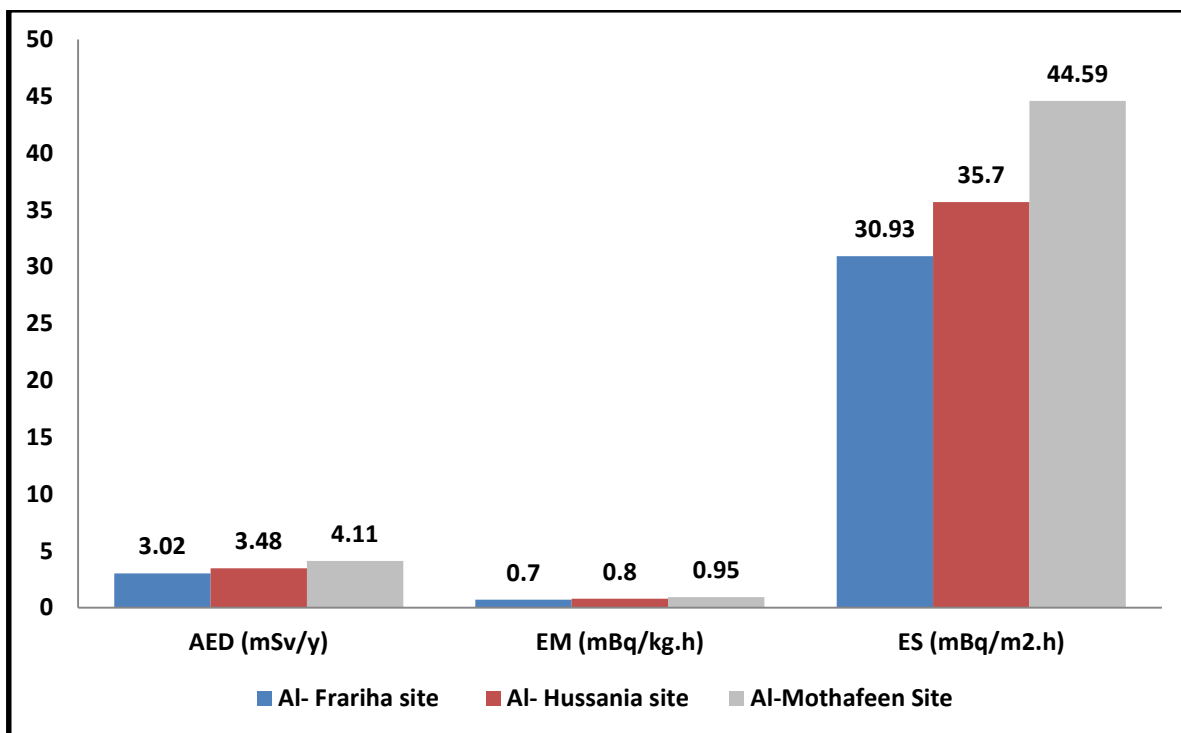


Figure (4-31): Comparing of radiological hazard due to alpha emitters in all locations under study.

The difference in radon levels can be attributed to the numerous components of these soil because of difference in the geological nature of each region and type of soil (clay or sand), as well as may be because the samples which are collected from the study area have been planted or treated with chemical fertilizers, usually, agricultural areas use high concentrations of chemical fertilizers, upon comparing the values of (C and C_{Rn}) With all the formulations that were investigated, it is clear that the concentration of radon within the study the sample is even higher than that in the tube airspace. The big disparity between the two values can be ascribed to the fact that the majority of the produced radon atoms within the sample decay before entering the space of the tube because they have allowed a decay time of 3.82 d. as well as due to the presence of radon parent (radium) inside

the sample, but not in the tube airspace. The activity concentration of radium varied in the formulations. That may be ascribed for the fact that the activity of concentrations of radium and other radionuclides were in a state of variation from one soil to another[141].

Activities of alpha attributable to radium in the soil samples were less than those due to radon. This is attributed to the fact that radon half-life (3.82 d) is less than radium (1600 y)[142]. The values of exhalation rates of soil samples vary from one sample to another this variation is due to the content of uranium and radium and to the porosity of the soil samples.

4.3.5 Compare the Results of Alpha Emitters Between Sites in Present Study

Table (4.18) shows comparison between the results of radon concentration in the soil sample in university of Kerbala and the results of the radon concentrations in the soil of several countries around the world. Therefore, from Table (4.18), it is found the average of radon concentration in soil of the university of Karbala are lower than that found in Pakistan, (Bahimber)[43] , Pakistan[44], Lebanon [57],India [52] Pakistan[39] Bulgaria[48], Iraq [143], Iraq(Kerbala) [144]Iraq(Al-Najaf) [53], Saudi Arabia [145] Egypt[146], Slovenia[147], Sudan[148], Iraq Maysan [149] Iraq (Karbala) [47] Foreland/ Modica[150] Iraq (Kerbala)[151] . while was greater than other values for a group of countries mentioned in the above table Turkey [46], Iraq [152] ,France[153]. While the results of radium activity in all present study was lower than the results of the other studies. As Well as the results of radium concentration in all present study was less than the results of the other studies and the results of uranium concentrations in all the new

research was less than the results from other studies with the exception of Iraq [143]. Shown in the below table.

Table (4.18): Comparison of the present study with others studies of many different countries.

No.	Country	$^{222}\text{Rn}(\text{kBq/m}^3)$	$^{226}\text{Ra}(\text{Bq/kg})$	$^{238}\text{Uppm}$	Ref.
1	Pakistan,(Bahimber)	48	-	-	[43]
2	Pakistan	95.1	-	-	[44]
3	Turkey	1.92	-	-	[46]
5	Bulgaria	26	-	-	[48]
6	India	-	-	3	[49]
7	India	4.561	-	-	[52]
8	Lebanon	-	1.079	1.467	[57]
9	Sudan	8.20	-	-	[148]
10	Egypt	4.35	-	-	[146]
11	Saudi Arabia	6.71	-	-	[145]
12	Slovenia	40.1	-	-	[147]
13	France	2.71	-	-	[153]
14	Foreland/ Modica	18	-	-	[150]
15	Iraq (kerbala)	2.87	-	-	[151]
16	Iraq (kerbala)	-	1.7921	-	[50]
17	Iraq(Hit City)	0.17	-	-	[152]
18	Iraq	-	58.927	0.05	[143]
19	Iraq(Kerbala)	-	0.317	0.345	[144]
20	Iraq Maysan,	776.98	37.79	-	[149]
21	Iraq (Karbala)	197.477	-	1.509	[47]
22	Iraq(AlNajaf)	894.21	136.18	1.5	[53]
Karbala (University)		4.14	0.10	0.24	This study

4.5. Correlation Between Gamma and Alpha Emitters

The numerical values of the correlation coefficient for gamma emitters ($C^{238}\text{U}$, $C^{232}\text{Th}$ and, $C^{40}\text{K}$) and alpha particles ($C^{222}\text{Rn}$, $C^{226}\text{Ra}$ and, $C^{238}\text{U}$) in samples of present study using two technical (NaI(Tl) and CN-85) are obtained in Tables (4.19), (4.20).

Table (4.19) Correlation between Gamma and Alpha Emitters in all value of Kerbala university

Element	$C^{238}\text{U}$	$C^{232}\text{Th}$	$C^{40}\text{K}$
C_{Rn}	0.886	0.268	0.264
C_{Ra}	0.885	0.270	0.261
C_{U}	0.884	0.274	0.266

Table (4.20) Correlation between Gamma and Alpha Emitters in present Study

Element	Freiha-Site			Al-Husseineya-Site			Al-Mothafeen- Site		
	$C^{238}\text{U}$	$C^{232}\text{Th}$	$C^{40}\text{K}$	$C^{238}\text{U}$	$C^{232}\text{Th}$	$C^{40}\text{K}$	$C^{238}\text{U}$	$C^{232}\text{Th}$	$C^{40}\text{K}$
C_{Rn}	0.89	0.35	0.47	0.88	0.20	0.03	0.89	0.14	0.12
C_{Ra}	0.88	0.35	0.46	0.89	0.20	0.02	0.90	0.13	0.11
C_{U}	0.89	0.36	0.48	0.88	0.18	0.04	0.89	0.14	0.31

From Table (4.19) and (4-20), it is found the high positively correlated values in soil samples in three sites and all value in present study (Freiha, Al-Husseineya, and Al-Mothafeen) between uranium-238 and radon-222. The study is proved the presence of a strong (positive) correlation factor for all the studied areas, and this is evidence that the soil under study is original and does not contain added exotic materials and thus the correct sequence of the uranium-238 basket can be achieved. Also, it is found week (negative) correlation for all sits in present study, between radon-222 with thorium-232 and potassium-40, this because no found the relation between radon-222 with thorium-232 series in side and potassium-40 from anther side.

Indeed, the current study is considered the first attempt at risk assessment that is related in soil samples at the university of Kerbala (Freiha, Al-Husseineya and Al-Mothafeen). It is found that the all results of gamma and alpha emitters in the samples under study was lower and not significant from a health risk point of view as shown in Figure (4-32) (4-33), (4-34) (4-35).

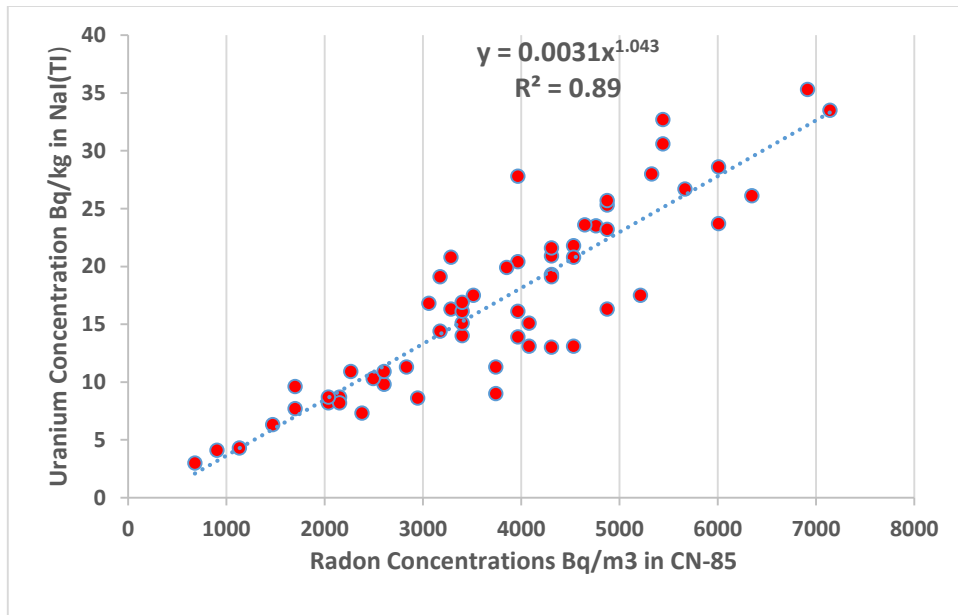


Figure (4.32) Correlation between ^{222}Rn for CN-85 and ^{238}U NaI(Tl) detectors for Freiha-site.

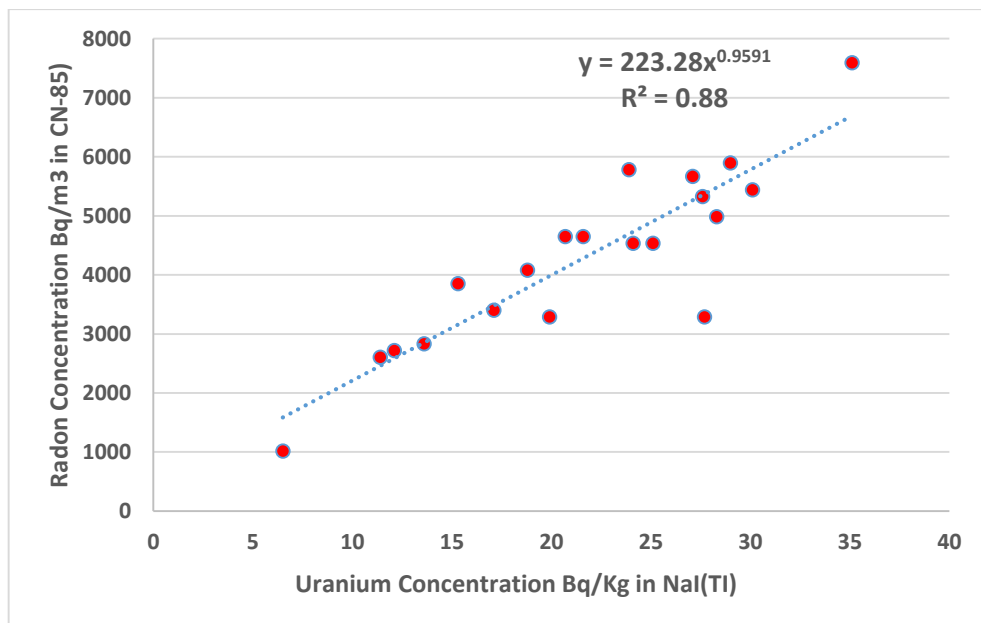


Figure (4.33) Correlation between ^{222}Rn for CN-85 and ^{238}U NaI(Tl) detectors for Al-Husseineya Site .

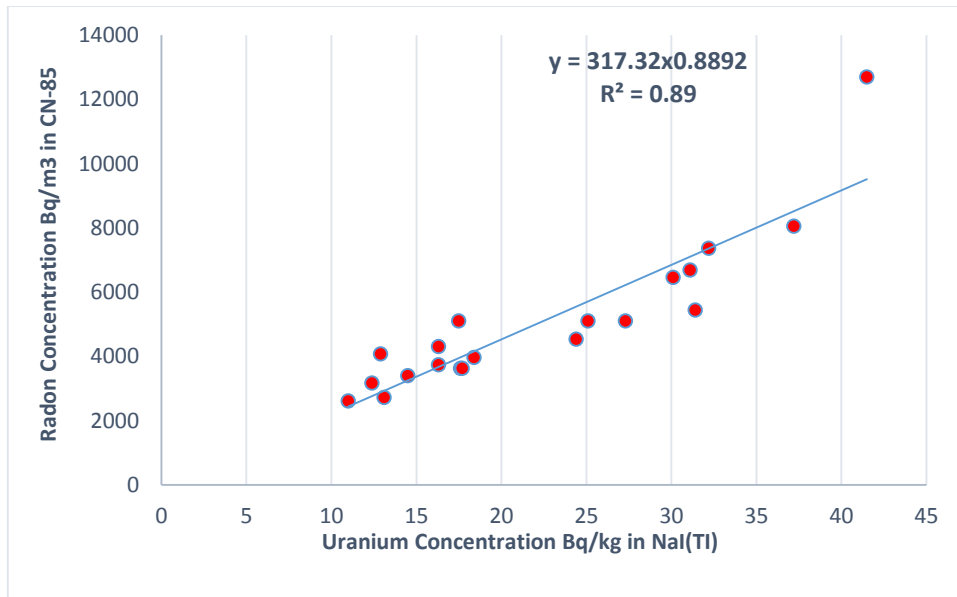


Figure (4.34) Correlation between ^{222}Rn for CN-85 and ^{238}U NaI(Tl) detectors for Al-Mothafeen Site.

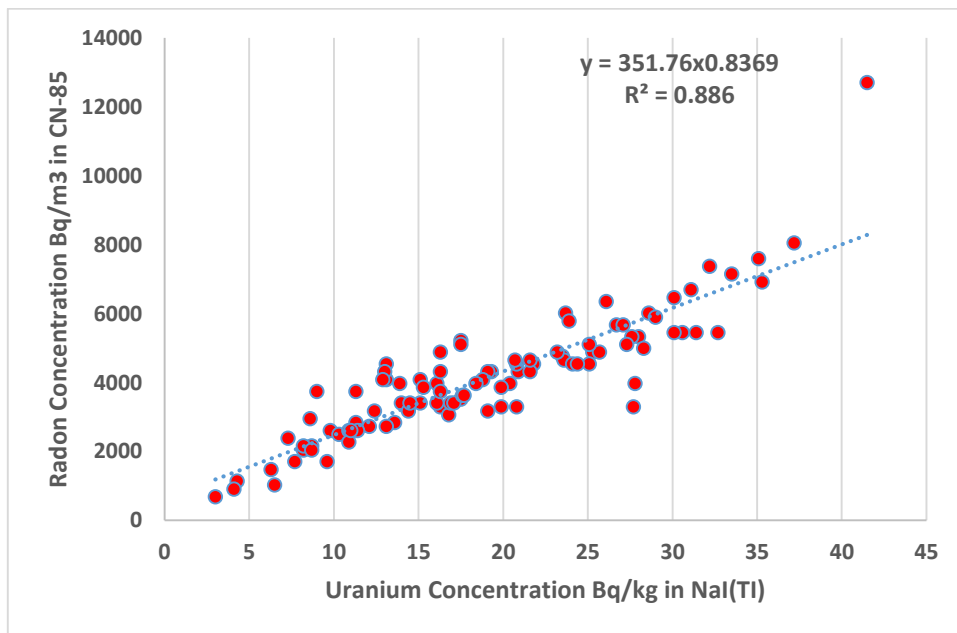


Figure (4.35) Correlation between ^{222}Rn for CN-85 and ^{238}U NaI(Tl) detectors for All values of Kerbala University.

4.6 Conclusions

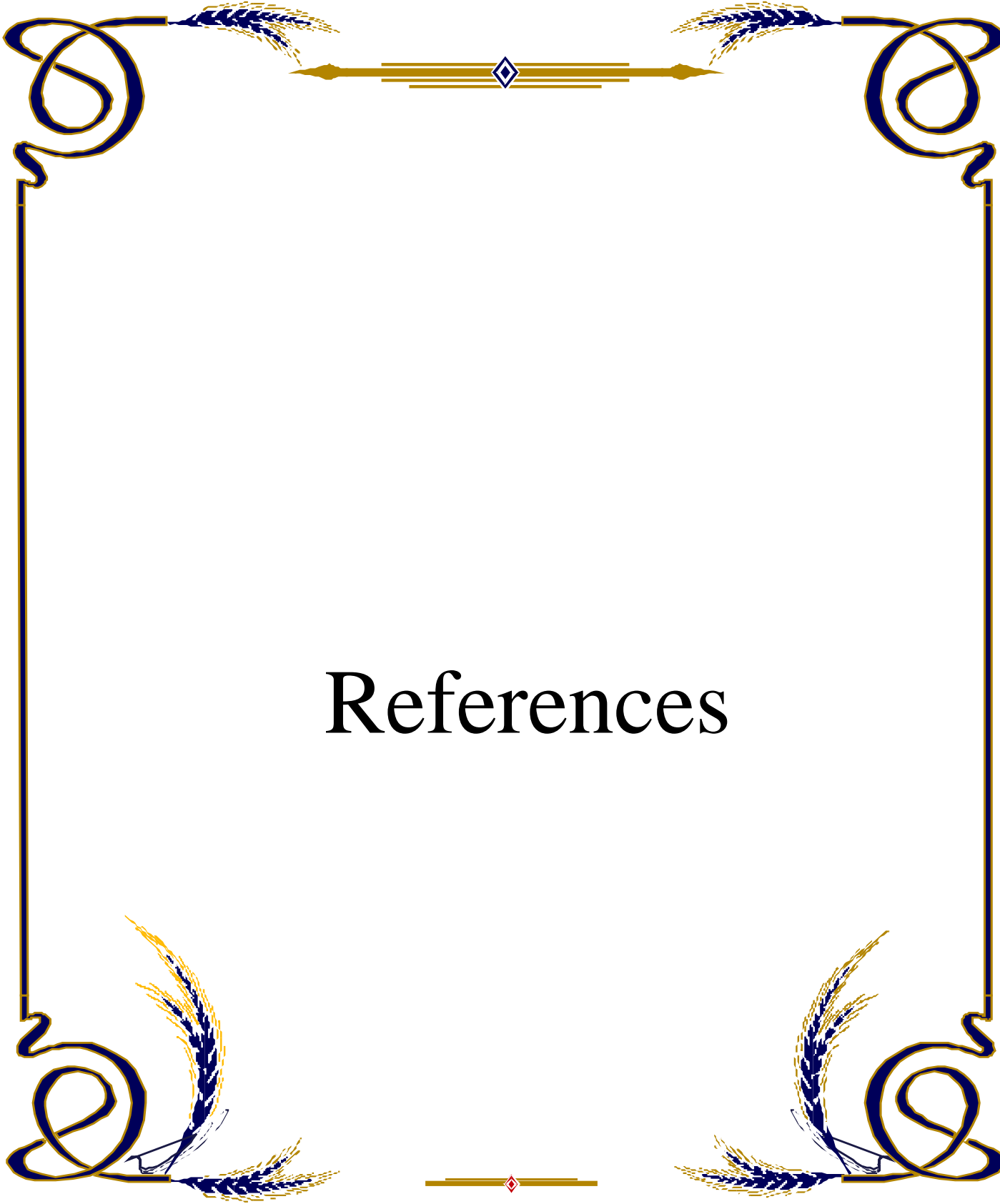
From the results, obtained the form gamma emitters and alpha emitters in 100 soil samples of in university of Kerbala can be concluded that:

1. The specific activity of uranium, thorium, and potassium in most samples were lower than the world average values according to UNSCEAR 2008.
2. The results of the ten radiological hazard parameters due to ^{238}U , ^{232}Th , and ^{40}K in all samples were lower than the world average according to the radiation protection report UNSCEAR2000, UNSCEAR2008, OECD, and ICRP1993.
3. The results of alpha emitters (^{222}Rn , ^{226}Ra and ^{238}U) also as well as AED and E_M , E_S altogether soil samples were lower than the typical of the worldwide level.
4. There is a good correlation between ^{238}U and alpha emitters using NaI(Tl) and CN-85 detector respectively, while no correlation between another gamma emitter with alpha emitters.
5. The average value of the results of the gamma and alpha emitter with the risk of the parameters calculated in the present research, the highest average of specific activity of ^{238}U and ^{232}Th were found in Al-Mothafeen site, while the highest average of specific activity ^{40}K was in Al-Husseineya
6. The Arc GIS statistical geographic tools analyzed gamma and alpha emitters in soil samples in the university of Kerbala (Freiha region, Al-Husseineya region, and Al-Mothafeen region) by mapping the elements.
7. As a result, gamma-ray and alpha particles levels and radiological hazard index current soil samples in the university of Kerbala, Iraq do not constitute a health hazard.

4.7 Recommendations

To the responsible authorities such as the Ministry of Health, Ministry Industry, Ministry of Environment, Local government, and survey of geology, in order to preserve the environment and public health from radiation hazards.

1. Forming a specialized work team to conduct a radiological survey of Karbala governorate, planning an integrated radiological princess, increasing the number of samples studied, and providing a study in all governorates of the country to draw the map.
2. Reducing the use of chemical fertilizers.
3. Conducting radiological surveys periodically to detect and monitor radiation changes of some kind in the governorate.
4. To provide modern enough scientific and research institutions to conduct their own systems of radiological environmental studies.
5. Using accurate and Complicated measuring devices to measure uranium and radon concentrations as well as radium content at a different time period
6. Photo-remediation one of a good method to rid high concentration of gas radon as well as some plants have god ability to absorb gas
7. Create a radiation map that includes measurement of all concentrations of radioactivity that all living creatures, especially humans, are exposed too. And to know the permissible limits locally for comparison with the global results.



References

References

- [1] Kennedy Jr, W.E., "Naturally occurring radioactive material (NORM V) proceedings of an international symposium", Spain 19-22 March Oxford University Press (2007)
- [2] Eisenbud, M. and T.F. Gesell, "Environmental radioactivity from natural, industrial and military sources: from natural, industrial and military sources". (1997)
- [3] Rosenberg, I., "Radiation oncology physics: a handbook for teachers and students". British journal of cancer, 98(5): p. 1020.(2008)
- [4] Annunziata, M.F., "Radioactivity introduction and history, from the quantum to quarks". (2016)
- [5] Cember, H., T.E. Johnson, and P. Alaei, "Introduction to health physics". Medical Physics, 35(12): p. 5959.(2008)
- [6] Cameron, J.R., J. G Skofronick ., Medical physics "Physics of the body". American Journal of Physics, 61: p.1156 (1993)
- [7] Whicker, F.W., M. Eisenbud, and T. Gesell, "Environmental radioactivity from natural, industrial, and military sources". Radiation Research. 148: p. 402.(1997)
- [8] UNSCEAR, "Sources and Effects of Ionizing Radiation, Report to the General Assembly". Annex J. Exposure and Effects of the Chernobyl Accident, p. 155.(2000)
- [9] Guidebook, A., "Measurement of Radionuclides in Food and the Environment". International Atomic Energy Agency IAEA, Vienna, Austria.(1989)
- [10] Al-Farouk, O., S.Al-Damluji., ALM.Al-Obaidi., "Experimental and numerical investigations of dissolution of gypsum in gypsiferous Iraqi soils". in Proceedings of the 17th International Conference on Soil Mechanics and Geotechnical Engineering: The academia and practice of geotechnical engineering, Alexandria, Egypt. (2009).
- [11] Tsoulfanidis, N., "Measurement and detection of radiation". CRC press.(2010)
- [12] Gilmore, G., "Practical Gamma Ray Spectrometry", J. Hemingway John Wiley and Sons, (1996)
- [13] Mahler, R., "Evaluation of water potential, fertilizer placement and incubation time on volatilization losses of urea in two northern Idaho soils". p.1991 En: Communications in Soil Science and Plant Analysis (USA). Vol. 25, (2004)

- [14] Da Conceicao, F.T. and D.M. Bonotto, "Radionuclides, heavy metals and fluorine incidence at Tapira phosphate rocks, Brazil, and their industrial (by) products". *Environmental Pollution*, 139(2): p.232 (2006)
- [15] Flores, O.B., A.M Estrada., R.R Suarez., J.T Zerquera., "Natural radionuclide content in building materials and gamma dose rate in dwellings in Cuba". *Journal of environmental radioactivity*, 99(12): p.1834 (2008)
- [16] Semmelrogge, W. and F. Sicilio, "A study of secular equilibrium using Ce_{144} — Pr_{144} ". *Journal of Chemical Education*, 42(8): p. 427.(1965)
- [17] College, A.o. and R. Libraries, Choice: "Publication of the Association of College and Research Libraries, a Division of the American Library Association". Vol. 23.Association of College and Research Libraries. (1985)
- [18] Outola, I., Nour, H.Kurosaki., K. Inn., J .La Rosa., "Investigation of radioactivity in selected drinking water samples from Maryland". *Journal of radioanalytical and nuclear chemistry*, 277(1): p. 155 (2008)
- [19] Carlson, S.K., K.L Classic., E.M Hadac ., "Quantitative molecular imaging of viral therapy for pancreatic cancer using an engineered measles virus expressing the sodium-iodide symporter reporter gene". *American journal of roentgenology*, 192(1): p. 279 (2009)
- [20] Zhang, W., "Suitable activated stable nuclide tracer technique and its applications in biology and medicine". *Nuclear Techniques*, 12(11): p.p 633-637.(1989)
- [21] Maphoto, K.P., "Determination of natural radioactivity concentrations in soil: a comparative study of Windows and Full Spectrum Analysis". University of the Western Cape. (2004)
- [22] Van Wijngaarden, M., M.,L,B Venema., RJ De Meijer., "Radiometric sand–mud characterisation in the Rhine–Meuse estuary": Part A. Fingerprinting. *Geomorphology*, 43(1-2): p.p87-101.(2002)
- [23] Al-Hamarneh, I.F. and M.I. Awadallah, "Soil radioactivity levels and radiation hazard assessment in the highlands of northern Jordan". *Radiation Measurements*, 44(1): p.p102-110.(2009)
- [24] Mandić, L.J., R. Dragović, and S. Dragović, "Distribution of lithogenic radionuclides in soils of the Belgrade region (Serbia)". *Journal of Geochemical Exploration*, 105(1-2): p.p43-49.(2010)

- [25] Al-Leswas, M., "Evaluation of natural radioactivity in Environmental samples. Master's thesis", University of Surrey, p.122 (2010).
- [26] Al-Sulaiti, H., P,H Regan, D,A Bradley, D ,Malain ., "A preliminary report on the determination of natural radioactivity levels of the State of Qatar using high-resolution gamma-ray spectrometry". Nuclear Instruments and Methods in Physics Research Section A: Accelerators, Spectrometers, Detectors and Associated Equipment, 619(1-3): p.p427-431.(2010)
- [27] Yousuf, R.M. and K.O. Abullah, "Measurement of Natural Radioactivity in Soil Collected from the Eastern of Sulaimany Governorate in Kurdistan–Region,physics of Iraq".(4) p:141-155 (2013).
- [28] Hatif, K.H., "Natural Radioactivity level and the measurement of soil gas Radon, Thoron concentrations in Hilla city". journal of kerbala university, 13(1): p.p103-114.(2015)
- [29] Abojassim, A.A., M.H. Oleiwi, and M. Hassan, "Evaluation of Radiation Hazard Indices duo to Gamma Radiation in Hattin Complex at Babylon Government". Middle-East Journal of Scientific Research, 24(7): p.p2196-203.(2016)
- [30] Jassim, A., H. Al-Gazaly, and A. Abojassim, "Natural radioactivity levels in soil samples for some locations of Missan government, Iraq". Journal of Environmental Science and Pollution Research, 2(1): p. 39-41.(2016)
- [31] Arnedo, M., J,G Rubiano., H, Alonso., A,Tejera., "Mapping natural radioactivity of soils in the eastern Canary Islands". Journal of environmental radioactivity, 166: p. 242 (2017)
- [32] Kadhim, I.H. and M.K. Muttaleb, "Measurement of radioactive nuclides present in soil samples of district Touirij of Karbala province for radiation safety purposes". Int. J. Chem. Tech. Res, 9: p. 228 (2016)
- [33] Abojassim,A,A., "Estimation of human radiation exposure from natural radioactivity and radon concentrations in soil samples at green zone in Al-Najaf, Iraq". Iranian Journal of Energy and Environment, 8(3): p.7 (2017)
- [34] Shayeb, M.A., A. Majid, and S. Zobidi, "Distribution of natural radioactivity and radiological hazard using a NaI (Tl) gamma-ray spectrometric system". Journal of Building Physics, 40(4):p. 324(2017)

- [35] Durusoy, A. and M. Yildirim, "Determination of radioactivity concentrations in soil samples and dose assessment for Rize Province, Turkey". *Journal of Radiation research and applied sciences*, 10(4): p. 348 (2017)
- [36] Saleh Kotahi, M., "Estimation of natural radioactivity and radiation exposure in environmental soil samples of Golestan, Iran". *Iranian Journal of Medical Physics*, 14(2): p. 98 (2017)
- [37] El-Taher, A., F. Alshahri, and R. Elsaman, "Environmental impacts of heavy metals, rare earth elements and natural radionuclides in marine sediment from Ras Tanura, Saudi Arabia along the Arabian Gulf". *Applied Radiation and Isotopes*, 132: p.p95-104.(2018)
- [38] Gbadamosi, M., T,A Afolabi., O,O Banjoko., A.L Ogunneye., "Spatial distribution and lifetime cancer risk due to naturally occurring radionuclides in soils around tar-sand deposit area of Ogun State, southwest Nigeria". *Chemosphere*, 193: p. 1036 (2018)
- [39] Abbasi, A., "Radiation hazards and natural radioactivity levels in surface soil samples from dwelling areas of North Cyprus". *Journal of radioanalytical and nuclear chemistry*, 324(1): p. 203 (2020)
- [40] Ibrahim, A., A. Hashim, and A. Abojasim, "The Impact of Long-Lived Gamma Emitters on Human Health in Selected Soil Samples at Karbala University-Fariha Site". *Prensa Med Argent*, 106: p. 5.(2020)
- [41] Ibrahim, A.A. and A.K. Hashim, A.A Abojasim "Comparing of the Natural Radioactivity in Soil Samples of University at Al-Husseineya and Al-Mothafeen Sites of Karbala, Iraq". *Jordan Journal of Physics*, 14(2): p.p177-191.(2021)
- [42] Mujahid, S., S. Hussain, and M. Ramzan, "Measurement of radon exhalation rate and soil gas radon concentration in areas of southern Punjab, Pakistan". *Radiation protection dosimetry*, 140(3): p.p300-303.(2010)
- [43] Rafique, M., S ,Rahman., S,U Rahman ., "Estimation of annual effective radon doses and risk of lung cancer in the residents of district Bhimber, Azad Kashmir, Pakistan". *Nuclear Technology and Radiation Protection*, 26(3): p.p218 (2011)
- [44] Iqbal, A., M,S,Baig., M,Akram., S,Khan ., "Indoor radon concentration: impact of geology in the 2005 Kashmir earthquake-affected Bagh area, Azad Jammu and Kashmir, Pakistan". *Radioprotection*, 46(3): p.p373-385.(2011)

- [45] Drweesh, E.M., L.M. Salih, and R.T. Abdulla, "Determination of uranium concentrations in some plants and soils samples from Baghdad-Iraq,"using CN-85 track detector". Journal of Madenat Alelem College 4(2): p.p124-134.(2012)
- [46] Tabar, E., M.N .Kumru., M.Ichedef., "Radioactivity level and the measurement of soil gas radon concentration in Dikili geothermal area, Turkey". International Journal of Radiation Research, 11(4): p.253.(2013)
- [47] Al-saadi, A.J., A.K. Hashim, and F.M. Hussein, "Measurement of Radon and Uranium Concentrations in the Dates and Their Seeds of Different Regions in Karbala Governorate". Journal of University of Babylon,. 21(6): p.2134 (2013)
- [48] Kunovska, B., K Ivanova, Z Stojanovska., "Measurements of radon concentration in soil gas of urban areas, Bulgaria". Romanian Journal of Physics, 58(S): p.p172-179.(2013)
- [49] Kakati, R.K., L. Kakati, and T. Ramachandran, "Measurement of uranium, radium and radon exhalation rate of soil samples from Karbi Anglong district of Assam, India using EDXRF and Can technique method". APCBEE procedia, 5(186): p.191.(2013)
- [50] Al-Saadi, A.J., A.K. Hashim, and H.J. Musa, "Determination of radium and radon exhalation rates in soil samples collected from Kerbala Governorate". International Journal of Physics, 3(5):p.p208-212.(2015)
- [51] Battawy, A.A., A.A. Aziz, and H.S. Ali, "Radon Concentration measurement in an Imported Tea using Nuclear Track Detector CN-85. Tikrit Journal of Pure Science, 21(1): p.p 68 (2016)
- [52] Mittal, S., A. Rani, and R. Mehra, "Estimation of radon concentration in soil and groundwater samples of Northern Rajasthan, India". Journal of Radiation research and applied sciences, 9(2): p.p 125-130.(2016)
- [53] Abojassim, A, A., "Alpha particles concentrations from soil samples of Al-Najaf/Iraq". Polish Journal of Soil Science, 50(2): p. 249.(2018)
- [54] Hashim, A.K. and S.S. Nayif, "Determination of the Radiation of Alpha Particles in the Air of Primary School Buildings in the City of Karbala". Indian Journal of Public Health Research & Development, 10(1): p.p531-537.(2019)
- [55] Bello, S., R Nasiru, NN Garba, DJ Adeyemo., "Annual effective dose associated with radon, gross alpha and gross beta radioactivity

- in soil from gold mining areas of Shanono and Bagwai, Kano state, Nigeria". *Microchemical Journal*, v.154: p. 104.(2020)
- [56] Ibrahim, A.A., A.K. Hashim, and A. A., Abojassim., "Determination of Alpha Activity in Soil Samples of Agricultural College of Kerbala University, Iraq". *Annals of Agri-Bio Research*, 26(1): p.p125-131.(2021)
- [57] Hashim, A.K., B.R. Al Safaay, and F.K. Fulyful, "Determination of Uranium concentration, Radium content and Radon Exhalations Rates in soil samples for Some Regions in Lebanon". *Journal of Kufa-physics*, 8(2): p.p1-9.(2016)
- [58] Hashim, A.K., E.I. Awad, and H.A. Mezher, "Measurement of annual effective dose for Radon in Kerbala University Campus, Freiha, Iraq". *Iraqi Journal of Public Health*, 1(1): p.p20-25.(2017)
- [59] Abid, A.A., A. A Mraity., Hussien, AA Husai., "Estimation of the excess lifetime cancer risk from radon exposure in some buildings of Kufa Technical Institute, Iraq". p.p276-286.(2017)
- [60] Saini, K. and B. Bajwa, "Mapping natural radioactivity of soil samples in different regions of Punjab, India". *Applied Radiation and Isotopes*, 127: p.p73-81.(2017)
- [61] Pourimani, R. and T. Davoodmaghami, "Radiological hazard resulting from natural radioactivity of soil in east of Shazand power plant". *Iranian Journal of Medical Physics*, 15(3): p.p192-199.(2018)
- [62] Günay, O., MM Saç, M İçhedef, C Taşköprü " Natural radioactivity analysis of soil samples from Ganos fault (GF)." *International Journal of Environmental Science and Technology*, 16(9): p. 5055-5058.(2019)
- [63] Bem, H., A. Gasiorowski, and P. Szajerski, "A fast method for the simultaneous determination of soil radon (^{222}Rn) and thoron (^{220}Rn) concentrations by liquid scintillation counting". *Science of The Total Environment*, 709: p. 135 (2020)
- [64] Stock, R., "Encyclopedia of nuclear physics and its applications". John Wiley & Sons p.166.(2013)
- [65] Rittersdorf, I., "Gamma ray spectroscopy". *Nuclear Engineering & Radiological Sciences*, p.p18-20.(2007)
- [66] De Grijs, R. and S. Cartwright, "An Introduction to Distance Measurement in Astronomy". Wiley Online Library p.127.(2011)
- [67] Erdi-Krausz, G., Matolin, M., Minty, B, Nicolet, J.P, "Guidelines for radioelement mapping using gamma ray spectrometry data: also as

- open access e-book". International Atomic Energy Agency (IAEA) p17.(2003)
- [68] Choppin, G.R. and P.J. Wong, "The chemistry of actinide behavior in marine systems". *Aquatic Geochemistry*, 4(1): p. 77-101.(1998)
- [69] Hodgson, P.E., E. Gadioli, and E.G. Erba, "Introductory nuclear physics". Clarendon Press Oxford.(1997)
- [70] Turner, J., Atoms, "radiation and radiation protection". v.(3) p.133. (2007).
- [71] Weidner, R.T. and R.L. Sells, "Elementary modern physics. (1960).
- [72] Lee, S., G. Tewolde, and J. Kwon. Design and implementation of vehicle tracking system using GPS/GSM/GPRS technology and smartphone application". in *IEEE world forum on internet of things (WF-IoT).IEEE.*(2014)
- [73] Ramadhan, R., "Measurement of Radon Concentration in Iraq and Imported ". *Journal of Thi-Qar Science*, 3(2): p.p210-215.(2012)
- [74] Crouthamel, C.E., F. Adams, and R. Dams, "Applied gamma-ray spectrometry". Vol. 41. Elsevier.(2013)
- [75] Beyzadeoglu, M., G. Ozyigit, and C. Ebruli, "Basic radiation oncology". Springer Science & Business Media.(2010)
- [76] Krane, E. and S. Kenneth, "Oregon state university". *Introductory Nuclear Physics*, John Wiley & Sons, New York, (1988).
- [77] Gordon, R., "Practical Gamma-ray Spectrometry–2nd Edition Gordon R. Gilmore Nuclear Training Services Ltd Warrington", UK, (2008).
- [78] Krstić, D., D Nikezić, N Stevanović, D Vučić ., "Radioactivity of some domestic and imported building materials from South Eastern Europe". *Radiation Measurements*, 42(10): p. 1731(2007)
- [79] Dwivedi, K., "Range and energy-loss of heavy ions by a nuclear track technique". *International Journal of Radiation Applications and Instrumentation. Part D. Nuclear Tracks and Radiation Measurements*, 19(1-4): p. 71(1991)
- [80] Fleischer, R.L., P.B. Price, and R.M. Walker, "Tracks of charged particles in solids". *Science*, 149(3682): p.p383-393.(1965)
- [81] Durrani, S.A. and R.K. Bull, "Solid state nuclear track detection: principles, methods and applications". Vol. 111. Elsevier.(2013)
- [82] Chadderton, L.T., S.A. Cruz, and D.W. Fink, "Theory for latent particle tracks in polymers". *Nuclear Tracks and Radiation Measurements*, 22(1-4): p. 29(1993)

- [83] Rehman, S., "Radon measurements with CR-39 detectors-implications for uranium ore analysis and risk assessment". Doctor thesis, PIEAS, (2005).
- [84] Mazzei, R. and O. Bernaola, Evidence for a dynamic process in track formation International Journal of Radiation Applications and Instrumentation. Part D. Nuclear Tracks and Radiation Measurements, 19(1-4): p. 101 (1991)
- [85] TSOULFANIDIS, N., " Measurement and detection of radiation(Book) ". Washington, DC, Hemisphere Publishing Corp., 586 p, (1983).
- [86] Haase, G., E. Schopper, and F. Granzer, "Solid state nuclear track detectors": Track forming, stabilizing and development processes. Radiation Effects, 34(1-3): p. 25 (1977)
- [87] Fleischer, R.L., P.B Price., R.M Walker., E.L Hubbard., "Nuclear tracks in solids": principles and applications.Univ of California Press.(1975)
- [88] Al-Baidhani, M.A., "Determination of the radioactivity in soil in Baghdad, Karbala and Basrah samples". M. Sc. Thesis, Al-Nahrain University, College of Science p:144(2006)
- [89] L'Annunziata, M.F., "Handbook of radioactivity analysis". Academic press.(2012)
- [90] Fleischer, R., P.B Price., R.M Walker., E.L Hubbard., "Criterion for registration in dielectric track detectors". Physical Review, 156(2): p. 353.(1967)
- [91] Bonfiglioli, G., A. Ferro, and A. Mojoni, "Electron microscope investigation on the nature of tracks of fission products in mica". Journal of Applied Physics, 32(12): p. 2499 (1961)
- [92] Obaid, H.A., S ,Shahid., KNBKN,Basim., "Modeling sewerage overflow in an urban residential area using storm water management model". Malaysian Journal of Civil Engineering, 26(2).p.133(2014)
- [93] Mohammed, E.A., Z.Y. Hani, and G.Q. Kadhim. "Assessing land cover/use changes in Karbala city (Iraq) using GIS techniques and remote sensing data". in Journal of Physics: Conference Series. IOP Publishing.(2018)
- [94] Almayahi, B., "Gamma spectroscopic of soil samples from Kufa in Najaf governorate, Iraq". World Applied Sciences Journal, 31(9): p. 1582(2014)
- [95] Rajamannan, B., G. Viruthagiri, and K. Suresh Jawahar, "Natural radionuclides in ceramic building materials available in Cuddalore

- district, Tamil Nadu, India". Radiation protection dosimetry,156(4): p. 531 (2013)
- [96] Gröning, M. and K. Rozanski, "Uncertainty assessment of environmental tritium measurements in soil" . Accreditation and quality assurance, 8(7-8): p.359(2003)
- [97] Lowenthal, G. and P. Airey, "Practical applications of radioactivity and nuclear radiations". Cambridge university press.(2001)
- [98] Currie, L., "Uncertainty in measurements close to detection limits: detection and quantification capabilities". Quantifying uncertainty in nuclear analytical measurements, p. 9.(2004)
- [99] Grupen, C. and B. Shwartz, "Particle detectors". Vol. 26. Cambridge university press.p:15-20 (2008)
- [100] Harb, S., A. Abbady, A.H El-Kamel, AI Abd El-Mageed, "Concentration of U-238, U-235, Ra-226, Th-232 and K-40 for some granite samples in eastern desert of Egypt". (2008)
- [101] Abojassim, A.A., M.H. Oleiwi, and M. Hassan, "Natural radioactivity and radiological effects in soil samples of the main electrical stations at Babylon Governorate". p. 308-315.(2016)
- [102] Harb, S.R.M., "On the human radiation exposure as derived from the analysis of natural and man-made radionuclides in soils". Hannover: Universität.(2004)
- [103] Krieger, R., "Radioactivity of construction materials". Betonwerk Fertigteil Techn, 47(5): p.p468-473.(1981)
- [104] Venturini, L. and M. Nisti, "Natural radioactivity of some Brazilian building materials". Radiation protection dosimetry, 71(3): p.p 227-229.(1997)
- [105] Mahler, R. and A. Hamid, "Evaluation of water potential, fertilizer placement and incubation time on volatilization losses of urea in two northern Idaho soils". Communications in soil science and plant analysis, 25(11-12): p. 1991 (2004).
- [106] Kahn, B., G.G. Eichholz, and F.J. Clarke, "Search for building materials as sources of elevated radiation dose. Health physics", 45(2): p.p349-361.(1983)
- [107] UNSCEAR, "Sources and Effects of Ionizing Radiation, Report to the General Assembly". Annex J. Exposure and Effects of the Chernobyl Accident, p. 155.(2000)
- [108] "UNSCEAR Sources and effects of ionizing radiation": Report to the general assembly, (United Nations, New York), with scientific annexes,2,1-219.(2008)

- [109] Arafa, W., Specific activity and hazards of granite samples collected from the Eastern Desert of Egypt. *Journal of environmental radioactivity*, 75(3): p.p315-327.(2004)
- [110] Okogbue, C. and M. Nweke, "The ^{226}Ra , ^{232}Th and ^{40}K contents in the Abakaliki baked shale construction materials and their potential radiological risk to public health, southeastern Nigeria". *J Environ Geol Vol*, 2(1): p. 14.(2018)
- [111] UNSCEAR, S., "Effects of ionizing radiation, United Nations Scientific Committee on the Effects of Atomic Radiation, Report to the General Assembly, with Scientific Annexes", United Nations Publication sales (1993).
- [112] Al-Hamidawi, A., "Assessment of radiation hazard indices and excess life time cancer risk due to dust storm for Al-Najaf, Iraq". *WSEAS Trans. Environ. Dev*, 10: p. 312.(2014)
- [113] Hamza, V.Z. and M.N. Mohankumar, "Cytogenetic damage in human blood lymphocytes exposed in vitro to radon". *Mutation Research/Fundamental and Molecular Mechanisms of Mutagenesis*, 661(1-2): p.p1-9.(2009)
- [114] Mohammad, A.I. and N.N. Al-Zubaidy, "Estimation of Natural Radioactivity in Soil in Some Villages of Irbid City". *Applied Physics Research*, 4(3): p. 39.(2012)
- [115] Khan, M.S., D. Srivastava, and A. Azam, "Study of radium content and radon exhalation rates in soil samples of northern India". *Environmental earth sciences*, 67(5): p.p1363-1371.(2012)
- [116] Mowlavi, A.A., A.A., M.R. Fornasier, ABinesh., "Indoor radon measurement and effective dose assessment of 150 apartments in Mashhad, Iran". *Environmental monitoring and assessment*, 184(2): p. 1085(2012)
- [117] Abumurad, K.M. and R.A. Al-Omari, "Indoor radon levels in irbid and health risk from internal doses". *Radiation Measurements*, 43: p.p389-391.(2008)
- [118] Shakir, K.M., A.H. Naqvi, A.Azam., "Radium and radon exhalation studies of soil". (2011).
- [119] Azam, A., A. Naqvi, and D. Srivastava, "Radium concentration and radon exhalation measurements using LR-115 type II plastic track detectors". *NuGeo*, 9(6): p.p653-657.(1995)
- [120] Khan, M.S., D. Srivastava, and A. Azam, "Study of radium content and radon exhalation rates in soil samples of northern India". *Environmental earth sciences*, 67(5): p. 1363 (2012)

- [121] Tykva, R. and J. Sabol, "Low-level environmental radioactivity: sources and evaluation". CRC Press.(1995)
- [122] AEA (International Atomic Energy Agency), Construction and Use of Calibration Facilities for Radiometric Field Equipment, Technical Report No. 309, Vienna, Austria, (1989).
- [123] IAEA (International Atomic Energy Agency), Guidelines for radioelement mapping using gamma ray spectrometry data, Technical Reports Series No. 1363, Vienna, Austria, (2003).
- [124] UNSCEAR Sources and effects of ionizing radiation: Report to the general assembly, (United Nations, New York), with scientific annexes,2,1-219. (2008)
- [125] Agency, N.E., "Exposure to radiation from the natural radioactivity in building materials: report". OECD.(1979)
- [126] Ravisankar, R., K Vanasunda, M Suganya, "Multivariate statistical analysis of radiological data of building materials used in Tiruvannamalai, Tamilnadu, India". Applied Radiation and Isotopes, 85: p. 114-127.(2014)
- [127] Charles, M., UNSCEAR Report 2000: sources and effects of ionizing radiation. Journal of Radiological Protection, 21(1): p. 83.(2001)
- [128] Thomas, R., "Ionising radiation exposure measurements at commercial jet aircraft altitudes". Radiation protection dosimetry, 48(1): p.p51-57.(1993)
- [129] Agency, O.N.E., "Guidelines for sea dumping packages of radioactive waste". Nuclear Energy Agency, Organisation for Economic Co-operation and Development.(1979)
- [130] against Radon, P., "222 at Home and at Work", ICRP Publ. No. 65. Ann. ICRP, 23(2): p.p782-785.(1993)
- [131] UNSCEAR, S., "Effects of ionizing radiation, United Nations Scientific Committee on the Effects of Atomic Radiation", Report to the General Assembly, with Scientific Annexes, United Nations Publication sales p.3(1993).
- [132] UNSCEAR, S., "Effects of Ionizing Radiation, United Nations Scientific Committee on the Effects of Atomic Radiation". Report to General, Assembly with Annexes, 2000.
- [133] Raghu R,Y., Chandrasekaran, A.,"Determination of natural radioactivity and the associated radiation hazards in building materials used in Polur, Tiruvannamalai District, Tamilnadu", India

- using gamma ray spectrometry with statistical approach. *Journal of Geochemical Exploration*, (163) p. 41, (2016)
- [134] Garribba, M., D. Energy, and D.D. Garribba, "International Commission on Radiological Protection". p.122. (2017).
- [135] Kaur, N., "Measurements of radon gas concentration in soil". *International Journal of Computer Applications*, (975) p.8887, (2015)
- [136] gainst Radon, P., "222 at Home and at Work", ICRP Publ. No. 65. *Ann. ICRP*, 23(2): p.p782-785. (1993)
- [137] de Carmoy, G., "Nuclear energy in France: An economic policy overview". *Energy Economics*, 1(3): p.p130-133. (1979)
- [138] UNSCEAR, S., " United Nations Scientific Committee on the Effects of Atomic Radiation". United Nations New York (2000).
- [139] NSCEAR Sources and effects of ionizing radiation: Report to the general assembly, (United Nations, Publications.), with Scientific annexes, 2, 1-219. (1994)
- [140] Ref, I., "International Commission on Radiological Protection Statement on Radon". (1990)
- [141] Archer, V.E., J.D. Gillam, and J.K. Wagoner, "Respiratory disease mortality among uranium miners". *Annals of the New York Academy of Sciences*, V 271: p.p280-293. (1976)
- [142] Nazaroff, W., Nero, A., Bodansky, D., Robkin, M.A., "Radon and Its Decay Products in Indoor Air and Indoor Radon and Its Hazards and Environmental Radon". *PhT*, 42(4) p.72. (1989)
- [143] Najam, L.A., E.J. Mohammed, and A.S. Hameed, "Estimation of Radon Exhalation Rate, Radium Activity and Uranium Concentration in Biscuit Samples in Iraq". *Iranian Journal of Medical Physics*, . 16(2): p.p152-157. (2019)
- [144] Hashim, A.K. and L.A. Najam, "Radium and Uranium Concentrations Measurements in Vegetables Samples of Iraq". *Detection*, 3(04): p. 21. (2015)
- [145] Farid, S., "Indoor radon in dwellings of Jeddah city, Saudi Arabia and its correlations with the radium and radon exhalation rates from soil". *Indoor and Built Environment*, 25(1): p.p269-278. (2016)
- [146] Korany, K., AE Shata and SF Hassan ., " Depth and seasonal variations for the soil radon-gas concentration levels at Wadi Naseib Area, southwestern Sinai, Egypt". *J. Phys. Chem. Biophys*, V(3): p. 123. (2013)

- [147] Brajnik, D., U. Miklavzic, and J. Tomsic, "Map of natural radioactivity in Slovenia and its correlation to the emanation of radon". *Radiation protection dosimetry*, 45(1-4): p. 27(1992)
- [148] Kumar, A., B. Singh, and S. Singh, "Uranium, radium and radon exhalation studies in some soil samples from Una district, Himachal Pradesh, India using track etching technique"v.144.p:55 (2001).
- [149] Abojassim, A., Sulahadi, K., Hamed ,A., Hashin, A., "Radon, Radium concentration and radiological parameters in soil samples of Amara at Maysan Iraq". *Asian Journal of Earth Sciences*3(2),p. 44-49, 2017
- [150] Antoci, C., Immè, G., La Delfa, S., Nigro, S.L., "Indoor and soil radon measurements in the Hyblean Foreland (South-East Sicily) ". *Annals of Geophysics*,50(4), 2007
- [151] Hashim, A.K. and E.J. Mohammed, "Measurement of radon concentration and the effective dose rate in the soil of the city of Karbala", *Iraq. J. Radiation and Nuclear Applications*, 1(1): p.p 17-23.2016
- [152] Mohammad, A.M., "Measurement of radon-222 concentration in soil samples of some sulfuric spring in hit city using CR-39 detector". *Baghdad Science Journal*, 8(4) p.972 (2011)
- [153] Climent H., Font L. I., Bacmeister G. U., Albarracin D. and Monnin M.M., "Using Passive Detectors in Soil and Indoors in Tow Mediterranean Locations for Radon Concentration Measurements" Vol.28, No.(1-6),pp713-716,1997

الخلاصة

يطلق على المصدر الرئيسي للنشاط الإشعاعي والإشعاع النووي النويدات المشعة والتي تمثل جزءا من حياتنا اليومية تمثل جسيمات الفا واشعة كما اهم انواع الاشعاعات المؤينة فالتربة تعتبر من المصادر المهمة للنشاط الإشعاعي الطبيعي مثل الإشعاع الأرضي الذي قد يكون له تأثير على صحة الإنسان.

تم جمع 100 عينة تربة من مواقع مختلفة لجامعة كربلاء والتي تتكون من مجموعه كليات موزعة على ثلاثة مواقع وهي منطقه فريجه و منطقه الحسينية (كلية الزراعة) و منطقة الموظفين. تم قياس النشاط الإشعاعي النوعي للنظائر (^{238}U , ^{232}Th , and ^{40}K) وبعثات الفا (^{222}Rn , ^{226}Ra , and ^{238}U) باستعمال الكواشف (NaI(Tl) و CN-85 على التوالي). كذلك تم تحديد عوامل الخطورة الإشعاعية بسبب باعثات كما و الفا في النماذج. تم استعمال تقنيه نظام المعلومات الجغرافية (GIS) لرسم خرائط لمعظم النتائج الرئيسية.

اظهرت النتائج أن قيم معدل الفعالية النوعية لكل من ^{238}U و ^{232}Th و ^{40}K لمنطقة فريجة كانت 17.02 ± 7.70 Bq/kg و 8.22 ± 2.9 Bq/kg و 301.02 ± 77.5 Bq/kg على التوالي ، بينما منطقة الحسينية كانت 21.75 ± 7.2 Bq/kg ، 9.43 ± 3.2 Bq/kg ، $82.2 \pm$ Bq/kg ، 335.88 على التوالي ، لكن منطقة الموظفين كانت 22.4 ± 8.8 Bq/kg 11.19 ± 3.3 Bq/kg ، 333.11 ± 70.7 Bq/kg ، بينما كانت قيم معدل الفعالية النوعية لكل من تراكيز الرادون ، وتراكيز الراديوم ، وتراكيز اليورانيوم في منطقة فريجة كانت 3769.71 ± 6.67 Bq/kg و 0.093 ± 0.03 Bq/kg و 2.7 ± 0.18 Bq/Kg على التوالي . بينما منطقة الحسينية كانت 4308.25 ± 7.17 Bq/m³ ، 0.106 ± 0.03 Bq/kg ، 3.15 ± 0.18 Bq/kg على التوالي ، لكن منطقة الموظفين كانت 5090.54 ± 155.31 Bq/m³ ، 0.125 ± 0.03 Bq/kg و 3.72 ± 0.12 Bq/kg على التوالي كذلك وجد علاقة ترابط جيدة للفعالية النوعية بين ^{238}U و ^{222}Rn (0.88). ووفقا لقيم معدل باعثات كما و الفا بالإضافة الى عوامل الخطورة الإشعاعية لتربة جامع كربلاء كانت ضمن الحدود العالمية الموصى بها لمنظمات UNSCEAR, OECD and ICRP. واخيرا يمكن استنتاج بانه لا يوجد خطر اشعاعي بسبب باعثات كما و الفا في نماذج التربة لمنطقة الدراسة على صحة الانسان.



جمهورية العراق

وزارة التعليم العالي والبحث العلمي

جامعة كربلاء

كلية العلوم

قسم الفيزياء

تحديد النشاط الاشعاعي الطبيعي لباعثات كاما والفا من تربة
جامعة كربلاء

رسالة

مقدمة الى مجلس كلية العلوم/جامعة كربلاء

كجزء من متطلبات نيل درجة الماجستير في علوم الفيزياء

مقدمة من قبل

ابرار عباس ابراهيم

بكالوريوس جامعة بابل 2017

بإشراف

أ.د. عبد الستار كريم هاشم

أ.د. علي عبد ابو جاسم